CHAPTER 34

DUCT DESIGN

BERNOULLI EQUATION 34.1
Head and Pressure 34.2
SYSTEM ANALYSIS 34.2
Pressure Changes in System 34.6
FLUID RESISTANCE 34.7
Friction Losses 34.7
Dynamic Losses 34.8
Ductwork Sectional Losses 34.12
FAN-SYSTEM INTERFACE 34.12
DUCT SYSTEM DESIGN 34.14
Design Considerations 34.14
Duct Design Methods 34.18
HVAC Duct Design Procedures 34.20
Industrial Exhaust System Duct Design 34.22
FITTING LOSS COEFFICIENTS 34.29

COMMERCIAL, industrial, and residential air duct system design must consider (1) space availability, (2) space air diffusion, (3) noise levels, (4) duct leakage, (5) duct heat gains and losses, (6) balancing, (7) fire and smoke control, (8) initial investment cost, and (9) system operating cost.

Deficiencies in duct design can result in systems that operate incorrectly or are expensive to own and operate. Poor air distribution can cause discomfort, loss of productivity and even adverse health effects; lack of sound attenuators may permit objectionable noise levels. Poorly designed ductwork can result in unbalanced systems. Faulty duct construction or lack of duct sealing produces inadequate airflow rates at the terminals. Proper duct insulation eliminates the problem caused by excessive heat gain or loss.

In this chapter, system design and the calculation of a system's frictional and dynamic resistance to airflow are considered. Chapter 16 of the 2000 *ASHRAE Handbook—Systems and Equipment* examines duct construction and presents construction standards for residential, commercial, and industrial heating, ventilating, air-conditioning, and exhaust systems.

BERNOULLI EQUATION

The Bernoulli equation can be developed by equating the forces on an element of a stream tube in a frictionless fluid flow to the rate of momentum change. On integrating this relationship for steady flow, the following expression (Osborne 1966) results:

$$\frac{v^2}{2} + \int \frac{dP}{\rho} + gz = \text{constant, N} \cdot \text{m/kg} \tag{1}$$

where

v = streamline (local) velocity, m/s
P = absolute pressure, Pa (N/m^2)
ρ = density, kg/m^3
g = acceleration due to gravity, m/s^2
z = elevation, m

Assuming constant fluid density within the system, Equation (1) reduces to

$$\frac{v^2}{2} + \frac{P}{\rho} + gz = \text{constant, N} \cdot \text{m/kg} \tag{2}$$

Although Equation (2) was derived for steady, ideal frictionless flow along a stream tube, it can be extended to analyze flow through ducts in real systems. In terms of pressure, the relationship for fluid resistance between two sections is

$$\frac{\rho_1 V_1^2}{2} + P_1 + g\rho_1 z_1 = \frac{\rho_2 V_2^2}{2} + P_2 + g\rho_2 z_2 + \Delta p_{t,1\text{-}2} \tag{3}$$

where

V = average duct velocity, m/s
$\Delta p_{t,1\text{-}2}$ = total pressure loss due to friction and dynamic losses between sections 1 and 2, Pa

In Equation (3), V (section average velocity) replaces v (streamline velocity) because experimentally determined loss coefficients allow for errors in calculating $\rho v^2/2$ (velocity pressure) across streamlines.

On the left side of Equation (3), add and subtract p_{z1}; on the right side, add and subtract p_{z2}, where p_{z1} and p_{z2} are the values of atmospheric air at heights z_1 and z_2. Thus,

$$\frac{\rho_1 V_1^2}{2} + P_1 + (p_{z1} - p_{z1}) + g\rho_1 z_1 = \frac{\rho_2 V_2^2}{2} + P_2 + (p_{z2} - p_{z2}) + g\rho_2 z_2 + \Delta p_{t,1\text{-}2} \tag{4}$$

The atmospheric pressure at any elevation (p_{z1} and p_{z2}) expressed in terms of the atmospheric pressure p_a at the same datum elevation is given by

$$p_{z1} = p_a - g\rho_a z_1 \tag{5}$$

$$p_{z2} = p_a - g\rho_a z_2 \tag{6}$$

Substituting Equations (5) and (6) into Equation (4) and simplifying yields the total pressure change between sections 1 and 2. Assume no change in temperature between sections 1 and 2 (no heat exchanger within the section); therefore, $\rho_1 = \rho_2$. When a heat exchanger is located within the section, the average of the inlet and outlet temperatures is generally used. Let $\rho = \rho_1 = \rho_2$. $(P_1 - p_{z1})$ and $(P_2 - p_{z2})$ are gage pressures at elevations z_1 and z_2.

$$\Delta p_{t,1\text{-}2} = \left(p_{s,1} + \frac{\rho V_1^2}{2}\right) - \left(p_{s,2} + \frac{\rho V_2^2}{2}\right) + g(\rho_a - \rho)(z_2 - z_1) \tag{7a}$$

$$\Delta p_{t,1\text{-}2} = \Delta p_t + \Delta p_{se} \tag{7b}$$

The preparation of this chapter is assigned to TC 5.2, Duct Design.

$$\Delta p_t = \Delta p_{t,1\text{-}2} - \Delta p_{se} \quad (7c)$$

where

$p_{s,1}$ = static pressure, gage at elevation z_1, Pa
$p_{s,2}$ = static pressure, gage at elevation z_2, Pa
V_1 = average velocity at section 1, m/s
V_2 = average velocity at section 2, m/s
ρ_a = density of ambient air, kg/m^3
ρ = density of air or gas within duct, kg/m^3
Δp_{se} = thermal gravity effect, Pa
Δp_t = total pressure change between sections 1 and 2, Pa
$\Delta p_{t,1-2}$ = total pressure loss due to friction and dynamic losses between sections 1 and 2, Pa

HEAD AND PRESSURE

The terms **head** and **pressure** are often used interchangeably; however, head is the height of a fluid column supported by fluid flow, while pressure is the normal force per unit area. For liquids, it is convenient to measure the head in terms of the flowing fluid. With a gas or air, however, it is customary to measure pressure on a column of liquid.

Static Pressure

The term $p/\rho g$ is static head; p is static pressure.

Velocity Pressure

The term $V^2/2g$ refers to velocity head, and the term $\rho V^2/2$ refers to velocity pressure. Although velocity head is independent of fluid density, velocity pressure, calculated by Equation (8), is not.

$$p_v = \rho V^2/2 \quad (8)$$

where

p_v = velocity pressure, Pa
V = fluid mean velocity, m/s

For air at standard conditions (1.204 kg/m^3), Equation (8) becomes

$$p_v = 0.602 V^2 \quad (9)$$

Velocity is calculated by Equation (10) or (11).

$$V = 1000 Q/A \quad (10)$$

where

Q = airflow rate, L/s
A = cross-sectional area of duct, mm^2

$$V = 0.001 Q/A \quad (11)$$

where A = cross-sectional area of duct, m^2.

Total Pressure

Total pressure is the sum of static pressure and velocity pressure:

$$p_t = p_s + \rho V^2/2 \quad (12)$$

or

$$p_t = p_s + p_v \quad (13)$$

where

p_t = total pressure, Pa
p_s = static pressure, Pa

Pressure Measurement

The range, precision, and limitations of instruments for measuring pressure and velocity are discussed in Chapter 14. The manometer is a simple and useful means for measuring partial vacuum and low pressure. Static, velocity, and total pressures in a duct system relative to atmospheric pressure are measured with a pitot tube connected to a manometer. Pitot tube construction and locations for traversing round and rectangular ducts are presented in Chapter 14.

SYSTEM ANALYSIS

The total pressure change due to friction, fittings, equipment, and net **thermal gravity effect (stack effect)** for each section of a duct system is calculated by the following equation:

$$\Delta p_{t_i} = \Delta p_{f_i} + \sum_{j=1}^{m} \Delta p_{ij} + \sum_{k=1}^{n} \Delta p_{ik} - \sum_{r=1}^{\lambda} \Delta p_{se_{ir}} \quad (14)$$

$$\text{for } i = 1, 2, \ldots, n_{up} + n_{dn}$$

where

Δp_{t_i} = net total pressure change for i-section, Pa
Δp_{f_i} = pressure loss due to friction for i-section, Pa
Δp_{ij} = total pressure loss due to j-fittings, including fan system effect (FSE), for i-section, Pa
Δp_{ik} = pressure loss due to k-equipment for i-section, Pa
$\Delta p_{se_{ir}}$ = thermal gravity effect due to r-stacks for i-section, Pa
m = number of fittings within i-section
n = number of equipment within i-section
λ = number of stacks within i-section
n_{up} = number of duct sections upstream of fan (exhaust/return air subsystems)
n_{dn} = number of duct sections downstream of fan (supply air subsystems)

From Equation (7), the thermal gravity effect for each nonhorizontal duct with a density other than that of ambient air is determined by the following equation:

$$\Delta p_{se} = 9.81(\rho_a - \rho)(z_2 - z_1) \quad (15)$$

where

Δp_{se} = thermal gravity effect, Pa
z_1 and z_2 = elevation from datum in direction of airflow (Figure 1), m
ρ_a = density of ambient air, kg/m^3
ρ = density of air or gas within duct, kg/m^3

Example 1. For Figure 1, calculate the thermal gravity effect for two cases: (a) air cooled to −34°C, and (b) air heated to 540°C. The density of air at −34°C and 540°C is 1.477 kg/m^3 and 0.434 kg/m^3, respectively. The density of the ambient air is 1.204 kg/m^3. Stack height is 15 m.

Solution:

$$\Delta p_{se} = 9.81(\rho_a - \rho)z$$

(a) For $\rho > \rho_a$ (Figure 1A),

$$\Delta p_{se} = 9.81(1.204 - 1.477)15$$
$$= -40 \text{ Pa}$$

(b) For $\rho < \rho_a$ (Figure 1B),

$$\Delta p_{se} = 9.81(1.204 - 0.434)15$$
$$= +113 \text{ Pa}$$

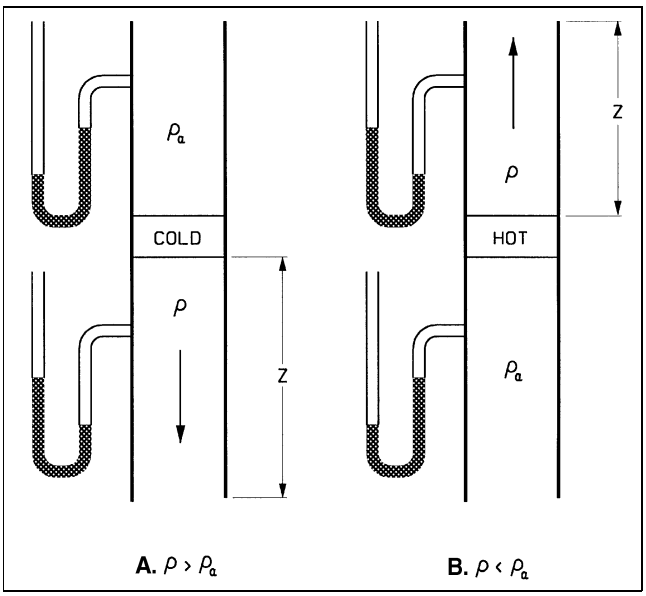

Fig. 1 Thermal Gravity Effect for Example 1

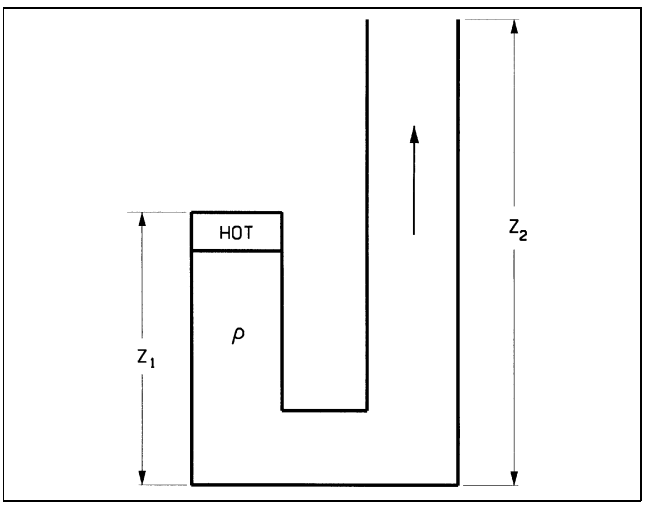

Fig. 2 Multiple Stacks for Example 2

Example 2. Calculate the thermal gravity effect for the two-stack system shown in Figure 2, where the air is 120°C and the stack heights are 15 and 30 m. The density of 120°C air is 0.898 kg/m^3; ambient air is 1.204 kg/m^3.

Solution:

$$\Delta p_{se} = 9.81(\rho_a - \rho)(z_2 - z_1)$$
$$= 9.81(1.204 - 0.898)(30 - 15)$$
$$= 45 \text{ Pa}$$

For the system shown in Figure 3, the direction of air movement created by the thermal gravity effect depends on the initiating force. The initiating force could be fans, wind, opening and closing doors, and turning equipment on and off. If for any reason air starts to enter the left stack (Figure 3A), it creates a buoyancy effect in the right stack. On the other hand, if flow starts to enter the right stack (Figure 3B), it creates a buoyancy effect in the left stack. In both cases the produced thermal gravity effect is stable and depends on the stack height and magnitude of heating. The starting direction of flow is important when using natural convection for ventilation.

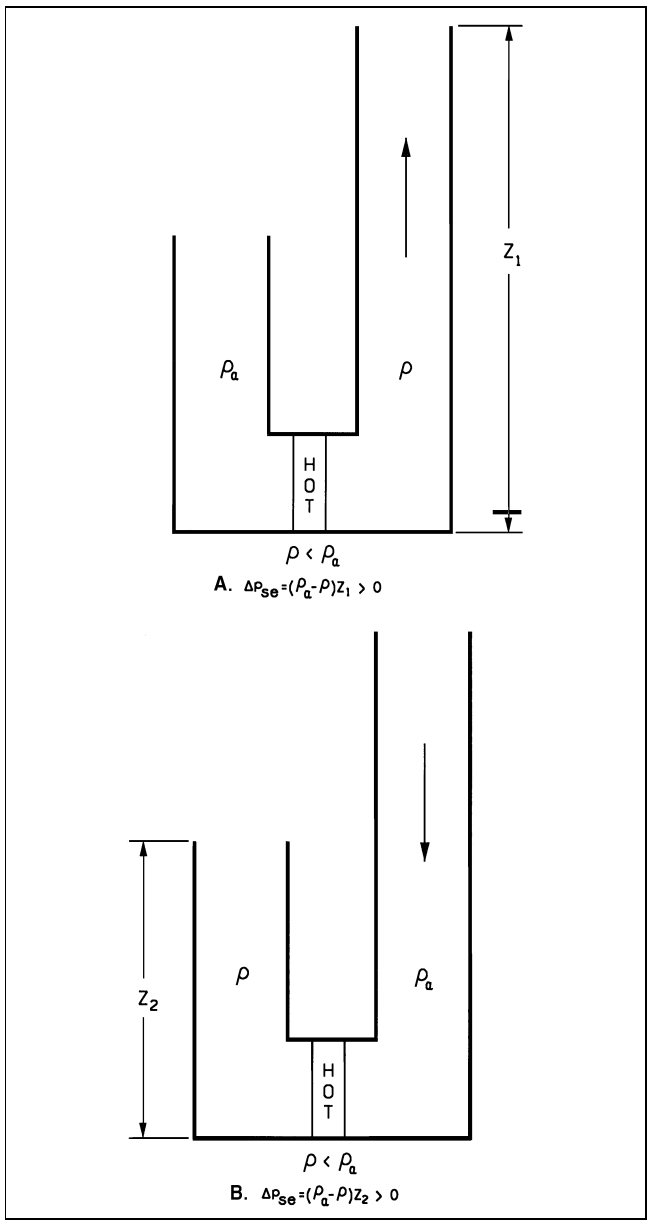

Fig. 3 Multiple Stack Analysis

To determine the fan total pressure requirement for a system, use the following equation:

$$P_t = \sum_{i \varepsilon F_{up}} \Delta p_{t_i} + \sum_{i \varepsilon F_{dn}} \Delta p_{t_i} \quad \text{for } i = 1, 2, \ldots, n_{up} + n_{dn} \quad (16)$$

where

F_{up} and F_{dn}=sets of duct sections upstream and downstream of a fan
P_t = fan total pressure, Pa
ε = symbol that ties duct sections into system paths from the exhaust/return air terminals to the supply terminals

Figure 4 illustrates the use of Equation (16). This system has three supply and two return terminals consisting of nine sections connected in six paths: 1-3-4-9-7-5, 1-3-4-9-7-6, 1-3-4-9-8, 2-4-9-7-5, 2-4-9-7-6, and 2-4-9-8. Sections 1 and 3 are unequal area; thus, they are assigned separate numbers in accordance with the rules for

identifying sections (see Step 4 in the section on HVAC Duct Design Procedures). To determine the fan pressure requirement, the following six equations, derived from Equation (16), are applied. These equations must be satisfied to attain pressure balancing for design airflow. Relying entirely on dampers is not economical and may create objectionable flow-generated noise.

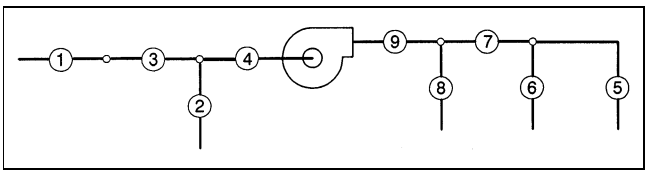

Fig. 4 Illustrative 6-Path, 9-Section System

$$\begin{cases} P_t = \Delta p_1 + \Delta p_3 + \Delta p_4 + \Delta p_9 + \Delta p_7 + \Delta p_5 \\ P_t = \Delta p_1 + \Delta p_3 + \Delta p_4 + \Delta p_9 + \Delta p_7 + \Delta p_6 \\ P_t = \Delta p_1 + \Delta p_3 + \Delta p_4 + \Delta p_9 + \Delta p_8 \\ P_t = \Delta p_2 + \Delta p_4 + \Delta p_9 + \Delta p_7 + \Delta p_5 \\ P_t = \Delta p_2 + \Delta p_4 + \Delta p_9 + \Delta p_7 + \Delta p_6 \\ P_t = \Delta p_2 + \Delta p_4 + \Delta p_9 + \Delta p_8 \end{cases} \quad (17)$$

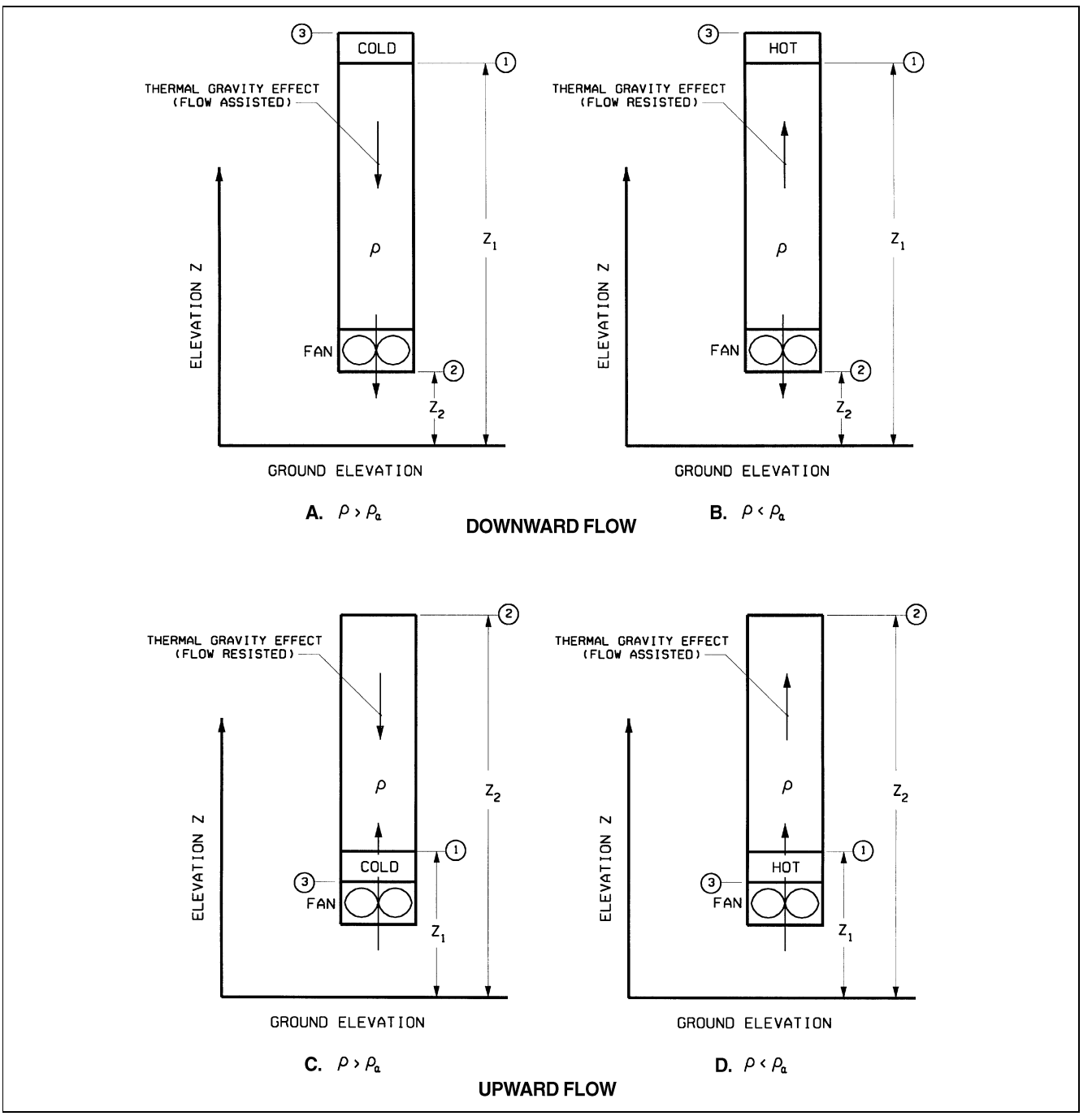

Fig. 5 Single Stack with Fan for Examples 3 and 4

Example 3. For Figures 5A and 5C, calculate the thermal gravity effect and fan total pressure required when the air is cooled to −34°C. The heat exchanger and ductwork (section 1 to 2) total pressure losses are 170 and 70 Pa respectively. The density of −34°C air is 1.477 kg/m^3; ambient air is 1.204 kg/m^3. Elevations are 21 m and 3 m as noted in the solutions below.

Solution.

(a) For Figure 5A (downward flow),

$$\begin{aligned}\Delta p_{se} &= 9.81(\rho_a - \rho)(z_2 - z_1)\\ &= 9.81(1.204 - 1.477)(3 - 21)\\ &= 48 \text{ Pa}\end{aligned}$$

$$\begin{aligned}P_t &= \Delta p_{t,3\text{-}2} - \Delta p_{se}\\ &= (170 + 70) - (48)\\ &= 192 \text{ Pa}\end{aligned}$$

(b) For Figure 5C (upward flow),

$$\begin{aligned}\Delta p_{se} &= 9.81(\rho_a - \rho)(z_2 - z_1)\\ &= 9.81(1.204 - 1.477)(21 - 3)\\ &= -48 \text{ Pa}\end{aligned}$$

$$\begin{aligned}P_t &= \Delta p_{t,3\text{-}2} - \Delta p_{se}\\ &= (170 + 70) - (-48)\\ &= 288 \text{ Pa}\end{aligned}$$

Example 4. For Figures 5B and 5D, calculate the thermal gravity effect and fan total pressure required when the air is heated to 120°C. The heat exchanger and ductwork (section 1 to 2) total pressure losses are 170 and 70 Pa respectively. The density of 120°C air is 0.898 kg/m^3; ambient air is 1.204 kg/m^3. Elevations are 21 m and 3 m as noted in the solutions below.

Solution:

(a) For Figure 5B (downward flow),

$$\begin{aligned}\Delta p_{se} &= 9.81(\rho_a - \rho)(z_2 - z_1)\\ &= 9.81(1.204 - 0.898)(3 - 21)\\ &= -54 \text{ Pa}\end{aligned}$$

$$\begin{aligned}P_t &= \Delta p_{t,3\text{-}2} - \Delta p_{se}\\ &= (170 + 70) - (-54)\\ &= 294 \text{ Pa}\end{aligned}$$

(b) For Figure 5D (upward flow),

$$\begin{aligned}\Delta p_{se} &= 9.81(\rho_a - \rho)(z_2 - z_1)\\ &= 9.81(1.204 - 0.898)(21 - 3)\\ &= 54 \text{ Pa}\end{aligned}$$

$$\begin{aligned}P_t &= \Delta p_{t,3\text{-}2} - \Delta p_{se}\\ &= (170 + 70) - (54)\\ &= 186 \text{ Pa}\end{aligned}$$

Example 5. Calculate the thermal gravity effect for each section of the system shown in Figure 6 and the net thermal gravity effect of the system. The density of ambient air is 1.204 kg/m^3, and the lengths are as follows: z_1 = 15 m, z_2 = 27 m, z_4 = 30 m, z_5 = 8 m, and z_9 = 60 m. The pressure required at section 3 is −25 Pa (−2.7 mm of water). Write the equation to determine the fan total pressure requirement.

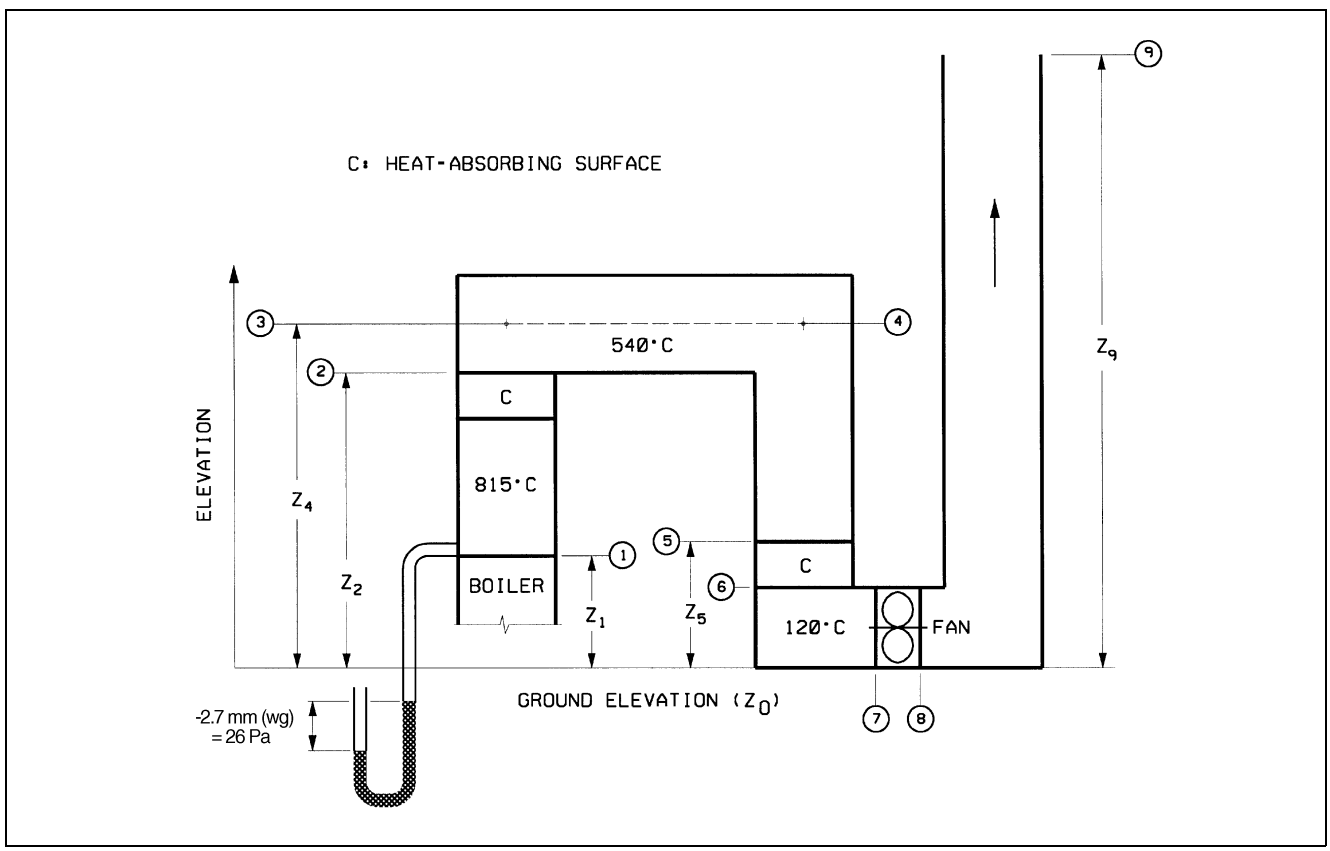

Fig. 6 Triple Stack System for Example 5

Solution: The following table summarizes the thermal gravity effect for each section of the system as calculated by Equation (15). The net thermal gravity effect for the system is 118 Pa. To select a fan, use the following equation:

$$P_t = 25 + \Delta p_{t,1\text{-}7} + \Delta p_{t,8\text{-}9} - \Delta p_{se}$$
$$= 25 + \Delta p_{t,1\text{-}7} + \Delta p_{t,8\text{-}9} - 118$$
$$= \Delta p_{t,1\text{-}7} + \Delta p_{t,8\text{-}9} - 93$$

Path (x-x')	Temp., °C	ρ, kg/m³	Δz ($z_{x'} - z_x$), m	$\Delta\rho$ ($\rho_a - \rho_{x-x'}$), kg/m³	Δp_{se}, Pa [Eq. (15)]
1-2	815	0.324	(27 – 15)	+0.880	+104
3-4	540	0.434	0	+0.770	0
4-5	540	0.434	(8 – 30)	+0.770	−166
6-7	120	0.898	0	+0.306	0
8-9	120	0.898	(60 – 0)	+0.306	+180
Net Thermal Gravity Effect					118

PRESSURE CHANGES IN SYSTEM

Figure 7 shows total and static pressure changes in a fan/duct system consisting of a fan with both supply and return air ductwork. Also shown are the total and static pressure gradients referenced to atmospheric pressure.

For all constant-area sections, the total and static pressure losses are equal. At the diverging transitions, velocity pressure decreases, absolute total pressure decreases, and absolute static pressure can increase. The static pressure increase at these sections is known as **static regain**.

At the converging transitions, velocity pressure increases in the direction of airflow, and the absolute total and absolute static pressures decrease.

At the exit, the total pressure loss depends on the shape of the fitting and the flow characteristics. Exit loss coefficients C_o can be greater than, less than, or equal to one. The total and static pressure grade lines for the various coefficients are shown in Figure 3. Note that for a loss coefficient less than one, static pressure upstream of the exit is less than atmospheric pressure (negative). The static pressure just upstream of the discharge fitting can be calculated by subtracting the upstream velocity pressure from the upstream total pressure.

At section 1, the total pressure loss depends on the shape of the entry. The total pressure immediately downstream of the entrance equals the difference between the upstream pressure, which is zero (atmospheric pressure), and the loss through the fitting. The static pressure of the ambient air is zero; several diameters downstream, static pressure is negative, equal to the sum of the total pressure (negative) and the velocity pressure (always positive).

System resistance to airflow is noted by the total pressure grade line in Figure 7. Sections 3 and 4 include fan system effect pressure losses. To obtain the fan static pressure requirement for fan selection where the fan total pressure is known, use

$$P_s = P_t - p_{v,o} \tag{18}$$

where

P_s = fan static pressure, Pa
P_t = fan total pressure, Pa
$p_{v,o}$ = fan outlet velocity pressure, Pa

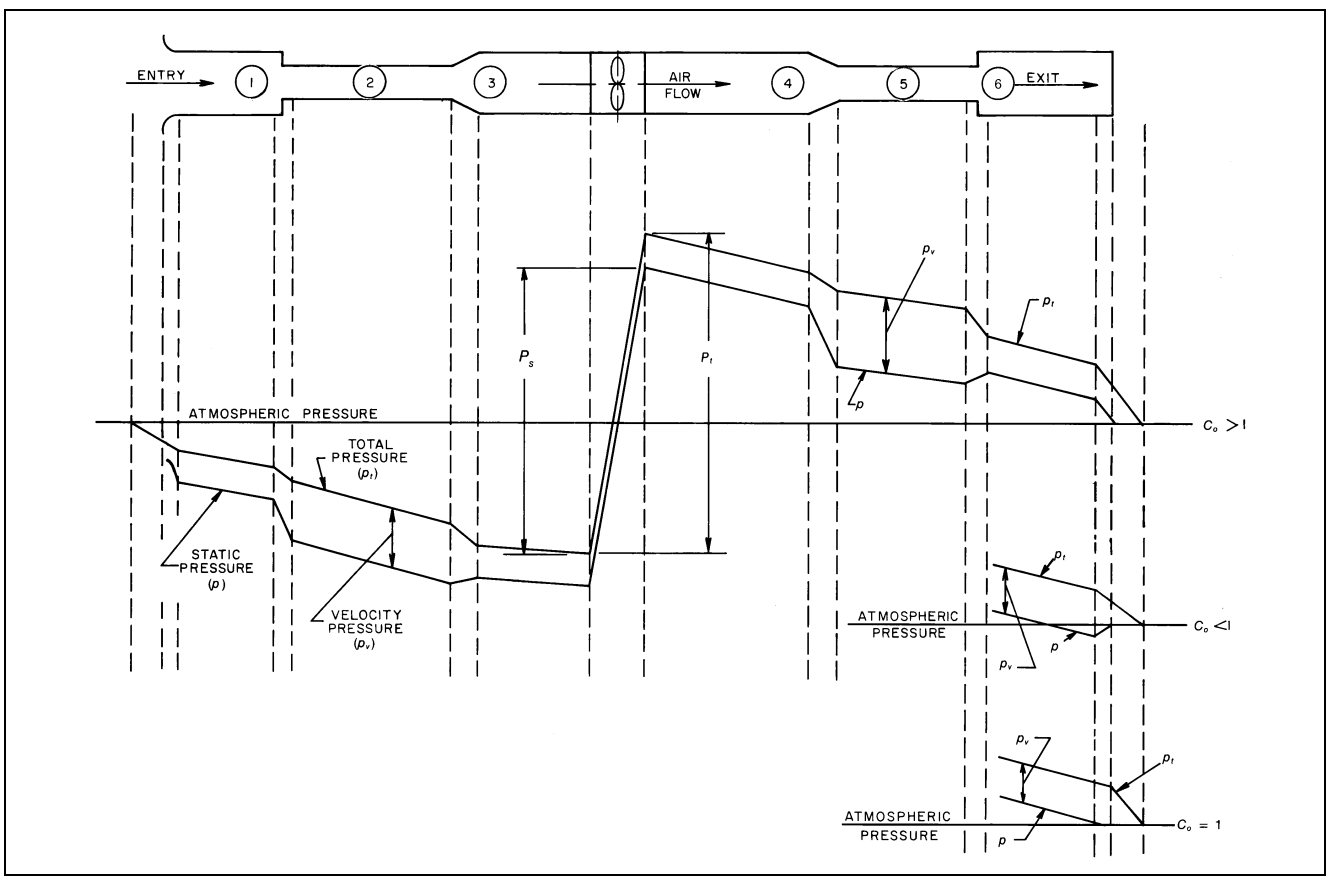

Fig. 7 Pressure Changes During Flow in Ducts

FLUID RESISTANCE

Duct system losses are the irreversible transformation of mechanical energy into heat. The two types of losses are (1) friction losses and (2) dynamic losses.

FRICTION LOSSES

Friction losses are due to fluid viscosity and are a result of momentum exchange between molecules in laminar flow and between individual particles of adjacent fluid layers moving at different velocities in turbulent flow. Friction losses occur along the entire duct length.

Darcy, Colebrook, and Altshul-Tsal Equations

For fluid flow in conduits, friction loss can be calculated by the Darcy equation:

$$\Delta p_f = \frac{1000 f L}{D_h} \frac{\rho V^2}{2} \tag{19}$$

where

Δp_f = friction losses in terms of total pressure, Pa
f = friction factor, dimensionless
L = duct length, m
D_h = hydraulic diameter [Equation (24)], mm
V = velocity, m/s
ρ = density, kg/m^3

Within the region of laminar flow (Reynolds numbers less than 2000), the friction factor is a function of Reynolds number only.

For completely turbulent flow, the friction factor depends on Reynolds number, duct surface roughness, and internal protuberances such as joints. Between the bounding limits of hydraulically smooth behavior and fully rough behavior, is a transitional roughness zone where the friction factor depends on both roughness and Reynolds number. In this transitionally rough, turbulent zone the friction factor f is calculated by Colebrook's equation (Colebrook 1938-39). Colebrook's transition curve merges asymptotically into the curves representing laminar and completely turbulent flow. Because Colebrook's equation cannot be solved explicitly for f, use iterative techniques (Behls 1971).

$$\frac{1}{\sqrt{f}} = -2 \log\left(\frac{\varepsilon}{3.7 D_h} + \frac{2.51}{\mathrm{Re}\sqrt{f}}\right) \tag{20}$$

where

ε = material absolute roughness factor, mm
Re = Reynolds number

A simplified formula for calculating friction factor, developed by Altshul (Altshul et al. 1975) and modified by Tsal, is

$$f' = 0.11\left(\frac{\varepsilon}{D_h} + \frac{68}{\mathrm{Re}}\right)^{0.25}$$
$$\text{If } f' \geq 0.018: \quad f = f' \tag{21}$$
$$\text{If } f' < 0.018: \quad f = 0.85 f' + 0.0028$$

Friction factors obtained from the Altshul-Tsal equation are within 1.6% of those obtained by Colebrook's equation.

Reynolds number (Re) may be calculated by using the following equation.

$$\mathrm{Re} = \frac{D_h V}{1000 \nu} \tag{22}$$

where ν = kinematic viscosity, m^2/s.

For standard air, Re can be calculated by

$$\mathrm{Re} = 66.4 D_h V \tag{23}$$

Roughness Factors

The roughness factors ε listed in Table 1 are recommended for use with the Colebrook or Altshul-Tsal equation [Equations (20) and (21), respectively]. These values include not only material, but also duct construction, joint type, and joint spacing (Griggs and Khodabakhsh-Sharifabad 1992). Roughness factors for other materials are presented in Idelchik et al. (1994). Idelchik summarizes roughness factors for 80 materials including metal tubes; conduits made from concrete and cement; and wood, plywood, and glass tubes.

Swim (1978) conducted tests on duct liners of varying densities, surface treatments, transverse joints (workmanship), and methods of attachment to sheet metal ducts. As a result of these tests, Swim recommends for design 4.6 mm for spray-coated liners and 1.5 mm for liners with a facing material cemented onto the air side. In both cases, the roughness factor includes the resistance offered by mechanical fasteners and assumes good joints. Liners cut too short result in (1) loss of thermal performance, (2) possible condensation problems, (3) potential damage to the liner (erosion of the blanket or tearing away from the duct surface), and (4) the collection of dirt and debris and the initiation of biological problems. Liner density does not significantly influence flow resistance.

Manufacturers' data indicate that the absolute roughness for fully extended nonmetallic flexible ducts ranges from 1.1 to 4.6 mm. For fully extended flexible metallic ducts, absolute roughness ranges from 0.1 to 2.1 mm. This range covers flexible duct with the supporting wire exposed to flow or covered by the material. Figure 8 provides a pressure drop correction factor for straight flexible duct when less than fully extended.

Table 1 Duct Roughness Factors

Duct Material	Roughness Category	Absolute Roughness ε, mm
Uncoated carbon steel, clean (Moody 1944) (0.05 mm) PVC plastic pipe (Swim 1982) (0.01 to 0.05 mm) Aluminum (Hutchinson 1953) (0.04 to 0.06 mm)	Smooth	0.03
Galvanized steel, longitudinal seams, 1200 mm joints (Griggs et al. 1987) (0.05 to 0.10 mm) Galvanized steel, continuously rolled, spiral seams, 3000 mm joints (Jones 1979) (0.06 to 0.12 mm) Galvanized steel, spiral seam with 1, 2, and 3 ribs, 3600 mm joints (Griggs et al. 1987) (0.09 to 0.12 mm)	Medium smooth	0.09
Galvanized steel, longitudinal seams, 760 mm joints (Wright 1945) (0.15 mm)	Average	0.15
Fibrous glass duct, rigid Fibrous glass duct liner, air side with facing material (Swim 1978) (1.5 mm)	Medium rough	0.9
Fibrous glass duct liner, air side spray coated (Swim 1978) (4.5 mm) Flexible duct, metallic (1.2 to 2.1 mm when fully extended) Flexible duct, all types of fabric and wire (1.0 to 4.6 mm when fully extended) Concrete (Moody 1944) (1.3 to 3.0 mm)	Rough	3.0

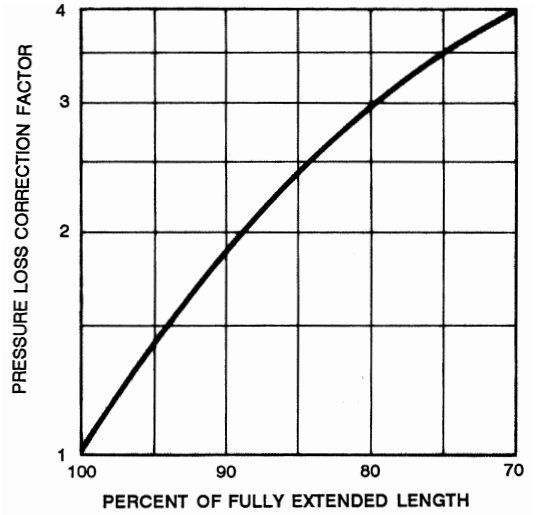

Fig. 8 Correction Factor for Unextended Flexible Duct

Friction Chart

Fluid resistance caused by friction in round ducts can be determined by the friction chart (Figure 9). This chart is based on standard air flowing through round galvanized ducts with beaded slip couplings on 1220 mm centers, equivalent to an absolute roughness of 0.09 mm.

Changes in barometric pressure, temperature, and humidity affect air density, air viscosity, and Reynolds number. No corrections to Figure 9 are needed for (1) duct materials with a medium smooth roughness factor, (2) temperature variations in the order of ±15 K from 20°C, (3) elevations to 500 m, and (4) duct pressures from –5 to +5 kPa relative to the ambient pressure. These individual variations in temperature, elevation, and duct pressure result in duct losses within ±5% of the standard air friction chart.

For duct materials other than those categorized as medium smooth in Table 1, and for variations in temperature, barometric pressure (elevation), and duct pressures (outside the range listed), calculate the friction loss in a duct by the Altshul-Tsal and Darcy equations [Equations (21) and (19), respectively].

Noncircular Ducts

A momentum analysis can relate average wall shear stress to pressure drop per unit length for fully developed turbulent flow in a passage of arbitrary shape but uniform longitudinal cross-sectional area. This analysis leads to the definition of **hydraulic diameter**:

$$D_h = 4A/P \tag{24}$$

where

D_h = hydraulic diameter, mm
A = duct area, mm^2
P = perimeter of cross section, mm

While the hydraulic diameter is often used to correlate noncircular data, exact solutions for laminar flow in noncircular passages show that such practice causes some inconsistencies. No exact solutions exist for turbulent flow. Tests over a limited range of turbulent flow indicated that fluid resistance is the same for equal lengths of duct for equal mean velocities of flow if the ducts have the same ratio of cross-sectional area to perimeter. From a series of experiments using round, square, and rectangular ducts having essentially the same hydraulic diameter, Huebscher (1948) found that each, for most purposes, had the same flow resistance at equal mean velocities. Tests by Griggs and Khodabakhsh-Sharifabad (1992) also indicated that experimental rectangular duct data for airflow over the range typical of HVAC systems can be correlated satisfactorily using Equation (20) together with hydraulic diameter, particularly when a realistic experimental uncertainty is accepted. These tests support using hydraulic diameter to correlate noncircular duct data.

Rectangular Ducts. Huebscher (1948) developed the relationship between rectangular and round ducts that is used to determine size equivalency based on equal flow, resistance, and length. This relationship, Equation (25), is the basis for Table 2.

$$D_e = \frac{1.30(ab)^{0.625}}{(a+b)^{0.250}} \tag{25}$$

where

D_e = circular equivalent of rectangular duct for equal length, fluid resistance, and airflow, mm
a = length one side of duct, mm
b = length adjacent side of duct, mm

To determine equivalent round duct diameter, use Table 2. Equations (21) or (20) and (19) must be used to determine pressure loss.

Flat Oval Ducts. To convert round ducts to spiral flat oval sizes, use Table 3. Table 3 is based on Equation (26) (Heyt and Diaz 1975), the circular equivalent of a flat oval duct for equal airflow, resistance, and length. Equations (21) or (20) and (19) must be used to determine friction loss.

$$D_e = \frac{1.55AR^{0.625}}{P^{0.250}} \tag{26}$$

where AR is the cross-sectional area of flat oval duct defined as

$$AR = (\pi a^2/4) + a(A-a) \tag{27}$$

and the perimeter P is calculated by

$$P = \pi a + 2(A-a) \tag{28}$$

where

P = perimeter of flat oval duct, mm
A = major axis of flat oval duct, mm
a = minor axis of flat oval duct, mm

DYNAMIC LOSSES

Dynamic losses result from flow disturbances caused by duct-mounted equipment and fittings that change the airflow path's direction and/or area. These fittings include entries, exits, elbows, transitions, and junctions. Idelchik et al. (1994) discuss parameters affecting fluid resistance of fittings and presents local loss coefficients in three forms: tables, curves, and equations.

Local Loss Coefficients

The dimensionless coefficient C is used for fluid resistance, because this coefficient has the same value in dynamically similar streams (i.e., streams with geometrically similar stretches, equal Reynolds numbers, and equal values of other criteria necessary for dynamic similarity). The fluid resistance coefficient represents the ratio of total pressure loss to velocity pressure at the referenced cross section:

$$C = \frac{\Delta p_j}{(\rho V^2/2)} = \frac{\Delta p_j}{p_v} \tag{29}$$

where

C = local loss coefficient, dimensionless
Δp_j = total pressure loss, Pa
ρ = density, kg/m^3
V = velocity, m/s
p_v = velocity pressure, Pa

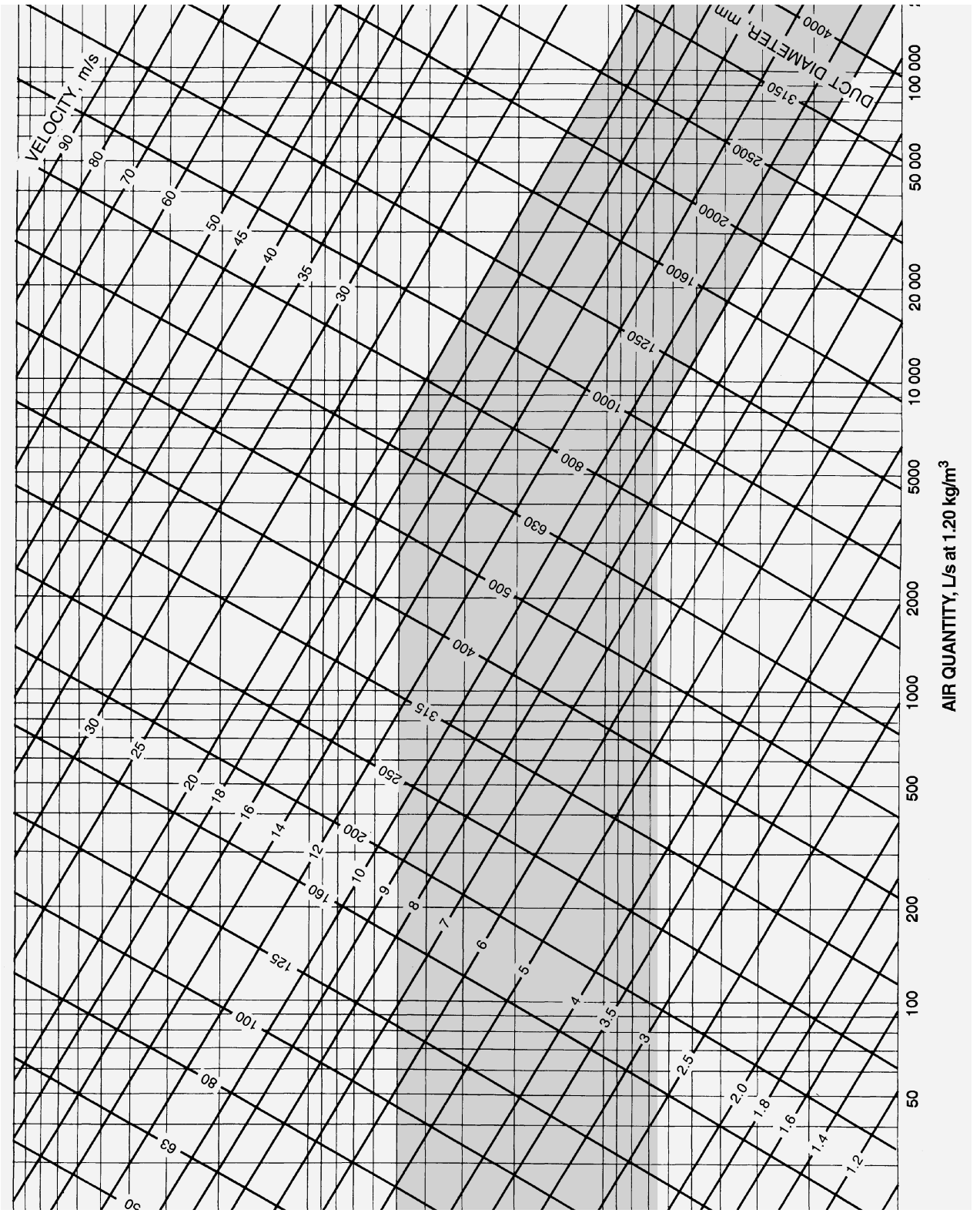

Fig. 9 Friction Chart for Round Duct (ρ = 1.20 kg/m^3 and ε = 0.09 mm)

Table 2 Circular Equivalents of Rectangular Duct for Equal Friction and Capacity[a]

	Length One Side of Rectangular Duct (a), mm																			
Lgth Adj.[b]	100	125	150	175	200	225	250	275	300	350	400	450	500	550	600	650	700	750	800	900
	Circular Duct Diameter, mm																			
100	109																			
125	122	137																		
150	133	150	164																	
175	143	161	177	191																
200	152	172	189	204	219															
225	161	181	200	216	232	246														
250	169	190	210	228	244	259	273													
275	176	199	220	238	256	272	287	301												
300	183	207	229	248	266	283	299	314	328											
350	195	222	245	267	286	305	322	339	354	383										
400	207	235	260	283	305	325	343	361	378	409	437									
450	217	247	274	299	321	343	363	382	400	433	464	492								
500	227	258	287	313	337	360	381	401	420	455	488	518	547							
550	236	269	299	326	352	375	398	419	439	477	511	543	573	601						
600	245	279	310	339	365	390	414	436	457	496	533	567	598	628	656					
650	253	289	321	351	378	404	429	452	474	515	553	589	622	653	683	711				
700	261	298	331	362	391	418	443	467	490	533	573	610	644	677	708	737	765			
750	268	306	341	373	402	430	457	482	506	550	592	630	666	700	732	763	792	820		
800	275	314	350	383	414	442	470	496	520	567	609	649	687	722	755	787	818	847	875	
900	289	330	367	402	435	465	494	522	548	597	643	686	726	763	799	833	866	897	927	984
1000	301	344	384	420	454	486	517	546	574	626	674	719	762	802	840	876	911	944	976	1037
1100	313	358	399	437	473	506	538	569	598	652	703	751	795	838	878	916	953	988	1022	1086
1200	324	370	413	453	490	525	558	590	620	677	731	780	827	872	914	954	993	1030	1066	1133
1300	334	382	426	468	506	543	577	610	642	701	757	808	857	904	948	990	1031	1069	1107	1177
1400	344	394	439	482	522	559	595	629	662	724	781	835	886	934	980	1024	1066	1107	1146	1220
1500	353	404	452	495	536	575	612	648	681	745	805	860	913	963	1011	1057	1100	1143	1183	1260
1600	362	415	463	508	551	591	629	665	700	766	827	885	939	991	1041	1088	1133	1177	1219	1298
1700	371	425	475	521	564	605	644	682	718	785	849	908	964	1018	1069	1118	1164	1209	1253	1335
1800	379	434	485	533	577	619	660	698	735	804	869	930	988	1043	1096	1146	1195	1241	1286	1371
1900	387	444	496	544	590	663	674	713	751	823	889	952	1012	1068	1122	1174	1224	1271	1318	1405
2000	395	453	506	555	602	646	688	728	767	840	908	973	1034	1092	1147	1200	1252	1301	1348	1438
2100	402	461	516	566	614	659	702	743	782	857	927	993	1055	1115	1172	1226	1279	1329	1378	1470
2200	410	470	525	577	625	671	715	757	797	874	945	1013	1076	1137	1195	1251	1305	1356	1406	1501
2300	417	478	534	587	636	683	728	771	812	890	963	1031	1097	1159	1218	1275	1330	1383	1434	1532
2400	424	486	543	597	647	695	740	784	826	905	980	1050	1116	1180	1241	1299	1355	1409	1461	1561
2500	430	494	552	606	658	706	753	797	840	920	996	1068	1136	1200	1262	1322	1379	1434	1488	1589
2600	437	501	560	616	668	717	764	810	853	935	1012	1085	1154	1220	1283	1344	1402	1459	1513	1617
2700	443	509	569	625	678	728	776	822	866	950	1028	1102	1173	1240	1304	1366	1425	1483	1538	1644
2800	450	516	577	634	688	738	787	834	879	964	1043	1119	1190	1259	1324	1387	1447	1506	1562	1670
2900	456	523	585	643	697	749	798	845	891	977	1058	1135	1208	1277	1344	1408	1469	1529	1586	1696

	Length One Side of Rectangular Duct (a), mm																			
Lgth Adj.[b]	1000	1100	1200	1300	1400	1500	1600	1700	1800	1900	2000	2100	2200	2300	2400	2500	2600	2700	2800	2900
	Circular Duct Diameter, mm																			
1000	1093																			
1100	1146	1202																		
1200	1196	1256	1312																	
1300	1244	1306	1365	1421																
1400	1289	1354	1416	1475	1530															
1500	1332	1400	1464	1526	1584	1640														
1600	1373	1444	1511	1574	1635	1693	1749													
1700	1413	1486	1555	1621	1684	1745	1803	1858												
1800	1451	1527	1598	1667	1732	1794	1854	1912	1968											
1900	1488	1566	1640	1710	1778	1842	1904	1964	2021	2077										
2000	1523	1604	1680	1753	1822	1889	1952	2014	2073	2131	2186									
2100	1558	1640	1719	1793	1865	1933	1999	2063	2124	2183	2240	2296								
2200	1591	1676	1756	1833	1906	1977	2044	2110	2173	2233	2292	2350	2405							
2300	1623	1710	1793	1871	1947	2019	2088	2155	2220	2283	2343	2402	2459	2514						
2400	1655	1744	1828	1909	1986	2060	2131	2200	2266	2330	2393	2453	2511	2568	2624					
2500	1685	1776	1862	1945	2024	2100	2173	2243	2311	2377	2441	2502	2562	2621	2678	2733				
2600	1715	1808	1896	1980	2061	2139	2213	2285	2355	2422	2487	2551	2612	2672	2730	2787	2842			
2700	1744	1839	1929	2015	2097	2177	2253	2327	2398	2466	2533	2598	2661	2722	2782	2840	2896	2952		
2800	1772	1869	1961	2048	2133	2214	2292	2367	2439	2510	2578	2644	2708	2771	2832	2891	2949	3006	3061	
2900	1800	1898	1992	2081	2167	2250	2329	2406	2480	2552	2621	2689	2755	2819	2881	2941	3001	3058	3115	3170

[a]Table based on $D_e = 1.30(ab)^{0.625}/(a + b)^{0.25}$.

[b]Length adjacent side of rectangular duct (b), mm.

Table 3 Equivalent Spiral Flat Oval Duct Dimensions

Circular Duct Diameter, mm	Minor Axis (a), mm																
	70	100	125	150	175	200	250	275	300	325	350	375	400	450	500	550	600
	Major Axis (A), mm																
125	205																
140	265	180															
160	360	235	190														
180	475	300	235	200													
200		380	290	245	215												
224		490	375	305	—	240											
250			475	385	325	290											
280				485	410	360	—	285									
315				635	525	—	—	345	325								
355				840	—	580	460	425	395	375							
400				1115	—	760	—	530	490	460	435						
450				1490	—	995	—	675	—	570	535	505					
500						1275	—	845	—	700	655	615	580				
560						1680	—	1085	—	890	820	765	720				
630								1425	—	1150	1050	970	905	810			
710										1505	1370	1260	1165	1025			
800											1800	1645	1515	1315	1170	1065	
900												2165	1985	1705	1500	1350	
1000														2170	1895	1690	
1120															2455	2170	1950
1250																2795	2495

Dynamic losses occur along a duct length and cannot be separated from friction losses. For ease of calculation, dynamic losses are assumed to be concentrated at a section (local) and to exclude friction. Frictional losses must be considered only for relatively long fittings. Generally, fitting friction losses are accounted for by measuring duct lengths from the centerline of one fitting to that of the next fitting. For fittings closely coupled (less than six hydraulic diameters apart), the flow pattern entering subsequent fittings differs from the flow pattern used to determine loss coefficients. Adequate data for these situations are unavailable.

For all fittings, except junctions, calculate the total pressure loss Δp_j at a section by

$$\Delta p_j = C_o p_{v,o} \tag{30}$$

where the subscript o is the cross section at which the velocity pressure is referenced. The dynamic loss is based on the actual velocity in the duct, not the velocity in an equivalent noncircular duct. For the cross section to reference a fitting loss coefficient, refer to Step 4 in the section on HVAC Duct Design Procedures. Where necessary (unequal area fittings), convert a loss coefficient from section o to section i using Equation (31), where V is the velocity at the respective sections.

$$C_i = \frac{C_o}{(V_i/V_o)^2} \tag{31}$$

For converging and diverging flow junctions, total pressure losses through the straight (main) section are calculated as

$$\Delta p_j = C_{c,s} p_{v,c} \tag{32}$$

For total pressure losses through the branch section,

$$\Delta p_j = C_{c,b} p_{v,c} \tag{33}$$

where $p_{v,c}$ is the velocity pressure at the common section c, and $C_{c,s}$ and $C_{c,b}$ are losses for the straight (main) and branch flow paths, respectively, each referenced to the velocity pressure at section c. To convert junction local loss coefficients referenced to straight and branch velocity pressures, use the following equation:

$$C_i = \frac{C_{c,i}}{(V_i/V_c)^2} \tag{34}$$

where

C_i = local loss coefficient referenced to section being calculated (see subscripts), dimensionless
$C_{c,i}$ = straight ($C_{c,s}$) or branch ($C_{c,b}$) local loss coefficient referenced to dynamic pressure at common section, dimensionless
V_i = velocity at section to which C_i is being referenced, m/s
V_c = velocity at common section, m/s

Subscripts:

b = branch
s = straight (main) section
c = common section

The junction of two parallel streams moving at different velocities is characterized by turbulent mixing of the streams, accompanied by pressure losses. In the course of this mixing, an exchange of momentum takes place between the particles moving at different velocities, finally resulting in the equalization of the velocity distributions in the common stream. The jet with higher velocity loses a part of its kinetic energy by transmitting it to the slower moving jet. The loss in total pressure before and after mixing is always large and positive for the higher velocity jet and increases with an increase in the amount of energy transmitted to the lower velocity jet. Consequently, the local loss coefficient, defined by Equation (29), will always be positive. The energy stored in the lower velocity jet increases as a result of mixing. The loss in total pressure and the local loss coefficient can, therefore, also have negative values for the lower velocity jet (Idelchik et al. 1994).

Table 4 Duct Fitting Codes

Fitting Function	Geometry	Category	Sequential Number
S: **S**upply	D: round (**D**iameter)	1. Entries 2. Exits	1,2,3...n
E: **E**xhaust/Return	R: **R**ectangular	3. Elbows 4. Transitions	
C: **C**ommon (supply and return)	F: **F**lat oval	5. Junctions 6. Obstructions 7. Fan and system interactions 8. Duct-mounted equipment 9. Dampers 10. Hoods	

Duct Fitting Database

A duct fitting database, developed by ASHRAE (1994), which includes 228 round and rectangular fittings with the provision to include flat oval fittings, is available from ASHRAE in electronic form with the capability to be linked to duct design programs.

The fittings are numbered (coded) as shown in Table 4. Entries and converging junctions are only in the exhaust/return portion of systems. Exits and diverging junctions are only in supply systems. Equal-area elbows, obstructions, and duct-mounted equipment are common to both supply and exhaust systems. Transitions and unequal-area elbows can be either supply or exhaust fittings. Fitting ED5-1 (see the section on Fitting Loss Coefficients) is an **E**xhaust fitting with a round shape (**D**iameter). The number 5 indicates that the fitting is a junction, and 1 is its sequential number. Fittings SR3-1 and ER3-1 are **S**upply and **E**xhaust fittings, respectively. The R indicates that the fitting is **R**ectangular, and the 3 identifies the fitting as an elbow. Note that the cross-sectional areas at sections 0 and 1 are not equal (see the section on Fitting Loss Coefficients). Otherwise, the elbow would be a **C**ommon fitting such as CR3-6. Additional fittings are reproduced in the section on Fitting Loss Coefficients to support the example design problems (see Table 12 for Example 8; see Table 14 for Example 9).

DUCTWORK SECTIONAL LOSSES

Darcy-Weisbach Equation

Total pressure loss in a duct section is calculated by combining Equations (19) and (29) in terms of Δp, where ΣC is the summation of local loss coefficients within the duct section. Each fitting loss coefficient must be referenced to that section's velocity pressure.

$$\Delta p = \left(\frac{1000 f L}{D_h} + \Sigma C\right)\left(\frac{\rho V^2}{2}\right) \quad (35)$$

FAN-SYSTEM INTERFACE

Fan Inlet and Outlet Conditions

Fan performance data measured in the field may show lower performance capacity than manufacturers' ratings. The most common causes of deficient performance of the fan/system combination are improper outlet connections, nonuniform inlet flow, and swirl at the fan inlet. These conditions alter the aerodynamic characteristics of the fan so that its full flow potential is not realized. One bad connection can reduce fan performance far below its rating. No data have been published that account for the effects of fan inlet and outlet flexible vibration connectors.

Normally, a fan is tested with open inlets and a section of straight duct attached to the outlet (ASHRAE *Standard* 51). This setup results in uniform flow into the fan and efficient static pressure recovery on the fan outlet. If good inlet and outlet conditions are not provided in the actual installation, the performance of the fan suffers. To select and apply the fan properly, these effects must be considered, and the pressure requirements of the fan, as calculated by standard duct design procedures, must be increased.

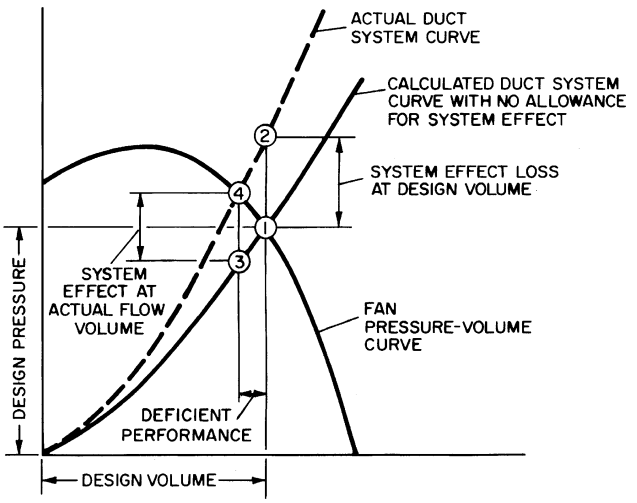

Fig. 10 Deficient System Performance with System Effect Ignored

Figure 10 illustrates deficient fan/system performance. The system pressure losses have been determined accurately, and a fan has been selected for operation at Point 1. However, no allowance has been made for the effect of system connections to the fan on fan performance. To compensate, a fan system effect must be added to the calculated system pressure losses to determine the actual system curve. The point of intersection between the fan performance curve and the actual system curve is Point 4. The actual flow volume is, therefore, deficient by the difference from 1 to 4. To achieve design flow volume, a fan system effect pressure loss equal to the pressure difference between Points 1 and 2 should be added to the calculated system pressure losses, and the fan should be selected to operate at Point 2.

Fan System Effect Coefficients

The system effect concept was formulated by Farquhar (1973) and Meyer (1973); the magnitudes of the system effect, called **system effect factors**, were determined experimentally in the laboratory of the Air Movement and Control Association (AMCA) (Brown 1973, Clarke et al. 1978) and published in their *Publication* 201 (AMCA 1990a). The system effect factors, converted to local loss coefficients, are in the *Duct Fitting Database* (ASHRAE 1994) for both centrifugal and axial fans. Fan system effect coefficients are only an approximation. Fans of different types and even fans of the same type, but supplied by different manufacturers, do not necessarily react to a system in the same way. Therefore, judgment based on experience must be applied to any design.

Fan Outlet Conditions. Fans intended primarily for duct systems are usually tested with an outlet duct in place (ASHRAE *Standard* 51). Figure 11 shows the changes in velocity profiles at various distances from the fan outlet. For 100% recovery, the duct, including transition, must meet the requirements for 100% effective duct length [L_e (Figure 11)], which is calculated as follows:

For $V_o > 13$ m/s,

$$L_e = \frac{V_o\sqrt{A_o}}{4500} \quad (36)$$

For $V_o \leq 13$ m/s,

$$L_e = \frac{\sqrt{A_o}}{350} \quad (37)$$

where

V_o = duct velocity, m/s
L_e = effective duct length, m
A_o = duct area, mm^2

As illustrated by Fitting SR7-1 in the section on Fitting Loss Coefficients, centrifugal fans should not abruptly discharge to the atmosphere. A diffuser design should be selected from Fitting SR7-2 (see the section on Fitting Loss Coefficients) or SR7-3 (see ASHRAE 1994).

Fan Inlet Conditions. For rated performance, air must enter the fan uniformly over the inlet area in an axial direction without prerotation. Nonuniform flow into the inlet is the most common cause of reduced fan performance. Such inlet conditions are not equivalent to a simple increase in the system resistance; therefore, they cannot be treated as a percentage decrease in the flow and pressure from the fan. A poor inlet condition results in an entirely new fan performance. An elbow at the fan inlet, for example Fitting ED7-2 (see the section on Fitting Loss Coefficients), causes turbulence and uneven flow into the fan impeller. The losses due to the fan system effect can be eliminated by including an adequate length of straight duct between the elbow and the fan inlet.

The ideal inlet condition allows air to enter axially and uniformly without spin. A spin in the same direction as the impeller rotation reduces the pressure-volume curve by an amount dependent on the intensity of the vortex. A counterrotating vortex at the inlet slightly increases the pressure-volume curve, but the power is increased substantially.

Inlet spin may arise from a great variety of approach conditions, and sometimes the cause is not obvious. Inlet spin can be avoided by providing an adequate length of straight duct between the elbow and the fan inlet. Figure 12 illustrates some common duct connections that cause inlet spin and includes recommendations for correcting spin.

Fans within plenums and cabinets or next to walls should be located so that air may flow unobstructed into the inlets. Fan performance is reduced if the space between the fan inlet and the enclosure is too restrictive. The system effect coefficients for fans in an enclosure or adjacent to walls are listed under Fitting ED7-1 (see the section on Fitting Loss Coefficients). The manner in which the airstream enters an enclosure in relation to the fan inlets also affects fan performance. Plenum or enclosure inlets or walls that are not symmetrical with the fan inlets cause uneven flow and/or inlet spin.

Testing, Adjusting, and Balancing Considerations

Fan system effects (FSEs) are not only to be used in conjunction with the system resistance characteristics in the fan selection process, but are also applied in the calculations of the results of testing, adjusting, and balancing (TAB) field tests to allow direct comparison to design calculations and/or fan performance data. Fan inlet swirl and the effect on system performance of poor fan inlet and outlet ductwork connections cannot be measured directly. Poor inlet flow patterns affect fan performance within the impeller wheel

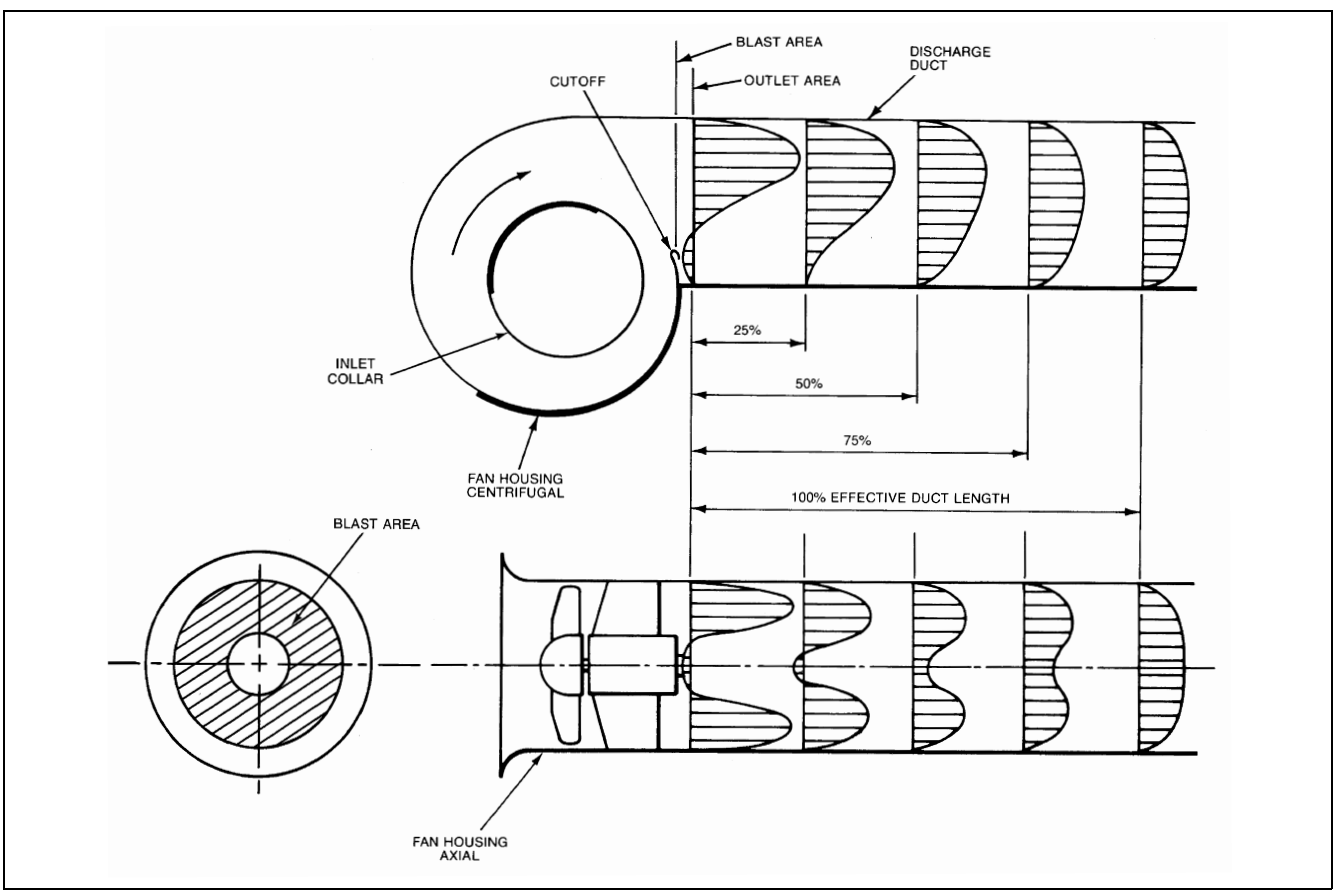

Fig. 11 Establishment of Uniform Velocity Profile in Straight Fan Outlet Duct
(Adapted by permission from AMCA *Publication* 201)

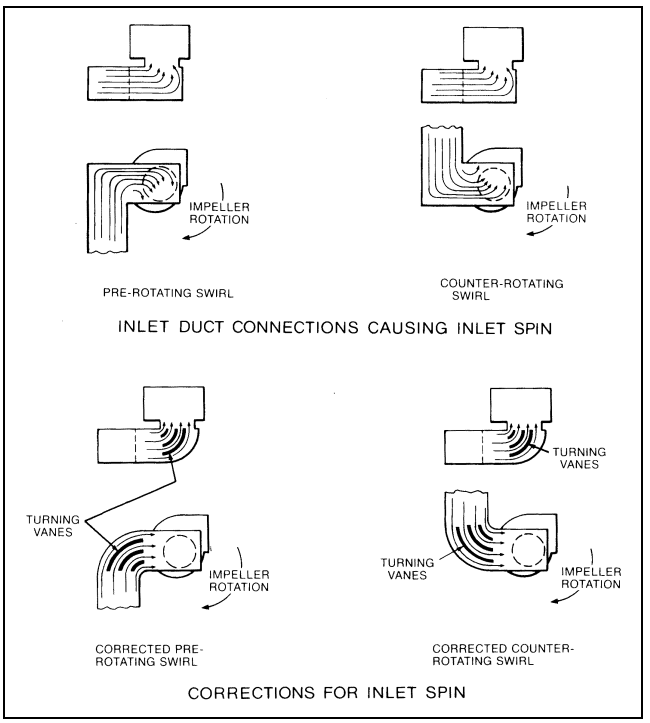

Fig. 12 Inlet Duct Connections Causing Inlet Spin and Corrections for Inlet Spin
(Adapted by permission from AMCA *Publication* 201)

(centrifugal fan) or wheel rotor impeller (axial fan), while the fan outlet system effect is flow instability and turbulence within the fan discharge ductwork.

The static pressure at the fan inlet and the static pressure at the fan outlet may be measured directly in some systems. In most cases, static pressure measurements for use in determining fan total (or static) pressure will not be made directly at the fan inlet and outlet, but at locations a relatively short distance from the fan inlet and downstream from the fan outlet. To calculate fan total pressure for this case from field measurements, use Equation (38), where $\Delta p_{x\text{-}y}$ is the summation of calculated total pressure losses between the fan inlet and outlet sections noted. Plane 3 is used to determine airflow rate. If necessary, use Equation (18) to calculate fan static pressure knowing fan total pressure. For locating measurement planes and calculation procedures, consult AMCA *Publication* 203 (AMCA 1990b).

$$P_t = (p_{s,5} + p_{v,5}) + \Delta p_{2\text{-}5} + \mathrm{FSE}_2 + (p_{s,4} + p_{v,4}) + \Delta p_{4\text{-}1} + \mathrm{FSE}_1 + \mathrm{FSE}_{1,sw} \quad (38)$$

where

P_t = fan total pressure, Pa
p_s = static pressure, Pa
p_v = velocity pressure, Pa
FSE = fan system effect, Pa
$\Delta p_{x\text{-}y}$ = summarization of total pressure losses between planes x and y, Pa

Subscripts (numerical subscripts same as used by AMCA *Publication* 203):

1 = fan inlet
2 = fan outlet
3 = plane of airflow measurement
4 = plane of static pressure measurement upstream of fan
5 = plane of static pressure measurement downstream of fan
sw = swirl

DUCT SYSTEM DESIGN

DESIGN CONSIDERATIONS

Space Pressure Relationships

Space pressure is determined by fan location and duct system arrangement. For example, a supply fan that pumps air into a space increases space pressure; an exhaust fan reduces space pressure. If both supply and exhaust fans are used, space pressure depends on the relative capacity of the fans. Space pressure is positive if supply exceeds exhaust and negative if exhaust exceeds supply (Osborne 1966). System pressure variations due to wind can be minimized or eliminated by careful selection of intake air and exhaust vent locations (Chapter 16).

Fire and Smoke Management

Because duct systems can convey smoke, hot gases, and fire from one area to another and can accelerate a fire within the system, fire protection is an essential part of air-conditioning and ventilation system design. Generally, fire safety codes require compliance with the standards of national organizations. NFPA *Standard* 90A examines fire safety requirements for (1) ducts, connectors, and appurtenances; (2) plenums and corridors; (3) air outlets, air inlets, and fresh air intakes; (4) air filters; (5) fans; (6) electric wiring and equipment; (7) air-cooling and -heating equipment; (8) building construction, including protection of penetrations; and (9) controls, including smoke control.

Fire safety codes often refer to the testing and labeling practices of nationally recognized laboratories, such as Factory Mutual and Underwriters Laboratories (UL). The *Building Materials Directory* compiled by UL lists fire and smoke dampers that have been tested and meet the requirements of UL *Standards* 555 and 555S. This directory also summarizes maximum allowable sizes for individual dampers and assemblies of these dampers. Fire dampers are 1.5 h or 3 h fire-rated. Smoke dampers are classified by (1) temperature degradation [ambient air or high temperature (120°C minimum)] and (2) leakage at 250 Pa and 1000 Pa pressure difference (2 kPa and 3 kPa classification optional). Smoke dampers are tested under conditions of maximum airflow. UL's *Fire Resistance Directory* lists the fire resistance of floor/roof and ceiling assemblies with and without ceiling fire dampers.

For a more detailed presentation of fire protection, see Chapter 51 of the 1999 *ASHRAE Handbook—Applications* and the NFPA *Fire Protection Handbook*.

Duct Insulation

In all new construction (except low-rise residential buildings), air-handling ducts and plenums installed as part of an HVAC air distribution system should be thermally insulated in accordance with Section 6.2.4.2 of ASHRAE *Standard* 90.1. Duct insulation for new low-rise residential buildings should be in compliance with ASHRAE *Standard* 90.2. Existing buildings should meet the requirements of ASHRAE *Standard* 100. The insulation thicknesses in these standards are minimum values. Economic and thermal considerations may justify higher insulation levels. Additional insulation, vapor retarders, or both may be required to limit vapor transmission and condensation.

Duct heat gains or losses must be known for the calculation of supply air quantities, supply air temperatures, and coil loads (see Chapter 29 of this volume and Chapter 2 of the 2000 *ASHRAE Handbook—Systems and Equipment*). To estimate duct heat transfer and entering or leaving air temperatures, use the following equations:

$$q_l = \frac{UPL}{1000}\left[\left(\frac{t_e + t_l}{2}\right) - t_a\right] \quad (39)$$

$$t_e = \frac{t_l(y+1) - 2t_a}{(y-1)} \quad (40)$$

$$t_l = \frac{t_e(y-1) + 2t_a}{(y+1)} \quad (41)$$

where

q_l = heat loss/gain through duct walls, W (negative for heat gain)
U = overall heat transfer coefficient of duct wall, W/(m^2·K)
P = perimeter of bare or insulated duct, mm
L = duct length, m
t_e = temperature of air entering duct, °C
t_l = temperature of air leaving duct, °C
t_a = temperature of air surrounding duct, °C
$y = 2.0AV\rho c_p/UPL$ for rectangular ducts
$= 0.5DV\rho c_p/UL$ for round ducts
A = cross-sectional area of duct, mm^2
V = average velocity, m/s
ρ = density of air, kg/m^3
c_p = specific heat of air, kJ/(kg·K)
D = diameter of duct, mm

Use Figure 13A to determine U-factors for insulated and uninsulated ducts. Lauvray (1978) has shown the effects of (1) compressing insulation wrapped externally on sheet metal ducts and (2) insulated flexible ducts with air-porous liners. For a 50 mm thick, 12 kg/m^3 fibrous glass blanket compressed 50% during installation, the heat transfer rate increases approximately 20% (see Figure 13A). Pervious flexible duct liners also influence heat transfer significantly (see Figure 13B). At 12.7 m/s, the pervious liner U-factor is 1.87 W/(m^2·K); for an impervious liner, U = 1.08 W/(m^2·K).

Example 6. A 20 m length of 600 mm by 900 mm uninsulated sheet metal duct, freely suspended, conveys heated air through a space maintained above freezing at 5°C. Based on heat loss calculations for the heated zone, 8100 L/s of standard air [c_p = 1.006 kJ/(kg·K)] at a supply air temperature of 50°C is required. The duct is connected directly to the heated zone. Determine the temperature of the air entering the duct and the duct heat loss.

Solution: Calculate duct velocity using Equation (10):

$$V = \frac{1000 \times 8100 \text{ L/s}}{600 \text{ mm} \times 900 \text{ mm}} = 15 \text{ m/s}$$

Calculate entering air temperature using Equation (40):

U = 4.16 W/(m^2 · K) (from Figure 13A)
P = 2(600 + 900) = 3000 mm

$$y = \frac{2.0(600\text{ mm})(900\text{ mm})(15\text{ m/s})(1.204\text{ kg/m}^3)(1.006)}{4.16\text{ W/(m}^2\cdot\text{K)} \times 3000\text{ mm} \times 20\text{ m}} = 78.6$$

$$t_e = \frac{50°\text{C}(78.6+1) - (2 \times 5°\text{C})}{(78.6-1)} = 51.2°\text{C}$$

Calculate duct heat loss using Equation (39):

$$q_l = \frac{4.16\text{ W/(m}^2\cdot\text{K)} \times 3000\text{ mm} \times 20\text{ m}}{1000} \times \left[\frac{51.2°\text{C} + 50°\text{C}}{2} - 5°\text{C}\right]$$

$$= 11\,400 \text{ W}$$

Example 7. Same as Example 6, except the duct is insulated externally with 50 mm thick fibrous glass with a density of 12 kg/m^3. The insulation is wrapped with 0% compression.

Solution: All values except U remain the same as in Example 6. From Figure 13A, U = 0.83 W/(m^2·K) at 15 m/s. Therefore,

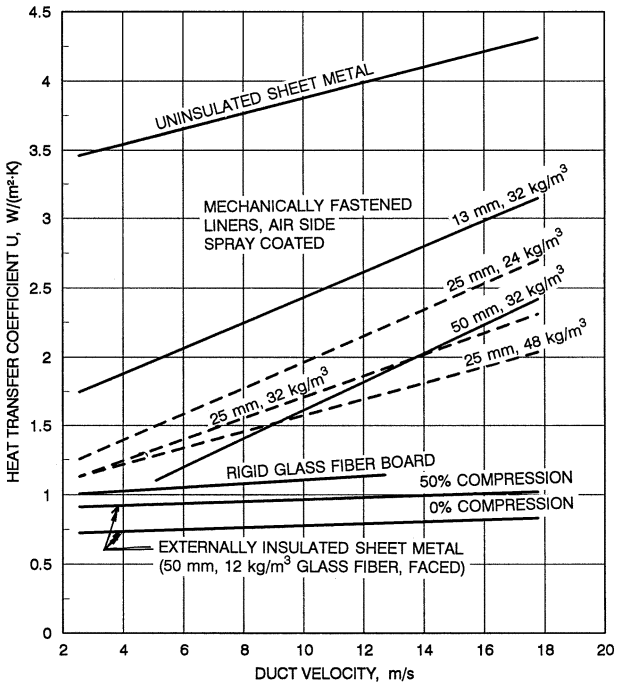

A. RIGID DUCTS

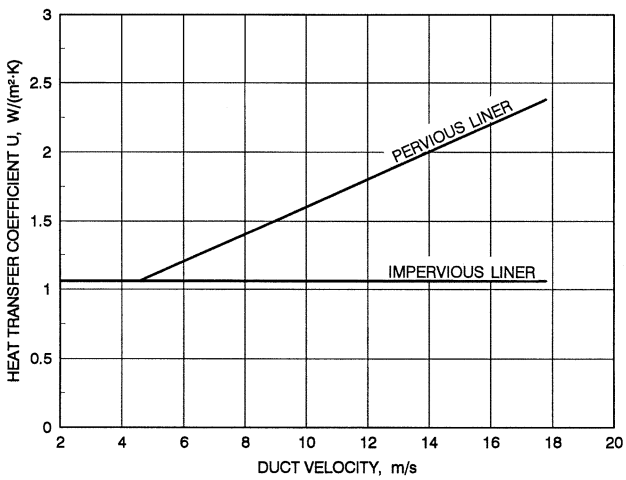

B. INSULATED FLEXIBLE DUCTS

Fig. 13 Duct Heat Transfer Coefficients

y = 394
t_e = 50.2°C
q_l = 2250 W

Insulating this duct reduces heat loss to 20% of the uninsulated value.

Duct System Leakage

Leakage in all unsealed ducts varies considerably with the fabricating machinery used, the methods for assembly, and installation workmanship. For sealed ducts, a wide variety of sealing methods and products exists. Sealed and unsealed duct leakage tests (AISI/SMACNA 1972, ASHRAE/SMACNA/TIMA 1985, Swim and Griggs 1995) have confirmed that longitudinal seam, transverse joint, and assembled duct leakage can be represented by Equation (42) and that for the same construction, leakage is not significantly different in the negative and positive modes. A range of leakage rates

Table 5 Unsealed Longitudinal Seam Leakage, Metal Ducts

Type of Duct/Seam	Leakage, L/s per metre Seam Length[a] Range	Average
Rectangular		
Pittsburgh lock	0.015 to 0.87	0.25
Button punch snaplock	0.015 to 0.25	0.10
Round		
Snaplock	0.06 to 0.22	0.17
Grooved	0.17 to 0.28	0.19

[a]Leakage rate is at 250 Pa static pressure.

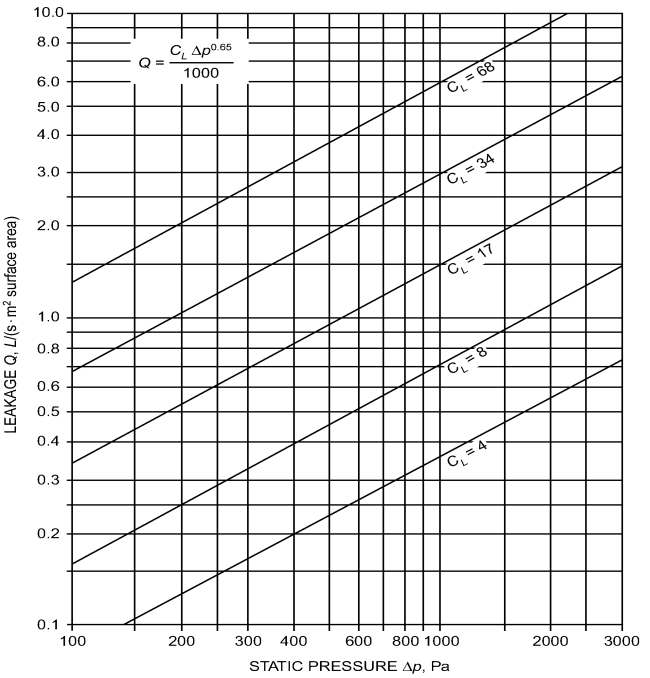

Fig. 14 Duct Leakage Classifications

for longitudinal seams commonly used in the construction of metal ducts is presented in Table 5. Longitudinal seam leakage for unsealed or unwelded metal ducts is about 10 to 15% of total duct leakage.

$$Q = C\Delta p_s^{\ N} \tag{42}$$

where

Q = duct leakage rate, L/s per m^2
C = constant reflecting area characteristics of leakage path
Δp_s = static pressure differential from duct interior to exterior, Pa
N = exponent relating turbulent or laminar flow in leakage path

Analysis of the AISI/ASHRAE/SMACNA/TIMA data resulted in the categorization of duct systems into **leakage classes** C_L based on Equation (43), where the exponent N is assumed to be 0.65. A selected series of leakage classes based on Equation (43) is shown in Figure 14.

$$C_L = \frac{1000Q}{\Delta p_s^{\ 0.65}} \tag{43}$$

where

Q = leakage rate, L/s per m^2 (surface area)
C_L = leakage class, mL/s·m^2 at 1 Pa

Table 6 Duct Leakage Classification[a]

Duct Type	Sealed[b,c] Predicted Leakage Class C_L	Sealed[b,c] Leakage Rate, L/(s·m^2) at 250 Pa	Unsealed[c] Predicted Leakage Class C_L	Unsealed[c] Leakage Rate, L/(s·m^2) at 250 Pa
Metal (flexible excluded)				
Round and flat oval	4	0.14	42 (8 to 99)	1.5 (0.3 to 3.6)
Rectangular				
≤ 500 Pa (both positive and negative pressures)	17	0.62	68 (17 to 155)	2.5 (0.6 to 5.6)
> 500 and ≤ 2500 Pa (both positive and negative pressures)	8	0.29	68 (17 to 155)	2.5 (0.6 to 5.6)
Flexible				
Metal, Aluminum	11	0.40	42 (17 to 76)	1.5 (0.6 to 2.8)
Nonmetal	17	0.62	30 (6 to 76)	1.5 (0.2 to 2.8)
Fibrous glass				
Round	4	0.14	na	na
Rectangular	8	0.29	na	na

[a]The leakage classes listed in this table are averages based on tests conducted by AISI/SMACNA (1972), ASHRAE/SMACNA/TIMA (1985), and Swim and Griggs (1995).
[b]The leakage classes listed in the sealed category are based on the assumptions that for metal ducts, all transverse joints, seams, and openings in the duct wall are sealed at pressures over 750 Pa, that transverse joints and longitudinal seams are sealed at 500 and 750 Pa, and that transverse joints are sealed below 500 Pa. Lower leakage classes are obtained by careful selection of joints and sealing methods.
[c]Leakage classes assigned anticipate about 0.82 joints per metre of duct. For systems with a high fitting to straight duct ratio, greater leakage occurs in both the sealed and unsealed conditions.

Table 6 is a forecast of the leakage class attainable for commonly used duct construction and sealing practices. Connections of ducts to grilles, diffusers, and registers are not represented in the test data. Leakage classes listed are for a specific duct type, not a system with a variety of duct types, access doors, and other duct-mounted equipment. The designer is responsible for assigning acceptable system leakage rates. It is recommended that this be accomplished by using Table 7 as a guideline to specify a ductwork leakage class or by specifying a duct seal level as recommended by Table 8. The designer should take into account attainable leakage rates by duct type and the fact that casings of volume-controlling air terminal units may leak 1 to 2% of their maximum flow. The effects of such leakage should be anticipated, if allowed, and the ductwork should not be expected to compensate for equipment leakage. When a system leakage class is specified by a designer, it is a performance specification that should not be compromised by prescriptive sealing. A portion of a system may exceed its leakage class if the aggregate system leakage meets the allowable rate. Table 9 can be used to estimate the system percent leakage based on the system design leakage class and system duct surface area. Table 9 is predicated on assessment at an average of upstream and downstream pressures because use of the highest pressure alone could indicate an artificially high rate. When several duct pressure classifications occur in a system, ductwork in each pressure class should be evaluated independently to arrive at an aggregate leakage for the system.

Leakage tests should be conducted in compliance with SMACNA's *HVAC Air Duct Leakage Test Manual* (1985) to verify the intent of the designer and the workmanship of the the installing contractor. Leakage tests used to confirm leakage class should be conducted at the pressure class for which the duct is constructed. Leakage testing is also addressed in ASHRAE *Standard* 90.1.

Limited performance standards for metal duct sealants and tapes exist. For guidance in their selection and use refer to SMACNA's *HVAC Duct Construction Standards* (1995). Fibrous glass ducts and their closure systems are covered by UL *Standards* 181and 181A.

Table 7 Recommended Ductwork Leakage Class by Duct Type

Duct Type	Leakage Class	Leakage Rate, L/(s·m²) at 250 Pa
Metal		
Round	4	0.14
Flat oval	4	0.14
Rectangular	8	0.29
Flexible	8	0.29
Fibrous glass		
Round	4	0.14
Rectangular	8	0.29

Table 8A Recommended Duct Seal Levels[a]

	Duct Type			
	Supply			
Duct Location	≤ 500 Pa	> 500 Pa	Exhaust	Return
Outdoors	A	A	A	A
Unconditioned spaces	B	A	B	B
Conditioned spaces (concealed ductwork)	C	B	B	C
Conditioned spaces (exposed ductwork)	A	A	B	B

[a]See Table 8B for definition of seal level.

Table 8B Duct Seal Levels

Seal Level	Sealing Requirements[a]
A	All transverse joints, longitudinal seams, and duct wall penetrations
B	All transverse joints and longitudinal seams
C	Transverse joints only

[a]Transverse joints are connections of two duct or fitting elements oriented perpendicular to flow. Longitudinal seams are joints oriented in the direction of airflow. Duct wall penetrations are openings made by screws, non-self-sealing fasteners, pipe, tubing, rods, and wire. Round and flat oval spiral lock seams need not be sealed prior to assembly, but may be coated after assembly to reduce leakage. All other connections are considered transverse joints, including but not limited to spin-ins, taps and other branch connections, access door frames, and duct connections to equipment.

For fibrous glass duct construction standards consult NAIMA (1997) and SMACNA (1992). Flexible duct performance and installation standards are covered by UL 181, UL 181B and ADC (1996). Soldered or welded duct construction is necessary where sealants are not suitable. Sealants used on exterior ducts must be resistant to weather, temperature cycles, sunlight, and ozone.

Shaft and compartment pressure changes affect duct leakage and are important to health and safety in the design and operation of contaminant and smoke control systems. Shafts should not be used for supply, return, and/or exhaust air without accounting for their leakage rates. Airflow around buildings, building component leakage, and the distribution of inside and outside pressures over the height of a building, including shafts, are discussed in Chapters 16 and 26. Smoke management system design is covered in Chapter 51 of the 1999 *ASHRAE Handbook—Applications* and in Klote and Milke (1992).

System Component Design Velocities

Table 10 summarizes face velocities for HVAC components in built-up systems. In most cases, the values are abstracted from pertinent chapters in the 2000 *ASHRAE Handbook—Systems and Equipment*; final selection of the components should be based on data in these chapters or from manufacturers.

Table 9 Leakage as Percentage of Airflow[a,b]

Leakage Class	System L/s per m² Duct Surface[c]	Static Pressure, Pa					
		125	250	500	750	1000	1500
68	10	15	24	38	49	59	77
	12.7	12	19	30	39	47	62
	15	10	16	25	33	39	51
	20	7.7	12	19	25	30	38
	25	6.1	9.6	15	20	24	31
34	10	7.7	12	19	25	30	38
	12.7	6.1	9.6	15	20	24	31
	15	5.1	8.0	13	16	20	26
	20	3.8	6.0	9.4	12	15	19
	25	3.1	4.8	7.5	9.8	12	15
17	10	3.8	6	9.4	12	15	19
	12.7	3.1	4.8	7.5	9.8	12	15
	15	2.6	4.0	6.3	8.2	9.8	13
	20	1.9	3.0	4.7	6.1	7.4	9.6
	25	1.5	2.4	3.8	4.9	5.9	7.7
8	10	1.9	3	4.7	6.1	7.4	9.6
	12.7	1.5	2.4	3.8	4.9	5.9	7.7
	15	1.3	2.0	3.1	4.1	4.9	6.4
	20	1.0	1.5	2.4	3.1	3.7	4.8
	25	0.8	1.2	1.9	2.4	3.0	3.8
4	10	1.0	1.5	2.4	3.1	3.7	4.8
	12.7	0.8	1.2	1.9	2.4	3.0	3.8
	15	0.6	1.0	1.6	2.0	2.5	3.2
	20	0.5	0.8	1.3	1.6	2.0	2.6
	25	0.4	0.6	0.9	1.2	1.5	1.9

[a]Adapted with permission from HVAC *Air Duct Leakage Test Manual* (SMACNA 1985, Appendix A).
[b]Percentage applies to the airflow entering a section of duct operating at an assumed pressure equal to the average of the upstream and downstream pressures.
[c]The ratios in this column are typical of fan volumetric flow rate divided by total system surface. Portions of the systems may vary from these averages.

Louvers require special treatment since the blade shapes, angles, and spacing cause significant variations in louver-free area and performance (pressure drop and water penetration). Selection and analysis should be based on test data obtained in accordance with AMCA *Standard* 500-L (1999). This standard presents both pressure drop and water penetration test procedures and a uniform method for calculating the free area of a louver. Tests are conducted on a 1220 mm square louver with the frame mounted flush in the wall. For the water penetration tests, the rainfall is 100 mm/h, no wind, and the water flow down the wall is 0.05 L/s per linear metre of louver width.

Use Figure 15 for preliminary sizing of air intake and exhaust louvers. For air quantities greater than 3300 L/s per louver, the air intake gross louver openings are based on 2 m/s; for exhaust louvers, 2.5 m/s is used for air quantities of 2400 L/s per louver and greater. For air quantities less than these, refer to Figure 15. These criteria are presented on a per louver basis (i.e., each louver in a bank of louvers) to include each louver frame. Representative production-run louvers were used in establishing Figure 15, and all data used in that analysis are based on AMCA standard tests. For louvers larger than 1.5 m², the free areas are greater than 45%, while for louvers less than 1.5 m², the free areas are less than 45%. Unless specific louver data are analyzed, no louver should have a face area less than 0.4 m². If debris collection on the screen of an intake louver is possible, or if louvers are located at grade with adjacent pedestrian traffic, louver face velocity should not exceed 0.5 m/s.

System and Duct Noise

The major sources of noise from air-conditioning systems are diffusers, grilles, fans, ducts, fittings, and vibrations. Chapter 46 of the 1999 *ASHRAE Handbook—Applications* discusses sound control for each of these sources. Sound control for terminal devices

Table 10 Typical Design Velocities for HVAC Components

Duct Element	Face Velocity, m/s
LOUVERS[a]	
Intake	
3300 L/s and greater	2
Less than 3300 L/s	See Figure 15
Exhaust	
2400 L/s and greater	2.5
Less than 2400 L/s	See Figure 15
FILTERS[b]	
Panel filters	
Viscous impingement	1 to 4
Dry-type, extended-surface	
Flat (low efficiency)	Duct velocity
Pleated media (intermediate efficiency)	Up to 3.8
HEPA	1.3
Renewable media filters	
Moving-curtain viscous impingement	2.5
Moving-curtain dry media	1
Electronic air cleaners	
Ionizing type	0.8 to 1.8
HEATING COILS[c]	
Steam and hot water	2.5 to 5 1 min., 8 max.
Electric	
Open wire	Refer to mfg. data
Finned tubular	Refer to mfg. data
DEHUMIDIFYING COILS[d]	2 to 3
AIR WASHERS[e]	
Spray type	1.5 to 3.0
Cell type	Refer to mfg. data
High-velocity spray type	6 to 9

[a]Based on assumptions presented in text.
[b]Abstracted from Chapter 24, 2000 *ASHRAE Handbook—Systems and Equipment*.
[c]Abstracted from Chapter 23, 2000 *ASHRAE Handbook—Systems and Equipment*.
[d]Abstracted from Chapter 21, 2000 *ASHRAE Handbook—Systems and Equipment*.
[e]Abstracted from Chapter 19, 2000 *ASHRAE Handbook—Systems and Equipment*.

consists of selecting devices that meet the design goal under all operating conditions and installing them properly so that no additional sound is generated. The sound power output of a fan is determined by the type of fan, airflow, and pressure. Sound control in the duct system requires proper duct layout, sizing, and provision for installing duct attenuators, if required. The noise generated by a system increases with both duct velocity and system pressure. Chapter 46 of the 1999 *ASHRAE Handbook—Applications* presents methods for calculating required sound attenuation.

Testing and Balancing

Each air duct system should be tested, adjusted, and balanced. Detailed procedures are given in Chapter 36 of the 1999 *ASHRAE Handbook—Applications*. To properly determine fan total (or static) pressure from field measurements taking into account fan system effect, refer to the section on Fan-System Interface. Equation (38) allows direct comparison of system resistance to design calculations and/or fan performance data. It is important that the system effect magnitudes be known prior to testing. If necessary, use Equation (18) to calculate fan static pressure knowing fan total pressure [Equation (38)]. For TAB calculation procedures of numerous fan/system configurations encountered in the field, refer to AMCA *Publication* 203 (AMCA 1990b).

DUCT DESIGN METHODS

Duct design methods for HVAC systems and for exhaust systems conveying vapors, gases, and smoke are the equal friction method, the static regain method, and the T-method. The section on Industrial Exhaust System Duct Design presents the design criteria and procedures for exhaust systems conveying particulates. Equal friction and static regain are nonoptimizing methods, while the T-method is a practical optimization method introduced by Tsal et al. (1988).

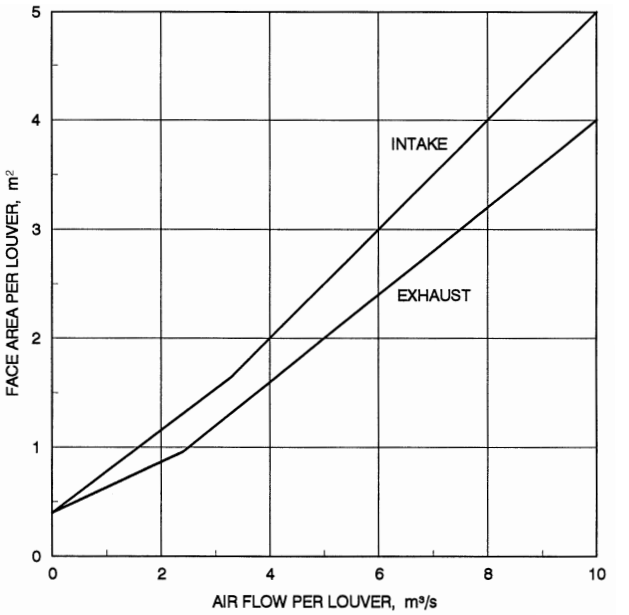

Parameters Used to Establish Figure	Intake Louver	Exhaust Louver
Minimum free area (1220 mm square test section), %	45	45
Water penetration, μL/(m²·s)	Negligible (less than 0.6)	na
Maximum static pressure drop, Pa	35	60

Fig. 15 Criteria for Louver Sizing

To ensure that system designs are acoustically acceptable, noise generation should be analyzed and sound attenuators and/or acoustically lined duct provided where necessary. Dampers must be installed throughout systems designed by equal friction, static regain, and the T-method because inaccuracies are introduced into these design methods by duct size round-off and the effect of close-coupled fittings on the total pressure loss calculations.

Equal Friction Method

In the equal friction method, ducts are sized for a constant pressure loss per unit length. The shaded area of the friction chart (Figure 9) is the suggested range of friction rate and air velocity. When energy cost is high and installed ductwork cost is low, a low friction rate design is more economical. For low energy cost and high duct cost, a higher friction rate is more economical. After initial sizing, calculate the total pressure loss for all duct sections, and then resize sections to balance pressure losses at each junction.

Static Regain Method

The objective of the static regain method is to obtain the same static pressure at diverging flow junctions by changing downstream duct sizes. This design objective can be developed by rearranging Equation (7a) and setting $p_{s,2}$ equal to $p_{s,1}$ (neglecting thermal gravity effect term). Thus,

$$p_{s,1} - p_{s,2} = \Delta p_{t,1\text{-}2} - \left[\frac{\rho V_1^2}{2} - \frac{\rho V_2^2}{2}\right] \quad (44)$$

and

$$\Delta p_{t,1\text{-}2} = \frac{\rho V_1^2}{2} - \frac{\rho V_2^2}{2} \quad (45)$$

where $\Delta p_{t,1\text{-}2}$ is the total pressure loss from upstream of junction 1 to upstream of junction 2, or the terminal of section 2. The immediate downstream duct size that satisfies Equation (45) is determined by iteration.

To start the design of a system, a maximum velocity is selected for the root section (duct section upstream and/or downstream of a fan). In Figure 17, section 6 is the root for the return air subsystem. Section 19 is the root for the supply air subsystem. The shaded area on the friction chart (Figure 9) is the suggested range of air velocity. When energy cost is high and installed ductwork cost is low, a lower initial velocity is more economical. For low energy cost and high duct cost, a higher velocity is more economical. All other sections, except terminal sections, are sized iteratively by Equation (45). In Figure 17, terminal sections are 1, 2, 4, 7, 8, 11, 12, 15, and 16. Knowing the terminal static pressure requirements, Equation (45) is used to calculate the duct size of terminal sections. If the terminal is an exit fitting rather than a register, diffuser, or terminal box, the static pressure at the exit of the terminal section is zero.

The classical static regain method (Carrier Corporation 1960, Chun-Lun 1983) is based on Equation (46), where R is the static pressure regain factor, and Δp_r is the static pressure regain between junctions.

$$\Delta p_r = R\left(\frac{\rho V_1^2}{2} - \frac{\rho V_2^2}{2}\right) \quad (46)$$

Typically R-values ranging from 0.5 to 0.95 have been used. Tsal and Behls (1988) show that this uncertainty exists because the splitting of mass at junctions and the dynamic (fitting) losses between junctions are ignored. The classical static regain method using an R-value should not be used because R is not predictable.

T-Method Optimization

T-method optimization (Tsal et al. 1988) is a dynamic programming procedure based on the tee-staging idea used by Bellman (1957), except that phase level vector tracing is eliminated by optimizing locally at each stage. This modification reduces the number of calculations but requires iteration.

Optimization Basis. The objective function, Equation (47), includes both initial system cost and the present worth of energy. Hours of operation, annual escalation and interest rates, and amortization period are also required for optimization.

$$E = E_p(\text{PWEF}) + E_s \quad (47)$$

where

E = present worth owning and operating cost
E_p = first year energy cost
E_s = initial cost
PWEF = present worth escalation factor (Smith 1968), dimensionless

Energy cost is determined by

$$E_p = Q_f\left[\frac{(E_d + E_c T)}{10^6 \eta_f \eta_e}\right] P_t \quad (48)$$

where

Q_f = fan airflow rate, L/s
E_c = unit energy cost, cost/kWh
E_d = energy demand cost, cost/kW
T = system operating time, h/year
P_t = fan total pressure, Pa
η_f = fan total efficiency, decimal
η_e = motor-drive efficiency, decimal

Energy cost depends on both applicable energy rates E_c and demand cost E_d. Since the difference in fan pressure between an optimized and a nonoptimized system is a small part of demand, it is usually neglected. Initial cost includes ducts and HVAC equipment, which is primarily the central handling unit. The cost of duct systems is given by the following equations:

$$Round \qquad E_s = S_d \pi DL/1000 \quad (49)$$

$$Rectangular \qquad E_s = 2S_d(H + W)L/1000 \quad (50)$$

where

S_d = unit ductwork cost/m^2 (including material and labor)
H = duct height, mm
W = duct width, mm
L = duct length, m

The cost of space required by ducts and equipment is another important factor of duct optimization. Including this cost reduces the size of ducts, thereby increasing energy consumption. Because the space available for ductwork is usually not used for anything else, its cost is ignored.

Both electrical energy rates and ductwork costs vary widely, by a factor of up to eight times for industrial users (DOE). Black iron rectangular ductwork can cost about 3.9 times that of spiral ductwork (Wendes 1989). Combining these ratios yields a factor of 30 to 1 based on locale and type of ductwork. Therefore, a great potential exists for reducing duct system life-cycle cost due to energy and ductwork cost variations.

The following constraints are necessary for duct optimization (Tsal and Adler 1987):

- *Continuity.* For each node, the flow in equals the flow out.
- *Pressure balancing*. The total pressure loss in each path must equal the fan total pressure; or, in effect, at any junction, the total pressure loss for all paths is the same.
- *Nominal duct size*. Ducts are constructed in discrete, nominal sizes. Each diameter of a round duct or height and width of a rectangular duct is rounded to the nearest increment, usually 25 or 50 mm. If a lower nominal size is selected, the initial cost decreases, but the pressure loss increases and may exceed the fan pressure. If the higher nominal size is selected, the opposite is true—the initial cost increases, but the section pressure loss decreases. However, this lower pressure at one section may allow smaller ducts to be selected for sections that follow. Therefore, optimization must consider size rounding.
- *Air velocity restriction*. The maximum allowable velocity is an acoustic limitation (ductwork regenerated noise).
- *Construction restriction*. Architectural limits may restrict duct sizes. If air velocity or construction constraints are violated during an iteration, a duct size must be calculated. The pressure loss calculated for this preselected duct size is considered a fixed loss.

Calculation Procedure. The T-method comprises the following major procedures:

- *System condensing*. This procedure condenses a multiple-section duct system into a single imaginary duct section with identical hydraulic characteristics and the same owning cost as the entire system. By Equation (1.41) in Tsal et al. (1988), two or more converging or diverging sections and the common section at a junction can be replaced by one condensed section. By applying this equation from junction to junction in the direction to the root section (fan), the entire supply and return systems can be condensed into one section (a single resistance).
- *Fan selection*. From the condensed system, the ideal optimum fan total pressure P_t^{opt} is calculated and used to select a fan. If a fan with a different pressure is selected, its pressure P^{opt} is considered optimum.
- *System expansion*. The expansion process distributes the available fan pressure P^{opt} throughout the system. Unlike the condensing procedure, the expansion procedure starts at the root section and continues in the direction of the terminals.

Economic Analysis. Tsal et al. (1988) describe the calculation procedure and include an economic analysis of the T-method.

T-Method Simulation

T-method simulation, also developed by Tsal et al. (1990), determines the flow in each duct section of an existing system with a known operating fan performance curve. The simulation version of the T-method converges very efficiently. Usually three iterations are sufficient to obtain a solution with a high degree of accuracy.

Calculation procedure. The simulation version of the T-method includes the following major procedures:

- *System condensing*. This procedure condenses a branched tee system into a single imaginary duct section with identical hydraulic characteristics. Two or more converging or diverging sections and the common section at a junction can be replaced by one condensed section [by Equation (18) in Tsal et al. (1990)]. By applying this equation from junction to junction in the direction to the root section (fan), the entire system, including supply and return subsystems, can be condensed into one imaginary section (a single resistance).
- *Fan operating point*. This step determines the system flow and pressure by locating the intersection of the fan performance and system curves, where the system curve is represented by the imaginary section from the last step.
- *System expansion*. Knowing system flow and pressure, the previously condensed imaginary duct section is expanded into the original system with flow distributed in accordance with the ratio of pressure losses calculated in the system condensing step.

Simulation Applications. The need for duct system simulation appears in many HVAC problems. In addition to the following concerns that can be clarified by simulation, the T-method is an excellent design tool for simulating the flow distribution within a system with various modes of operation.

- Flow distribution in a variable air volume (VAV) system due to terminal box flow diversity
- Airflow redistribution due to HVAC system additions and/or modifications
- System airflow analysis for partially occupied buildings
- Necessity to replace fans and/or motors when retrofitting an air distribution system
- Multiple-fan system operating condition when one or more fans shut down
- Pressure differences between adjacent confined spaces within a nuclear facility when a design basis accident (DBA) occurs (Farajian et al. 1992)
- Smoke management system performance during a fire, when certain fire/smoke dampers close and others remain open

HVAC DUCT DESIGN PROCEDURES

The general procedure for HVAC system duct design is as follows:

1. Study the building plans, and arrange the supply and return outlets to provide proper distribution of air within each space. Adjust calculated air quantities for duct heat gains or losses and duct leakage. Also, adjust the supply, return, and/or exhaust air quantities to meet space pressurization requirements.
2. Select outlet sizes from manufacturers' data (see Chapter 32).
3. Sketch the duct system, connecting supply outlets and return intakes with the air-handling units/air conditioners. Space allocated for supply and return ducts often dictates system layout and ductwork shape. Use round ducts whenever feasible and avoid close-coupled fittings.
4. Divide the system into sections and number each section. A duct system should be divided at all points where flow, size, or shape changes. Assign fittings to the section toward the supply and return (or exhaust) terminals. The following examples are for the fittings identified for Example 6 (Figure 16), and system section numbers assigned (Figure 17). For converging flow fitting 3, assign the straight-through flow to section 1 (toward terminal 1), and the branch to section 2 (toward terminal 4). For diverging flow fitting 24, assign the straight-through flow to section 13 (toward terminals 26 and 29) and the branch to section 10 (toward terminals 43 and 44). For transition fitting 11, assign the fitting to upstream section 4 [toward terminal 9 (intake louver)]. For fitting 20, assign the unequal area elbow to downstream section 9 (toward diffusers 43 and 44). The fan outlet diffuser, fitting 42, is assigned to section 19 (again, toward the supply duct terminals).
5. Size ducts by the selected design method. Calculate system total pressure loss; then select the fan (refer to Chapter 18 of the 2000 *ASHRAE Handbook—Systems and Equipment*).
6. Lay out the system in detail. If duct routing and fittings vary significantly from the original design, recalculate the pressure losses. Reselect the fan if necessary.
7. Resize duct sections to approximately balance pressures at each junction.
8. Analyze the design for objectionable noise levels, and specify sound attenuators as necessary. Refer to the section on System and Duct Noise.

Example 8. For the system illustrated by Figures 16 and 17, size the ductwork by the equal friction method, and pressure balance the system by changing duct sizes (use 10 mm increments). Determine the system resistance and total pressure unbalance at the junctions. The airflow quantities are actual values adjusted for heat gains or losses, and ductwork is sealed (assume no leakage), galvanized steel ducts with transverse joints on 1200 mm centers (ε = 0.09 mm). Air is at 1.204 kg/m^3 density.

Because the primary purpose of Figure 16 is to illustrate calculation procedures, its duct layout is not typical of any real duct system. The layout includes fittings from the local loss coefficient tables, with emphasis on converging and diverging tees and various types of entries and discharges. The supply system is constructed of rectangular ductwork; the return system, round ductwork.

Solution: See Figure 17 for section numbers assigned to the system. The duct sections are sized within the suggested range of friction rate shown on the friction chart (Figure 9). Tables 11 and 12 give the total pressure loss calculations and the supporting summary of loss coefficients by sections. The straight duct friction factor and pressure loss were calculated by Equations (19) and (20). The fitting loss coefficients are from the *Duct Fitting Database* (ASHRAE 1994). Loss coefficients were calculated automatically by the database program (not by manual interpolation). The pressure loss values in Table 11 for the diffusers (fittings 43 and 44), the louver (fitting 9), and the air-measuring station (fitting 46) are manufacturers' data.

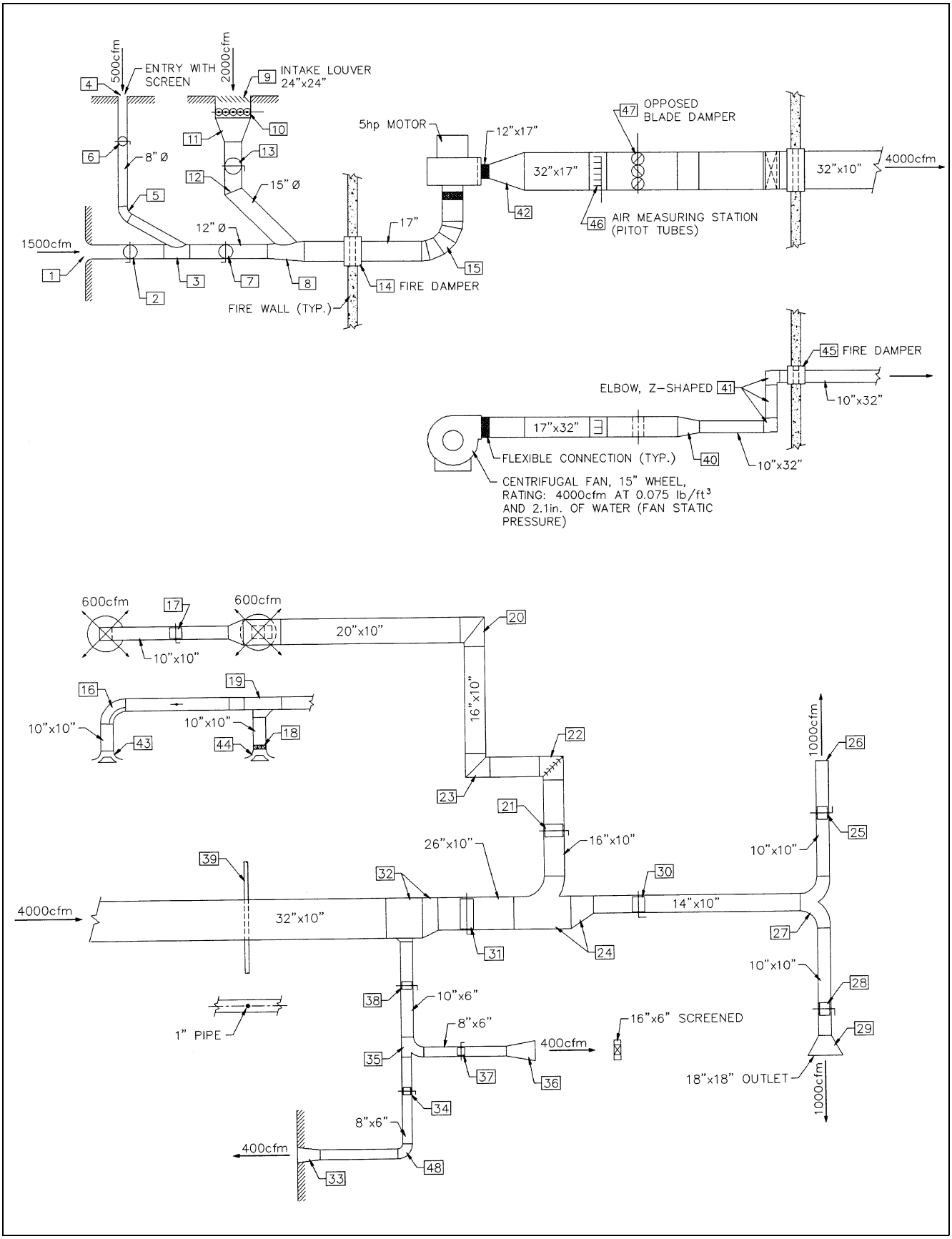

Fig. 16 Schematic for Example 8

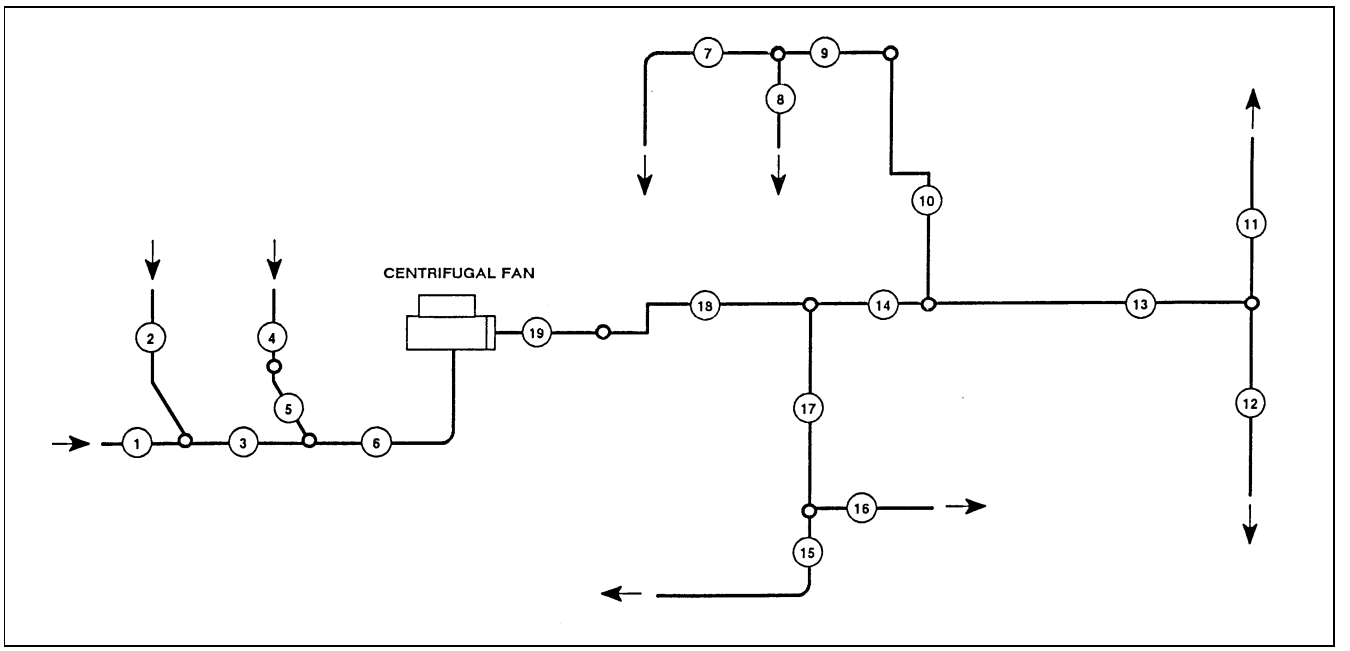

Fig. 17 System Schematic with Section Numbers for Example 8

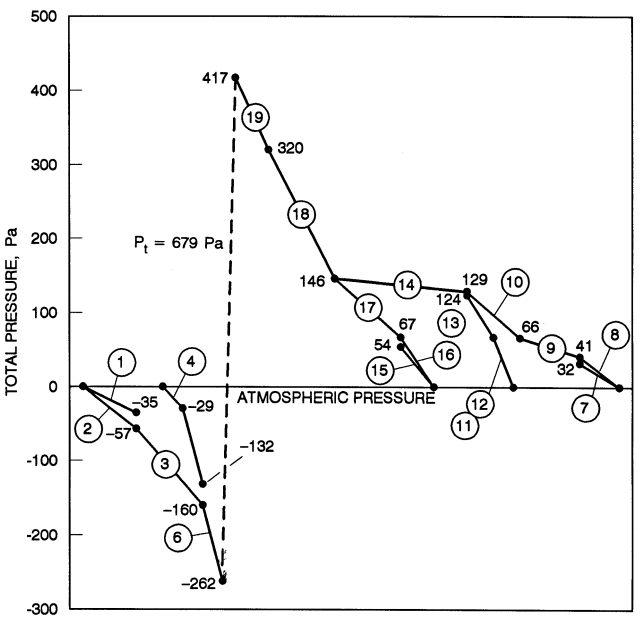

Fig. 18 Total Pressure Grade Line for Example 8

The pressure unbalance at the junctions may be noted by referring to Figure 18, the total pressure grade line for the system. The system resistance P_t is 679 Pa. Noise levels and the need for duct silencers were not evaluated. To calculate the fan static pressure, use Equation (18):

$$P_s = 679 - 119 = 560 \text{ Pa}$$

where 119 Pa is the fan outlet velocity pressure.

INDUSTRIAL EXHAUST SYSTEM DUCT DESIGN

Chapter 29 of the 1999 *ASHRAE Handbook—Applications* discusses design criteria, including hood design, for industrial exhaust systems. Exhaust systems conveying vapors, gases, and smoke can be designed by equal friction, or T-method. Systems conveying particulates are designed by the constant velocity method at duct velocities adequate to convey particles to the system air cleaner. For contaminant transport velocities, see Table 5 in Chapter 29 of the 1999 *ASHRAE Handbook—Applications*.

Two pressure-balancing methods can be considered when designing industrial exhaust systems. One method uses balancing devices (e.g., dampers, blast gates) to obtain design airflow through each hood. The other approach balances systems by adding resistance to ductwork sections (i.e., changing duct size, selecting different fittings, and increasing airflow). This self-balancing method is preferred, especially for systems conveying abrasive materials. Where potentially explosive or radioactive materials are conveyed, the prebalanced system is mandatory because contaminants could accumulate at the balancing devices. To balance systems by increasing airflow, use Equation (51), which assumes that all ductwork has the same diameter and that fitting loss coefficients, including main and branch tee coefficients, are constant.

$$Q_c = Q_d(P_h/P_l)^{0.5} \tag{51}$$

where

Q_c = airflow rate required to increase P_l to P_h, L/s
Q_d = total airflow rate through low-resistance duct run, L/s
P_h = absolute value of pressure loss in high-resistance ductwork section(s), Pa
P_l = absolute value of pressure loss in low-resistance ductwork section(s), Pa

For systems conveying particulates, use elbows with a large centerline radius-to-diameter ratio (r/D), greater than 1.5 whenever possible. If r/D is 1.5 or less, abrasion in dust-handling systems can reduce the life of elbows. Elbows are often made of seven or more gores, especially in large diameters. For converging flow fittings, a 30° entry angle is recommended to minimize energy losses and abrasion in dust-handling systems. For the entry loss coefficients of hoods and equipment for specific operations, refer to Chapter 29 of the 1999 *ASHRAE Handbook—Applications* and to ACGIH (1998).

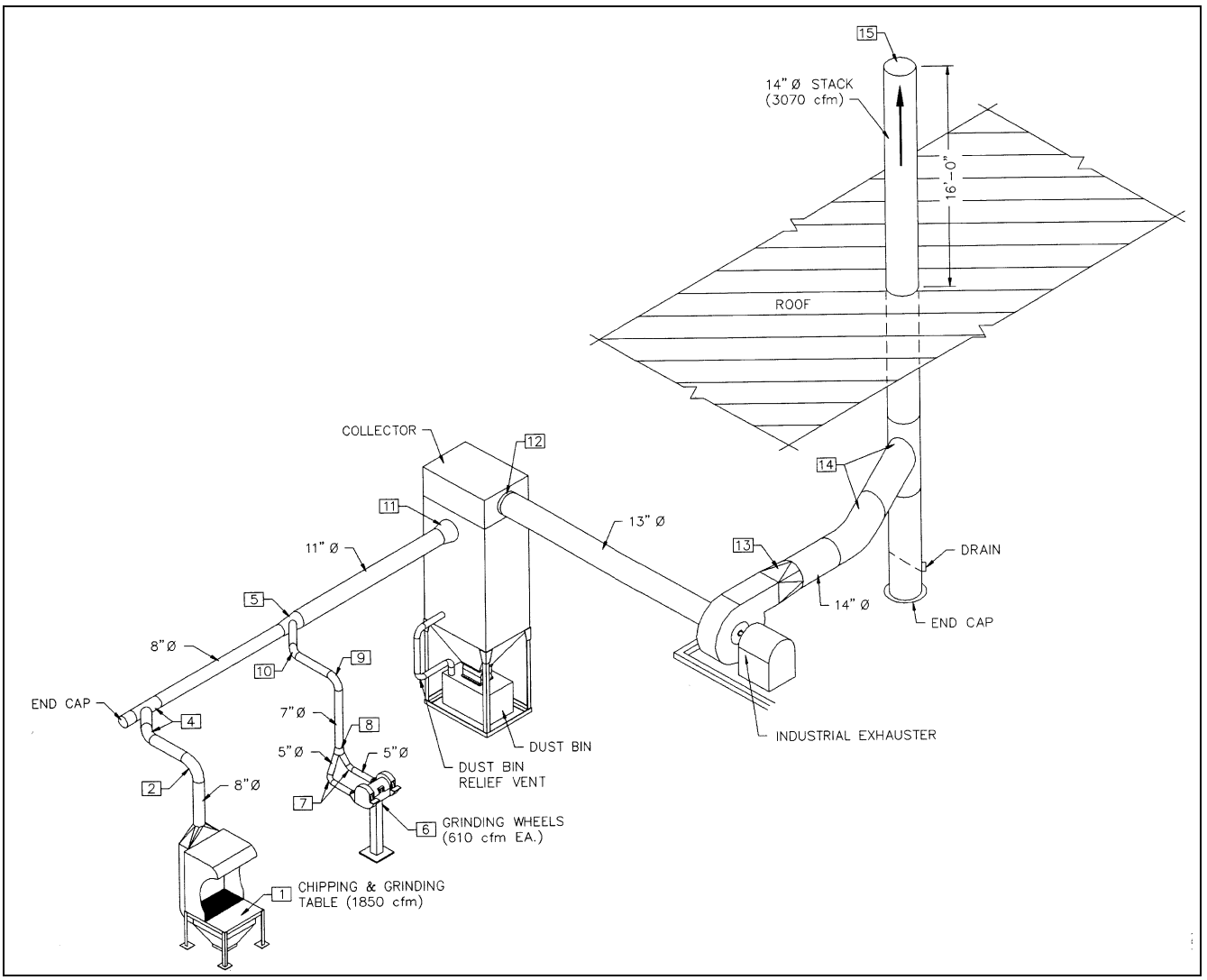

Fig. 19 Metalworking Exhaust System for Example 9

Example 9. For the metalworking exhaust system in Figures 19 and 20, size the ductwork and calculate the fan static pressure requirement for an industrial exhaust designed to convey granular materials. Pressure balance the system by changing duct sizes and adjusting airflow rates. The minimum particulate transport velocity for the chipping and grinding table ducts (sections 1 and 5, Figure 20) is 20 m/s. For the ducts associated with the grinder wheels (sections 2, 3, 4, and 5), the minimum duct velocity is 23 m/s. Ductwork is galvanized steel, with the absolute roughness being 0.09 mm. Assume standard air and use ISO diameter sizes, given in the following table:

Standard Circular Duct Diameters (ISO 1983)

63	180	500
71	200	560
80	224	630
90	250	710
100	280	800
112	315	900
125	355	1000
140	400	1120
160	450	1250

Note: Dimensions listed are in millimetres.

The building is one story, and the design wind velocity is 9 m/s. For the stack, use Design J shown in Figure 13 in Chapter 16 for complete

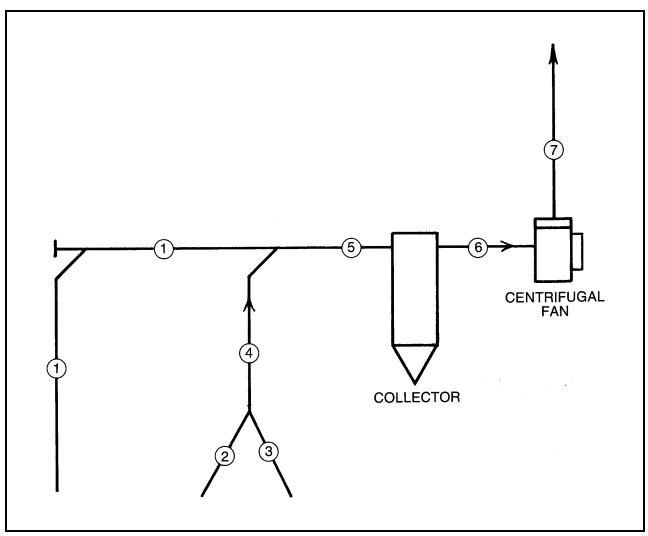

Fig. 20 System Schematic with Section Numbers for Example 9

Table 11 Total Pressure Loss Calculations by Sections for Example 8

Duct Section[a]	Fitting No.[b]	Duct Element	Airflow, L/s	Duct Size (Equivalent Round)	Velocity, m/s	Velocity Pressure, Pa	Duct Length,[c] m	Summary of Fitting Loss Coefficients[d]	Duct Pressure Loss,[e] Pa/m	Total Pressure Loss, Pa	Section Pressure Loss, Pa
1	—	Duct	700	300 mm ϕ	9.9	—	4.6	—	3.5	16	
	—	Fittings	700	—	9.9	59	—	0.32	—	19	35
2	—	Duct	250	200 mm ϕ	8.0	—	18.3	—	3.8	70	
	—	Fittings	250	—	8.0	38	—	−0.34	—	−13	57
3	—	Duct	950	300 mm ϕ	13.4	—	6.1	—	6.2	38	
	—	Fittings	950	—	13.4	109	—	0.60	—	65	103
4	—	Duct	950	600 mm × 600 mm (656)	2.6	—	1.5	—	0.1	0	
	—	Fittings	950	—	2.6	4	—	1.09	—	4	
	9	Louver	950	600 mm × 600 mm	—	—	—	—	—	25[f]	29
5	—	Duct	950	380 mm ϕ	8.4	—	18.3	—	1.9	35	
	—	Fittings	950	—	8.4	42	—	1.61	—	68	103
6	—	Duct	1900	450 mm ϕ	11.9	—	9.1	—	3.0	27	
	—	Fittings	1900	—	11.9	86	—	0.87	—	75	102
7	—	Duct	275	250 mm × 250 mm (273)	4.4	—	4.3	—	0.9	4	
	—	Fittings	275	—	4.4	12	—	0.26	—	3	
	43	Diffuser	275	250 mm × 250 mm	—	—	—	—	—	25[f]	32
8	—	Duct	275	250 mm × 250 mm (273)	4.4	—	1.2	—	0.9	1	
	—	Fittings	275	—	4.4	12	—	1.25	—	15	
	44	Diffuser	275	250 mm × 250 mm	—	—	—	—	—	25[f]	41
9	—	Duct	550	500 mm × 250 mm (381)	4.4	—	7.6	—	0.6	5	
	—	Fittings	550	—	4.4	12	—	1.67	—	20	25
10	—	Duct	550	400 mm × 250 mm (343)	5.5	—	13.7	—	1.1	15	
	—	Fittings	550	—	5.5	18	—	2.69	—	48	63
11	—	Duct	475	250 mm × 250 mm (273)	7.6	—	3.0	—	2.6	8	
	—	Fittings	475	—	7.6	35	—	1.68	—	59	67
12	—	Duct	475	250 mm × 250 mm (273)	7.6	—	6.7	—	2.6	17	
	—	Fittings	475	—	7.6	35	—	1.44	—	50	67
13	—	Duct	950	350 mm × 250 mm (322)	10.9	—	10.7	—	4.2	45	
	—	Fittings	950	—	10.9	71	—	0.17	—	12	57
14	—	Duct	1500	660 mm × 250 mm (414)	9.1	—	4.6	—	2.2	10	
	—	Fittings	1500	—	9.1	50	—	0.13	—	7	17
15	—	Duct	200	200 mm × 150 mm (189)	6.7	—	12.2	—	3.2	39	
	—	Fittings	200	—	6.7	27	—	0.57	—	15	54
16	—	Duct	200	200 mm × 150 mm (189)	6.7	—	6.1	—	3.2	20	
	—	Fittings	200	—	6.7	27	—	1.74	—	47	67
17	—	Duct	400	250 mm × 150 mm (210)	10.7	—	4.2	—	6.9	29	
	—	Fittings	400	—	10.7	69	—	0.73	—	50	79
18	—	Duct	1900	800 mm × 250 mm (470)	9.5	—	7.0	—	2.3	16	
	—	Fittings	1900	—	9.5	54	—	2.93	—	158	174
19	—	Duct	1900	800 mm × 450 mm (649)	5.3	—	3.7	—	0.5	2	
	—	Fittings	1900	—	5.3	17	—	4.71	—	80	
	46	Air-measuring station	1900	—	—	—	—	—	—	15[f]	97

[a]See Figure 17.
[b]See Figure 16.
[c]Duct lengths are to fitting centerlines.
[d]See Table 12.
[e]Duct pressure based on a 0.09 mm absolute roughness factor.
[f]Pressure drop based on manufacturers' data.

Table 12 Loss Coefficient Summary by Sections for Example 8

Duct Section	Fitting Number	Type of Fitting	ASHRAE Fitting No.[a]	Parameters	Loss Coefficient
1	1	Entry	ED1-3	$r/D = 0.2$	0.03
	2	Damper	CD9-1	$\theta = 0°$	0.19
	3	Wye (30°), main	ED5-1	$A_s/A_c = 1.0$, $A_b/A_c = 0.444$, $Q_s/Q_c = 0.75$	0.10 (C_s)
	Summation of Section 1 loss coefficients				0.32
2	4	Entry	ED1-1	$L = 0$, $t = 1.61$ mm (16 gage)	0.50
	4	Screen	CD6-1	$n = 0.70$, $A_1/A_o = 1$	0.58
	5	Elbow	CD3-6	60°, $r/D = 1.5$, pleated	0.27
	6	Damper	CD9-1	$\theta = 0°$	0.19
	3	Wye (30°), branch	ED5-1	$A_s/A_c = 1.0$, $A_b/A_c = 0.444$, $Q_b/Q_c = 0.25$	−1.88 (C_b)
	Summation of Section 2 loss coefficients				−0.34
3	7	Damper	CD9-1	$\theta = 0°$	0.19
	8	Wye (45°), main	ED5-2	$A_s/A_c = 0.445$, $A_b/A_c = 0.713$, $Q_s/Q_c = 0.5$	0.41 (C_s)
	Summation of Section 3 loss coefficients				0.60

[a]*Duct Fitting Database* (ASHRAE 1994) data for fittings reprinted in the section on Fitting Loss Coefficients.

Table 12 Loss Coefficient Summary by Sections for Example 8 (*Concluded*)

Duct Section	Fitting Number	Type of Fitting	ASHRAE Fitting No.[a]	Parameters	Loss Coefficient	
4	10	Damper	CR9-4	$\theta = 0°$, 5 blades (opposed), $L/R = 1.25$	0.52	
	11	Transition	ER4-3	$L = 750$ mm, $A_o/A_1 = 3.17$, $\theta = 17°$	0.57	
	Summation of Section 4 loss coefficients				1.09	
5	12	Elbow	CD3-17	45°, mitered	0.34	
	13	Damper	CD9-1	$\theta = 0°$	0.19	
	8	Wye (45°), branch	ED5-2	$Q_b/Q_c = 0.5$, $A_s/A_c = 0.445$, $A_b/A_c = 0.713$	1.08	(C_b)
	Summation of Section 5 loss coefficients				1.61	
6	14	Fire damper	CD9-3	Curtain type, Type C	0.12	
	15	Elbow	CD3-9	90°, 5 gore, $r/D = 1.5$	0.15	
	—	Fan and system interaction	ED7-2	90° elbow, 5 gore, $r/D = 1.5$, $L = 900$ mm	0.60	
	Summation of Section 6 loss coefficients				0.87	
7	16	Elbow	CR3-3	90°, $r/W = 0.70$, 1 splitter vane	0.14	
	17	Damper	CR9-1	$\theta = 0°$, $H/W = 1.0$	0.08	
	19	Tee, main	SR5-13	$Q_s/Q_c = 0.5$, $A_s/A_c = 0.50$	0.04	(C_s)
	Summation of Section 7 loss coefficients				0.26	
8	19	Tee, branch	SR5-13	$Q_b/Q_c = 0.5$, $A_b/A_c = 0.50$	0.73	(C_b)
	18	Damper	CR9-4	$\theta = 0°$, 3 blades (opposed), $L/R = 0.75$	0.52	
	Summation of Section 8 loss coefficients				1.25	
9	20	Elbow	SR3-1	90°, mitered, $H/W_1 = 0.625$, $W_o/W_1 = 1.25$	1.67	
	Summation of Section 9 loss coefficients				1.67	
10	21	Damper	CR9-1	$\theta = 0°$, $H/W = 0.625$	0.08	
	22	Elbow	CR3-10	90°, single-thickness vanes, design 2	0.12	
	23	Elbow	CR3-6	$\theta = 90°$, mitered, $H/W = 0.625$	1.25	
	24	Tee, branch	SR5-1	$r/W_b = 1.0$, $Q_b/Q_c = 0.367$, $A_s/A_c = 0.530$, $A_b/A_c = 0.606$	1.24	(C_b)
	Summation of Section 10 loss coefficients				2.69	
11	25	Damper	CR9-1	$\theta = 0°$, $H/W = 1.0$	0.08	
	26	Exit	SR2-1	$H/W = 1.0$, Re = 125 400	1.00	
	27	Wye, dovetail	SR5-14	$r/W_c = 1.5$, $Q_{b1}/Q_c = 0.5$, $A_{b1}/A_c = 0.714$	0.60	(C_b)
	Summation of Section 11 loss coefficients				1.68	
12	28	Damper	CR9-1	$\theta = 0°$, $H/W = 1.0$	0.08	
	29	Exit	SR2-5	$\theta = 19°$, $A_1/A_o = 3.24$, Re = 130 000	0.76	
	27	Wye, dovetail	SR5-14	$r/W_c = 1.5$, $Q_{b2}/Q_c = 0.5$, $A_{b2}/A_c = 0.714$	0.60	(C_b)
	Summation of Section 12 loss coefficients				1.44	
13	30	Damper	CR9-1	$\theta = 0°$, $H/W = 0.71$	0.08	
	24	Tee, main	SR5-1	$r/W_b = 1.0$, $Q_s/Q_c = 0.633$, $A_s/A_c = 0.530$, $A_b/A_c = 0.606$	0.09	(C_s)
	Summation of Section 13 loss coefficients				0.17	
14	31	Damper	CR9-1	$\theta = 0°$, $H/W = 0.38$	0.08	
	32	Tee, main	SR5-13	$Q_s/Q_c = 0.79$, $A_s/A_c = 0.825$	0.05	(C_s)
	Summation of Section 14 loss coefficients				0.13	
15	48	Elbow	CR3-1	$\theta = 90°$, $r/W = 1.5$, $H/W = 0.75$	0.19	
	33	Exit	SR2-6	$L = 500$ mm, $D_h = 187$	0.27	
	34	Damper	CR9-1	$\theta = 0°$, $H/W = 0.75$	0.08	
	35	Tee, main	SR5-1	$r/W_b = 1.0$, $Q_s/Q_c = 0.5$, $A_s/A_c = 0.80$, $A_b/A_c = 0.80$	0.03	(C_s)
	Summation of Section 15 loss coefficients				0.57	
16	36	Exit	SR2-3	$\theta = 20°$, $A_1/A_o = 2.0$, Re = 75 000	0.63	
	36	Screen	CR6-1	$n = 0.8$, $A_1/A_o = 2.0$	0.08	
	37	Damper	CR9-1	$\theta = 0°$, $H/W = 0.75$	0.08	
	35	Tee, branch	SR5-1	$r/W_b = 1.0$, $Q_b/Q_c = 0.5$, $A_s/A_c = 0.80$, $A_b/A_c = 0.80$	0.95	(C_b)
	Summation of Section 16 loss coefficients				1.74	
17	38	Damper	CR9-1	$\theta = 0°$, $H/W = 0.6$	0.08	
	32	Tee, branch	SR5-13	$Q_b/Q_c = 0.21$, $A_b/A_c = 0.187$	0.65	(C_b)
	Summation of Section 17 loss coefficients				0.73	
18	39	Obstruction, pipe	CR6-4	Re = 15 000, $y = 0$, $d = 25$ mm, $S_m/A_o = 0.1$, $y/H = 0$	0.17	
	40	Transition	SR4-1	$\theta = 25°$, $A_o/A_1 = 0.556$, $L = 450$ mm	0.04	
	41	Elbows, Z-shaped	CR3-17	$L = 1000$ mm, $L/W = 4.0$, $H/W = 3.2$, Re = 240 000	2.53	
	45	Fire damper	CR9-6	Curtain type, Type B	0.19	
	Summation of Section 18 loss coefficients				2.93	
19	42	Diffuser, fan	SR7-17	$\theta_1 = 28°$, $L = 1000$ mm, $A_o/A_1 = 2.67$, $C_1 = 0.59$	4.19	(C_o)
	47	Damper	CR9-4	$\theta = 0°$, 8 blades (opposed), $L/R = 1.44$	0.52	
	Summation of Section 19 loss coefficients				4.71	

[a]*Duct Fitting Database* (ASHRAE 1994) data for fittings reprinted in the section on Fitting Loss Coefficients.

rain protection. The stack height, determined by calculations from Chapter 16, is 4.9 m above the roof. This stack height is based on minimized stack downwash; therefore, the stack discharge velocity must exceed 1.5 times the design wind velocity.

Solution: For the contaminated ducts upstream of the collector, initial duct sizes and transport velocities are summarized below. The 22.8 m/s velocity in section 4 is acceptable because the transport velocity is not significantly lower than 23 m/s. For the next available duct size (160 mm diameter), the duct velocity is 28.8 m/s, significantly higher than 23 m/s.

Duct Section	Design Airflow, L/s	Transport Velocity, m/s	Duct Diameter, mm	Duct Velocity, m/s
1	850	20	224	21.6
2,3	290 each	23	125	23.6
4	580	23	180	22.8
5	1430	23	280	23.2

The following tabulation summarizes design calculations up through the junction after sections 1 and 4.

Design No.	D_1, mm	Δp_1, Pa	Δp_{2+4}, Pa	Imbalance, $\Delta p_1 - \Delta p_{2+4}$
1	224	411	794	−383
2	200	762	850	−88
3	180	1320	712	+609

Q_1 = 850 L/s
Q_2 = 290 L/s; D_2 = 125 mm dia.
Q_3 = 290 L/s; D_3 = 125 mm dia.
Q_4 = 850 L/s; D_4 = 180 mm dia.

For the initial design, Design 1, the imbalance between section 1 and section 2 (or 3) is 383 Pa, with section 1 requiring additional resistance. Decreasing section 1 duct diameter by ISO sizes results in the least imbalance, 88 Pa, when the duct diameter is 200 mm (Design 3). Because section 1 requires additional resistance, estimate the new airflow rate using Equation (51):

$$Q_{c,1} = 850(850/762)^{0.5} = 900 \text{ L/s}$$

At 900 L/s flow in section 1, 130 Pa imbalance remains at the junction of sections 1 and 4. By trial-and-error solution, balance is attained when the flow in section 1 is 860 L/s. The duct between the collector and the fan inlet is 355 mm round to match the fan inlet (340 mm diameter). To minimize downwash, the stack discharge velocity must exceed 13.5 m/s, 1.5 times the design wind velocity (9 m/s) as stated in the problem definition. Therefore, the stack is 355 mm round, and the stack discharge velocity is 14.5 m/s.

Table 13 summarizes the system losses by sections. The straight duct friction factor and pressure loss were calculated by Equations (19) and (20). Table 14 lists fitting loss coefficients and input parameters necessary to determine the loss coefficients. The fitting loss coefficients are from the *Duct Fitting Database* (ASHRAE 1994). The fitting loss coefficient tables are included in the section on Fitting Loss Coefficients for illustration but can not be obtained exactly by manual interpolation since the coefficients were calculated by the duct fitting database algorithms (more significant figures). For a pressure grade line of the system, see Figure 21. The fan total pressure, calculated by Equation (16), is 1992 Pa. To calculate the fan static pressure, use Equation (18):

$$P_s = 1992 - 192 = 1800 \text{ Pa}$$

where 192 Pa is the fan outlet velocity pressure. The fan airflow rate is 1440 L/s, and its outlet area is 0.081 m^2 (260 mm by 310 mm). Therefore, the fan outlet velocity is 17.9 m/s.

The hood suction for the chipping and grinding table hood is 560 Pa, calculated by Equation (18) from Chapter 29 of the 1999 *ASHRAE Handbook—Applications* [*HS* = (1 + 0.25) (451) = 560 Pa, where 0.25 is the

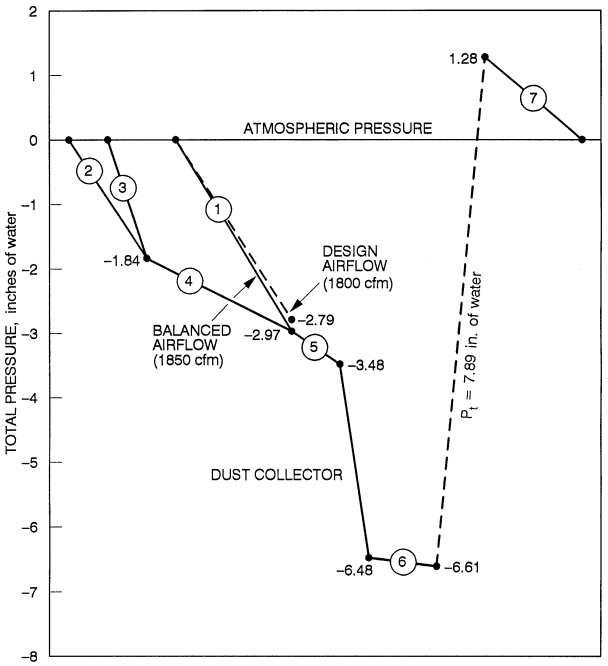

Fig. 21 Total Pressure Grade Line for Example 9

Table 13 Total Pressure Loss Calculations by Sections for Example 9

Duct Section[a]	Duct Element	Airflow, L/s	Duct Size	Velocity, m/s	Velocity Pressure, Pa	Duct Length,[b] m	Summary of Fitting Loss Coefficients[c]	Duct Pressure Loss, Pa/m[d]	Total Pressure Loss, Pa	Section Pressure Loss, Pa
1	Duct	860	200 mm ϕ	27.4	—	7.0	—	40	280	
	Fittings	860	—	27.4	451	—	1.12	—	505	785
2,3	Duct	290	125 mm ϕ	23.6	—	2.7	—	54	146	
	Fittings	290	—	23.6	336	—	1.06	—	356	502
4	Duct	580	180 mm ϕ	22.8	—	3.84	—	32	123	
	Fittings	580	—	22.8	313	—	0.51	—	160	283
5	Duct	1440	280 mm ϕ	23.4	—	2.7	—	20	54	
	Fittings	1440	—	23.4	329	—	0.22	—	72	126
—	Collector,[e] fabric	1440	—	—	—	—	—	—	750	750
6	Duct	1440	355 mm ϕ	14.5	—	3.7	—	6	22	
	Fittings	1440	—	14.5	127	—	0.00	—	0	22
7	Duct	1440	355 mm ϕ	14.5	—	8.5	—	6	51	
	Fittings	1440	—	14.5	127	—	2.03	—	258	309

[a]See Figure 20.
[b]Duct lengths are to fitting centerlines.
[c]See Table 14.
[d]Duct pressure based on a 0.09 mm absolute roughness factor.
[e]Collector manufacturers set the fabric bag cleaning mechanism to actuate at a pressure difference of 750 Pa between the inlet and outlet plenums. The pressure difference across the clean media is approximately 400 Pa.

Table 14 Loss Coefficient Summary by Sections for Example 9

Duct Section	Fitting Number	Type of Fitting	ASHRAE Fitting No.[a]	Parameters	Loss Coefficient
1	1	Hood[b]	—	Hood face area: 0.9 m by 1.2 m	0.25
	2	Elbow	CD3-10	90°, 7 gore, $r/D = 2.5$	0.11
	4	Capped wye (45°), with 45° elbow	ED5-6	$A_b/A_c = 1$	0.64 (C_b)
	5	Wye (30°), main	ED5-1	$Q_s/Q_c = 0.60$, $A_s/A_c = 0.510$, $A_b/A_c = 0.413$	0.12 (C_s)
	Summation of Section 1 loss coefficients				1.12
2,3	6	Hood[c]	—	Type hood: For double wheels, dia. = 560 mm each, wheel width = 100 mm each; type takeoff: tapered	0.40
	7	Elbow	CD3-12	90°, 3 gore, $r/D = 1.5$	0.34
	8	Symmetrical wye (60°)	ED5-9	$Q_b/Q_c = 0.5$, $A_b/A_c = 0.482$	0.32 (C_b)
	Summation of Sections 2 and 3 loss coefficients				1.06
4	9	Elbow	CD3-10	90°, 7 gore, $r/D = 2.5$	0.11
	10	Elbow	CD3-13	60°, 3 gore, $r/D = 1.5$	0.19
	5	Wye (30°), branch	ED5-1	$Q_b/Q_c = 0.40$, $A_s/A_c = 0.510$, $A_b/A_c = 0.413$	0.21 (C_b)
	Summation of Section 4 loss coefficients				0.51
5	11	Exit, conical diffuser to collector	ED2-1	$L = 600$ mm, $L/D_o = 2.14$, $A_1/A_o \approx 16$	0.22
	Summation of Section 5 loss coefficients				0.22
6	12	Entry, bellmouth from collector	ER2-1	$r/D_1 = 0.20$	0.00 (C_1)
	Summation of Section 6 loss coefficients				0.00
7	13	Diffuser, fan outlet[d]	SR7-17	Fan outlet size: 260 mm by 310 mm, $A_o/A_1 = 1.563$ (assume 355 mm by 355 mm outlet rather than 355 mm round), $L = 460$ mm	0.39 (C_o)
	14	Capped wye (45°), with 45° elbow	ED5-6	$A_b/A_c = 1$	0.64 (C_b)
	15	Stackhead	SD2-6	$D_e/D = 1$	1.0
	Summation of Section 7 loss coefficients				2.03

[a] *Duct Fitting Database* (ASHRAE 1994) data for fittings reprinted in the section on Fitting Loss Coefficients.
[b] From *Industrial Ventilation* (ACGIH 1998, Figure VS-80-19).
[c] From *Industrial Ventilation* (ACGIH 1998, Figure VS-80-11).
[d] Fan specified: Industrial exhauster for granular materials: 530 mm wheel diameter, 340 mm inlet diameter, 260 mm by 310 mm outlet, 6 kW motor.

hood entry loss coefficient C_o, and 451 Pa is the duct velocity pressure P_v a few diameters downstream from the hood]. Similarly, the hood suction for each of the grinder wheels is 470 Pa:

$$HS_{2,3} = (1 + 0.4)(336) = 470 \text{ Pa}$$

where 0.4 is the hood entry loss coefficient, and 336 Pa is the duct velocity pressure.

REFERENCES

ACGIH. 1998. *Industrial ventilation: A manual of recommended practice*, 23rd ed. American Conference of Governmental Industrial Hygienists, Lansing, MI.

ADC. 1996. Flexible duct performance and installation standards, 3rd ed. Air Diffusion Council.

AISI/SMACNA. 1972. Measurement and analysis of leakage rates from seams and joints of air handling systems.

Altshul, A.D., L.C. Zhivotovckiy, and L.P. Ivanov. 1987. *Hydraulics and aerodynamics.* Stroisdat Publishing House, Moscow.

AMCA. 1999. Laboratory method of testing louvers for rating. *Standard* 500-L. Air Movement and Control Association, Arlington Heights, IL.

AMCA. 1990a. Fans and systems. *Publication* 201.

AMCA. 1990b. Field performance measurement of fan systems. *Publication* 203.

ASHRAE. 1993. Energy-efficient design of new low-rise residential buildings. ASHRAE *Standard* 90.2-1993.

ASHRAE. 1994. *Duct fitting database.*

ASHRAE. 1995. Energy conservation in existing buildings. ASHRAE/IESNA *Standard* 100-1995. Addendum 1-1996.

ASHRAE. 1999. Energy standard for buildings except low-rise residential buildings. ASHRAE/IESNA *Standard* 90.1-1999.

ASHRAE. 1999. Laboratory methods for testing fans for aerodynamic performance rating. ANSI/ASHRAE *Standard* 51-1999. Also ANSI/AMCA 210-99.

ASHRAE/SMACNA/TIMA. 1985. Investigation of duct leakage. ASHRAE *Research Project* 308.

Behls, H.F. 1971. Computerized calculation of duct friction. *Building Science Series* 39, p. 363. National Institute of Standards and Technology, Gaithersburg, MD.

Bellman, R.E. 1957. *Dynamic programming.* Princeton University Press, New York.

Brown, R.B. 1973. Experimental determinations of fan system effect factors. In *Fans and systems*, ASHRAE Symposium Bulletin LO-73-1, Louisville, KY (June).

Carrier Corporation. 1960. Air duct design. Chapter 2 in *System design manual,* Part 2: Air distribution. pp.17-63. Syracuse, NY.

Chun-Lun, S. 1983. Simplified static-regain duct design procedure. *ASHRAE Transactions* 89(2A):78.

Clarke, M.S., J.T. Barnhart, F.J. Bubsey, and E. Neitzel. 1978. The effects of system connections on fan performance. *ASHRAE Transactions* 84(2): 227-63.

Colebrook, C.F. 1938-39. Turbulent flow in pipes, with particular reference to the transition region between the smooth and rough pipe laws. *Journal of the Institution of Civil Engineers* 11:133. London.

DOE. *Electrical sales and revenue*, latest edition. Department of Energy, Washington, D.C. (To purchase, call Energy Information Administration 202-512-1800.)

Farajian, T., G. Grewal, and R.J. Tsal. 1992. Post-accident air leakage analysis in a nuclear facility via T-method airflow simulation. 22nd DOE/NRC Nuclear Air Cleaning and Treatment Conference, Denver, CO, October.

Farquhar, H.F. 1973. System effect values for fans. In *Fans and systems*, ASHRAE Symposium Bulletin LO-73-1, Louisville, KY (June).

Griggs, E.I. and F. Khodabakhsh-Sharifabad. 1992. Flow characteristics in rectangular ducts. *ASHRAE Transactions* 98(1).

Griggs, E.I., W.B. Swim, and G.H. Henderson. 1987. Resistance to flow of round galvanized ducts. *ASHRAE Transactions* 93(1):3-16.

Heyt, J.W. and M.J. Diaz. 1975. Pressure drop in flat-oval spiral air duct. *ASHRAE Transactions* 81(2):221-32.

Huebscher, R.G. 1948. Friction equivalents for round, square and rectangular ducts. *ASHVE Transactions* 54:101-18.

Hutchinson, F.W. 1953. Friction losses in round aluminum ducts. *ASHVE Transactions* 59:127-38.

Idelchik, I.E., M.O. Steinberg, G.R. Malyavskaya, and O.G. Martynenko. 1994. *Handbook of hydraulic resistance*, 3rd ed. CRC Press/Begell House, Boca Raton, Ann Arbor, London, Tokyo.

ISO. 1983. Air distribution—Straight circular sheet metal ducts with a lock type spiral seam and straight rectangular sheet metal ducts—Dimensions. *Standard* 7807:1983. International Organization for Standardization, Geneva.

Jones, C.D. 1979. Friction factor and roughness of United Sheet Metal Company spiral duct. United Sheet Metal, Division of United McGill Corp., Westerville, OH (August). Based on data contained in Friction loss tests, United Sheet Metal Company Spiral Duct, Ohio State University Engineering Experiment Station, File No. T-1011, September, 1958.

Klote, J.H. and J. Milke. 1992. *Design of smoke management systems.* ASHRAE, Atlanta.

Lauvray, T.L. 1978. Experimental heat transmission coefficients for operating air duct systems. *ASHRAE Journal* (June):69.

Meyer, M.L. 1973. A new concept: The fan system effect factor. In *Fans and systems*, ASHRAE Symposium Bulletin LO-73-1, Louisville, KY (June).

Moody, L.F. 1944. Friction factors for pipe flow. *ASME Transactions* 66:671.

NAIMA. 1997. Fibrous glass duct construction standards, 3rd ed. North American Insulation Manufacturers Association.

NFPA. *Fire protection handbook*, latest ed. National Fire Protection Association, Quincy, MA.

NFPA. Installation of air conditioning and ventilating systems. ANSI/NFPA *Standard* 90A, latest ed.

Osborne, W.C. 1966. *Fans*. Pergamon Press Ltd., London.

SMACNA. 1985. *HVAC air duct leakage manual.* Sheet Metal and Air Conditioning Contractors' National Association, Chantilly, VA.

SMACNA. 1992. Fibrous glass duct construction standards, 6th ed.

SMACNA. 1995. HVAC duct construction standards, metal and flexible, 2nd ed.

Smith, G.W. 1968. *Engineering economy: Analysis of capital expenditures.* The Iowa State University Press, Ames, IA.

Swim, W.B. 1978. Flow losses in rectangular ducts lined with fiberglass. *ASHRAE Transactions* 84(2):216.

Swim, W.B. 1982. Friction factor and roughness for airflow in plastic pipe. *ASHRAE Transactions* 88(1):269.

Swim, W.B. and E.I. Griggs. 1995. Duct leakage measurement and analysis. *ASHRAE Transactions* 101(1).

Tsal, R.J. and M.S. Adler. 1987. Evaluation of numerical methods for ductwork and pipeline optimization. *ASHRAE Transactions* 93(1):17-34.

Tsal, R.J. and H.F. Behls. 1988. Fallacy of the static regain duct design method. *ASHRAE Transactions* 94(2):76-89.

Tsal, R.J., H.F. Behls, and R. Mangel. 1988. T-method duct design, Part I: Optimization theory; Part II: Calculation procedure and economic analysis. *ASHRAE Transactions* 94(2):90-111.

Tsal, R.J., H.F. Behls, and R. Mangel. 1990. T-method duct design, Part III: Simulation. *ASHRAE Transactions* 96(2).

UL. Published annually. *Building materials directory.* Underwriters Laboratories, Northbrook, IL.

UL. Published annually. *Fire resistance directory.*

UL. Factory-made air ducts and air connectors. UL *Standard* 181, latest ed.

UL. Closure systems for use with rigid air ducts and air connectors. UL *Standard* 181A, latest ed.

UL. Closure systems for use with rigid air ducts and air connectors. UL *Standard* 181B, latest ed.

UL. Fire dampers. *Standard* UL 555, latest ed.

UL. Smoke dampers. *Standard* 555S, latest ed.

Wendes, H.C. 1989. *Sheet metal estimating.* Wendes Mechanical Consulting Services, Elk Grove Village, IL.

Wright, D.K., Jr. 1945. A new friction chart for round ducts. *ASHVE Transactions* 51:303-16.

BIBLIOGRAPHY

SMACNA. 1987. Duct research destroys design myths. Videotape (VHS). Sheet Metal and Air Conditioning Contractors' National Association, Chantilly, VA.

FITTING LOSS COEFFICIENTS

Fittings to support Examples 8 and 9 and some of the more common fittings are reprinted here.

For the complete fitting database see the *Duct Fitting Database* (ASHRAE 1994).

ROUND FITTINGS

CD3-1 Elbow, Die Stamped, 90 Degree, *r*/*D* = 1.5

***D*, mm**	**75**	**100**	**125**	**150**	**180**	**200**	**230**	**250**
C_o	0.30	0.21	0.16	0.14	0.12	0.11	0.11	0.11

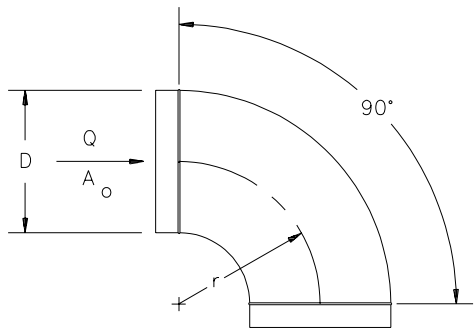

CD3-3 Elbow, Die Stamped, 45 Degree, *r*/*D* = 1.5

***D*, mm**	**75**	**100**	**125**	**150**	**180**	**200**	**230**	**250**
C_o	0.18	0.13	0.10	0.08	0.07	0.07	0.07	0.07

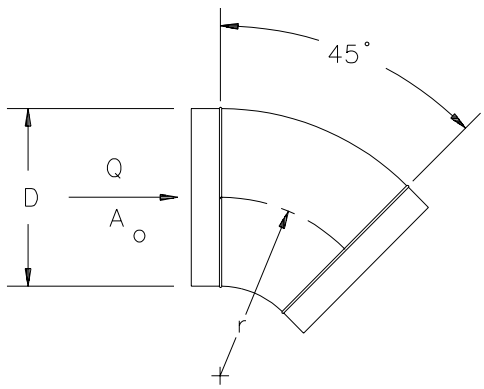

CD3-5 Elbow, Pleated, 90 Degree, *r*/*D* = 1.5

***D*, mm**	**100**	**150**	**200**	**250**	**300**	**350**	**400**
C_o	0.57	0.43	0.34	0.28	0.26	0.25	0.25

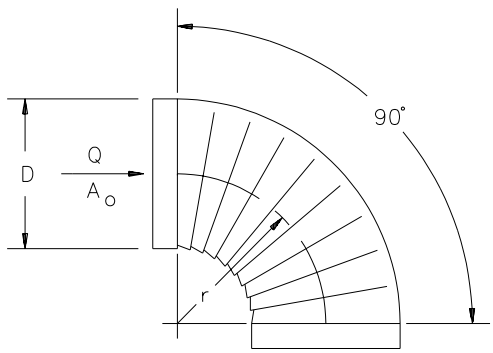

CD3-6 Elbow, Pleated, 60 Degree, *r*/*D* = 1.5

***D*, mm**	**100**	**150**	**200**	**250**	**300**	**350**	**400**
C_o	0.45	0.34	0.27	0.23	0.20	0.19	0.19

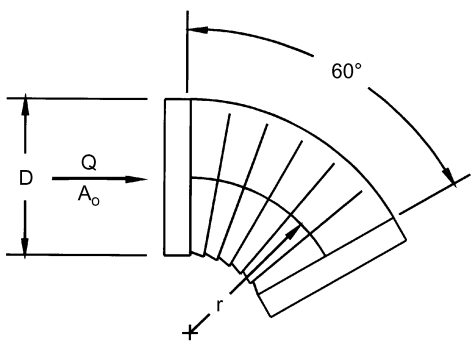

CD3-7 Elbow, Pleated, 45 Degree, r/D = 1.5

D, mm	100	150	200	250	300	350	400
C_o	0.34	0.26	0.21	0.17	0.16	0.15	0.15

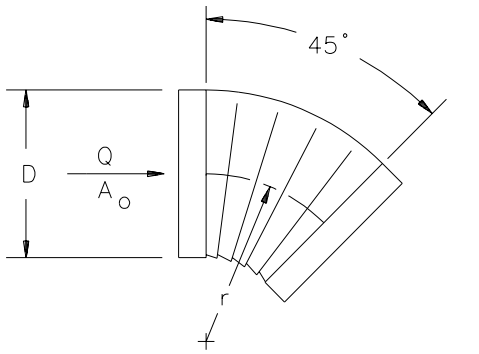

CD3-9 Elbow, 5 Gore, 90 Degree, r/D = 1.5

D, mm	75	150	230	300	380	450	530	600	690	750	1500
C_o	0.51	0.28	0.21	0.18	0.16	0.15	0.14	0.13	0.12	0.12	0.12

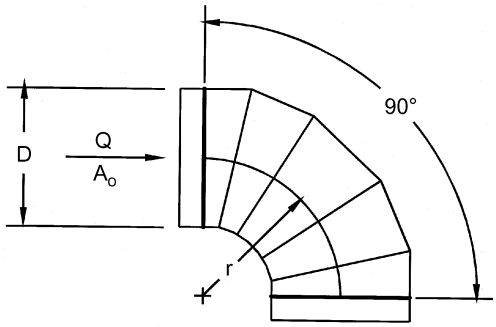

CD3-10 Elbow, 7 Gore, 90 Degree, r/D = 2.5

D, mm	75	150	230	300	380	450	690	1500
C_o	0.16	0.12	0.10	0.08	0.07	0.06	0.05	0.03

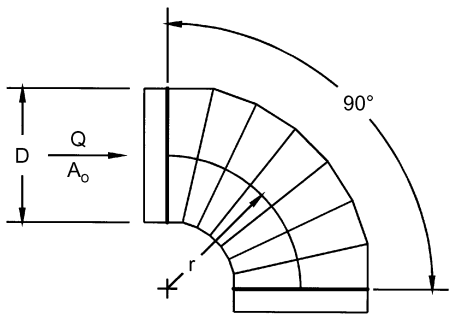

CD3-12 Elbow, 3 Gore, 90 Degree, r/D = 0.75 to 2.0

r/D	0.75	1.00	1.50	2.00
C_o	0.54	0.42	0.34	0.33

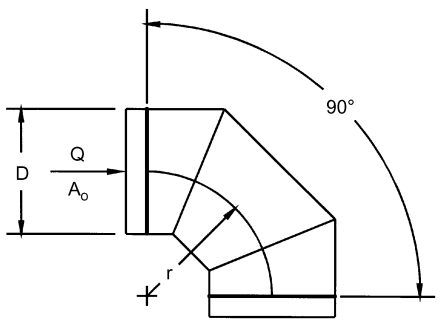

CD3-13 Elbow, 3 Gore, 60 Degree, r/D = 1.5

D, mm	75	150	230	300	380	450	530	600	690	750	1500
C_o	0.40	0.21	0.16	0.14	0.12	0.12	0.11	0.10	0.09	0.09	0.09

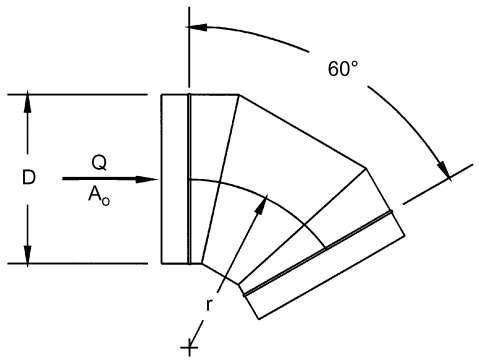

CD3-14 Elbow, 3 Gore, 45 Degree, *r*/*D* = 1.5

D, mm	75	150	230	300	380	450	530	600	690	750	1500
C_o	0.31	0.17	0.13	0.11	0.11	0.09	0.08	0.08	0.07	0.07	0.07

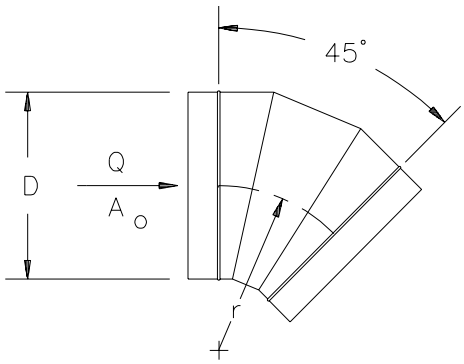

CD3-17 Elbow, Mitered, 45 Degree

D, mm	75	150	230	300	380	450	530	600	690	1500
C_o	0.34	0.34	0.34	0.34	0.34	0.34	0.34	0.34	0.34	0.34

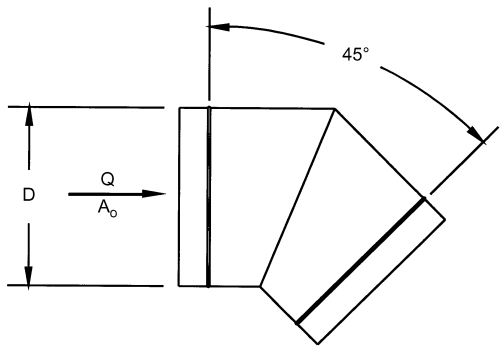

CD6-1 Screen (Only)

	C_o Values n												
A_1/A_o	0.30	0.35	0.40	0.45	0.50	0.55	0.60	0.65	0.70	0.75	0.80	0.90	1.00
0.2	155.00	102.50	75.00	55.00	41.25	31.50	24.25	18.75	14.50	11.00	8.00	3.50	0.00
0.3	68.89	45.56	33.33	24.44	18.33	14.00	10.78	8.33	6.44	4.89	3.56	1.56	0.00
0.4	38.75	25.63	18.75	13.75	10.31	7.88	6.06	4.69	3.63	2.75	2.00	0.88	0.00
0.5	24.80	16.40	12.00	8.80	6.60	5.04	3.88	3.00	2.32	1.76	1.28	0.56	0.00
0.6	17.22	11.39	8.33	6.11	4.58	3.50	2.69	2.08	1.61	1.22	0.89	0.39	0.00
0.7	12.65	8.37	6.12	4.49	3.37	2.57	1.98	1.53	1.18	0.90	0.65	0.29	0.00
0.8	9.69	6.40	4.69	3.44	2.58	1.97	1.52	1.17	0.91	0.69	0.50	0.22	0.00
0.9	7.65	5.06	3.70	2.72	2.04	1.56	1.20	0.93	0.72	0.54	0.40	0.17	0.00
1.0	6.20	4.10	3.00	2.20	1.65	1.26	0.97	0.75	0.58	0.44	0.32	0.14	0.00
1.2	4.31	2.85	2.08	1.53	1.15	0.88	0.67	0.52	0.40	0.31	0.22	0.10	0.00
1.4	3.16	2.09	1.53	1.12	0.84	0.64	0.49	0.38	0.30	0.22	0.16	0.07	0.00
1.6	2.42	1.60	1.17	0.86	0.64	0.49	0.38	0.29	0.23	0.17	0.13	0.05	0.00
1.8	1.91	1.27	0.93	0.68	0.51	0.39	0.30	0.23	0.18	0.14	0.10	0.04	0.00
2.0	1.55	1.03	0.75	0.55	0.41	0.32	0.24	0.19	0.15	0.11	0.08	0.04	0.00
2.5	0.99	0.66	0.48	0.35	0.26	0.20	0.16	0.12	0.09	0.07	0.05	0.02	0.00
3.0	0.69	0.46	0.33	0.24	0.18	0.14	0.11	0.08	0.06	0.05	0.04	0.02	0.00
4.0	0.39	0.26	0.19	0.14	0.10	0.08	0.06	0.05	0.04	0.03	0.02	0.01	0.00
6.0	0.17	0.11	0.08	0.06	0.05	0.04	0.03	0.02	0.02	0.01	0.01	0.00	0.00

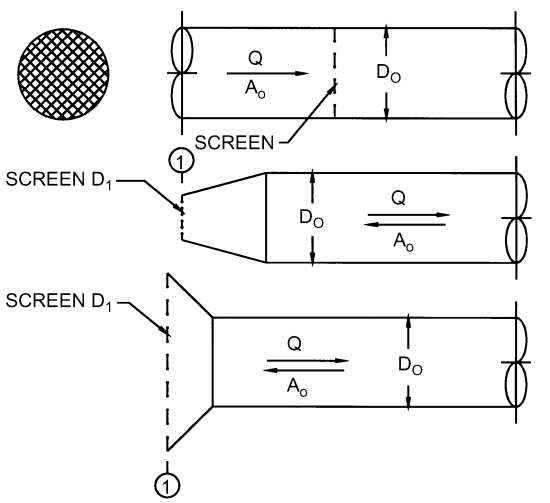

n = free area ratio of screen
A_o = area of duct
A_1 = cross-sectional area of duct or fitting where screen is located

CD6-4 Round Duct, Depressed to Avoid an Obstruction

$C_o = 0.24$

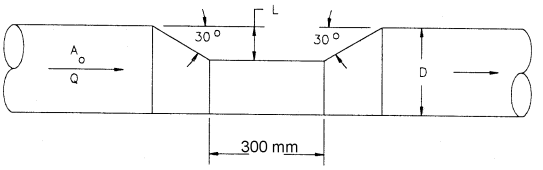

CD9-1 Damper, Butterfly

	C_o Values											
	θ											
D/D_o	0	10	20	30	40	50	60	70	75	80	85	90
0.5	0.19	0.27	0.37	0.49	0.61	0.74	0.86	0.96	0.99	1.02	1.04	1.04
0.6	0.19	0.32	0.48	0.69	0.94	1.21	1.48	1.72	1.82	1.89	1.93	2.00
0.7	0.19	0.37	0.64	1.01	1.51	2.12	2.81	3.46	3.73	3.94	4.08	6.00
0.8	0.19	0.45	0.87	1.55	2.60	4.13	6.14	8.38	9.40	10.30	10.80	15.00
0.9	0.19	0.54	1.22	2.51	4.97	9.57	17.80	30.50	38.00	45.00	50.10	100.00
1.0	0.19	0.67	1.76	4.38	11.20	32.00	113.00	619.00	2010.00	10350.00	99999.00	99999.00

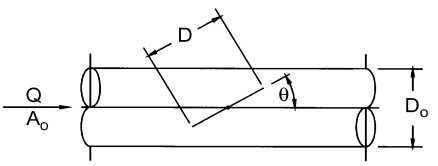

CD9-3 Fire Damper, Curtain Type, Type C

$C_o = 0.12$

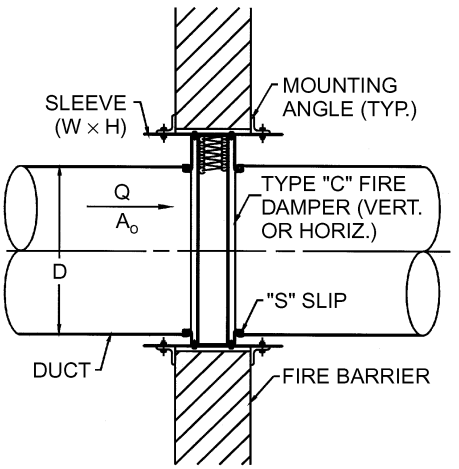

ED1-1 Duct Mounted in Wall

	C_o Values								
	L/D								
t/D	0.00	0.002	0.01	0.05	0.10	0.20	0.30	0.50	10.00
0.00	0.50	0.57	0.68	0.80	0.86	0.92	0.97	1.00	1.00
0.02	0.50	0.51	0.52	0.55	0.60	0.66	0.69	0.72	0.72
0.05	0.50	0.50	0.50	0.50	0.50	0.50	0.50	0.50	0.50
10.00	0.50	0.50	0.50	0.50	0.50	0.50	0.50	0.50	0.50

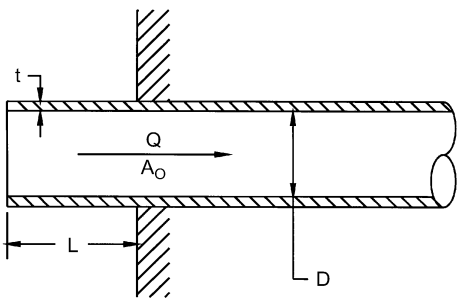

ED1-3 Bellmouth, with Wall

r/D	0.00	0.01	0.02	0.03	0.04	0.05	0.06	0.08	0.10	0.12	0.16	0.20	10.00
C_o	0.50	0.44	0.37	0.31	0.26	0.22	0.20	0.15	0.12	0.09	0.06	0.03	0.03

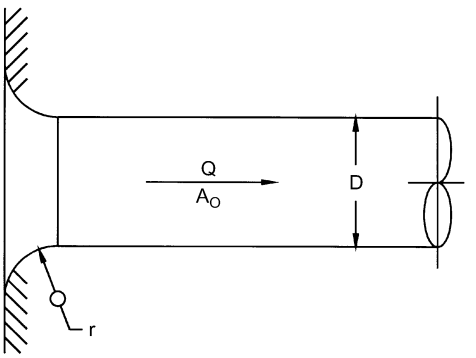

ED2-1 Conical Diffuser, Round to Plenum, Exhaust/Return Systems

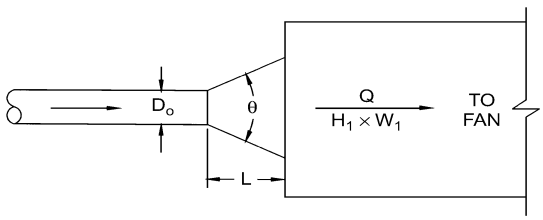

	C_o Values										
	L/D_o										
A_1/A_o	**0.5**	**1.0**	**2.0**	**3.0**	**4.0**	**5.0**	**6.0**	**8.0**	**10.0**	**12.0**	**14.0**
1.5	0.03	0.02	0.03	0.03	0.04	0.05	0.06	0.08	0.10	0.11	0.13
2.0	0.08	0.06	0.04	0.04	0.04	0.05	0.05	0.06	0.08	0.09	0.10
2.5	0.13	0.09	0.06	0.06	0.06	0.06	0.06	0.06	0.07	0.08	0.09
3.0	0.17	0.12	0.09	0.07	0.07	0.06	0.06	0.07	0.07	0.08	0.08
4.0	0.23	0.17	0.12	0.10	0.09	0.08	0.08	0.08	0.08	0.08	0.08
6.0	0.30	0.22	0.16	0.13	0.12	0.10	0.10	0.09	0.09	0.09	0.08
8.0	0.34	0.26	0.18	0.15	0.13	0.12	0.11	0.10	0.09	0.09	0.09
10.0	0.36	0.28	0.20	0.16	0.14	0.13	0.12	0.11	0.10	0.09	0.09
14.0	0.39	0.30	0.22	0.18	0.16	0.14	0.13	0.12	0.10	0.10	0.10
20.0	0.41	0.32	0.24	0.20	0.17	0.15	0.14	0.12	0.11	0.11	0.10
	Optimum Angle θ										
A_1/A_o	**0.5**	**1.0**	**2.0**	**3.0**	**4.0**	**5.0**	**6.0**	**8.0**	**10.0**	**12.0**	**14.0**
1.5	34	20	13	9	7	6	4	3	2	2	2
2.0	42	28	17	12	10	9	8	6	5	4	3
2.5	50	32	20	15	12	11	10	8	7	6	5
3.0	54	34	22	17	14	12	11	10	8	8	6
4.0	58	40	26	20	16	14	13	12	10	10	9
6.0	62	42	28	22	19	16	15	12	11	10	9
8.0	64	44	30	24	20	18	16	13	12	11	10
10.0	66	46	30	24	22	19	17	14	12	11	10
14.0	66	48	32	26	22	19	17	14	13	11	11
20.0	68	48	32	26	22	20	18	15	13	12	11

ED4-1 Transition, Round to Round, Exhaust/Return Systems

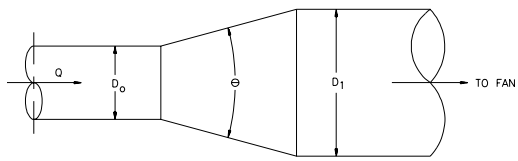

	C_o Values									
	θ									
A_o/A_1	**10**	**15**	**20**	**30**	**45**	**60**	**90**	**120**	**150**	**180**
0.06	0.21	0.29	0.38	0.60	0.84	0.88	0.88	0.88	0.88	0.88
0.10	0.21	0.28	0.38	0.59	0.76	0.80	0.83	0.84	0.83	0.83
0.25	0.16	0.22	0.30	0.46	0.61	0.68	0.64	0.63	0.62	0.62
0.50	0.11	0.13	0.19	0.32	0.33	0.33	0.32	0.31	0.30	0.30
1.00	0.00	0.00	0.00	0.00	0.00	0.00	0.00	0.00	0.00	0.00
2.00	0.20	0.20	0.20	0.20	0.22	0.24	0.48	0.72	0.96	1.04
4.00	0.80	0.64	0.64	0.64	0.88	1.12	2.72	4.32	5.60	6.56
6.00	1.80	1.44	1.44	1.44	1.98	2.52	6.48	10.10	13.00	15.10
10.00	5.00	5.00	5.00	5.00	6.50	8.00	19.00	29.00	37.00	43.00

ED4-2 Transition, Round to Rectangular, Exhaust/Return Systems

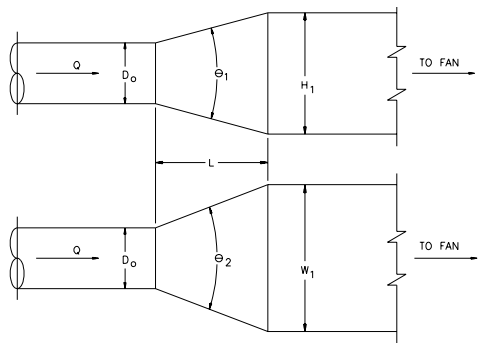

	C_o Values									
	θ									
A_o/A_1	**10**	**15**	**20**	**30**	**45**	**60**	**90**	**120**	**150**	**180**
0.06	0.30	0.54	0.53	0.65	0.77	0.88	0.95	0.98	0.98	0.93
0.10	0.30	0.50	0.53	0.64	0.75	0.84	0.89	0.91	0.91	0.88
0.25	0.25	0.36	0.45	0.52	0.58	0.62	0.64	0.64	0.64	0.64
0.50	0.15	0.21	0.25	0.30	0.33	0.33	0.33	0.32	0.31	0.30
1.00	0.00	0.00	0.00	0.00	0.00	0.00	0.00	0.00	0.00	0.00
2.00	0.24	0.28	0.26	0.20	0.22	0.24	0.49	0.73	0.97	1.04
4.00	0.89	0.78	0.79	0.70	0.88	1.12	2.72	4.33	5.62	6.58
6.00	1.89	1.67	1.59	1.49	1.98	2.52	6.51	10.14	13.05	15.14
10.00	5.09	5.32	5.15	5.05	6.50	8.05	19.06	29.07	37.08	43.05

ED5-1 Wye, 30 Degree, Converging

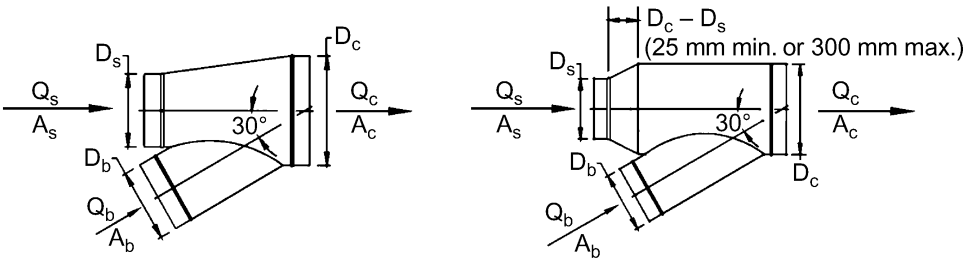

		C_b Values								
		Q_b/Q_c								
A_s/A_c	A_b/A_c	0.1	0.2	0.3	0.4	0.5	0.6	0.7	0.8	0.9
0.2	0.2	−24.17	−3.78	−0.60	0.30	0.64	0.77	0.83	0.88	0.98
	0.3	−55.88	−9.77	−2.57	−0.50	0.25	0.55	0.67	0.70	0.71
	0.4	−99.93	−17.94	−5.13	−1.45	−0.11	0.42	0.62	0.68	0.68
	0.5	−156.51	−28.40	−8.37	−2.62	−0.52	0.30	0.62	0.71	0.69
	0.6	−225.62	−41.13	−12.30	−4.01	−0.99	0.20	0.66	0.78	0.75
	0.7	−307.26	−56.14	−16.90	−5.61	−1.51	0.11	0.73	0.90	0.86
	0.8	−401.44	−73.44	−22.18	−7.44	−2.08	0.04	0.84	1.06	1.01
	0.9	−508.15	−93.02	−28.15	−9.49	−2.71	−0.03	0.99	1.27	1.20
	1.0	−627.39	−114.89	−34.80	−11.77	−3.39	−0.08	1.18	1.52	1.43
0.3	0.2	−13.97	−1.77	0.08	0.59	0.77	0.84	0.88	0.92	1.06
	0.3	−33.06	−5.33	−1.09	0.10	0.51	0.66	0.71	0.72	0.74
	0.4	−59.43	−10.08	−2.52	−0.41	0.32	0.59	0.67	0.68	0.66
	0.5	−93.24	−16.11	−4.30	−1.00	0.14	0.56	0.69	0.70	0.66
	0.6	−134.51	−23.45	−6.44	−1.68	−0.03	0.57	0.76	0.77	0.70
	0.7	−183.25	−32.08	−8.93	−2.45	−0.21	0.61	0.87	0.88	0.79
	0.8	−239.47	−42.01	−11.77	−3.32	−0.38	0.69	1.02	1.03	0.91
	0.9	−303.16	−53.25	−14.97	−4.27	−0.56	0.80	1.21	1.23	1.07
	1.0	−374.32	−65.79	−18.53	−5.32	−0.73	0.94	1.45	1.47	1.27
0.4	0.2	−9.20	−0.85	0.39	0.71	0.82	0.87	0.90	0.94	1.09
	0.3	−22.31	−3.24	−0.38	0.39	0.64	0.73	0.76	0.78	0.85
	0.4	−40.52	−6.48	−1.37	0.02	0.48	0.64	0.67	0.66	0.65
	0.5	−63.71	−10.50	−2.50	−0.33	0.40	0.63	0.69	0.67	0.63
	0.6	−92.00	−15.37	−3.84	−0.71	0.33	0.67	0.75	0.71	0.65
	0.7	−125.40	−21.08	−5.40	−1.13	0.28	0.75	0.85	0.80	0.70
	0.8	−163.90	−27.65	−7.16	−1.59	0.25	0.86	1.00	0.93	0.80
	0.9	−207.52	−35.07	−9.14	−2.09	0.25	1.02	1.18	1.10	0.93
	1.0	−256.25	−43.35	−11.33	−2.63	0.26	1.21	1.42	1.31	1.09
0.5	0.2	−6.62	−0.36	0.54	0.77	0.85	0.88	0.90	0.95	1.11
	0.3	−16.42	−2.11	−0.01	0.54	0.72	0.78	0.80	0.83	0.96
	0.4	−30.26	−4.59	−0.79	0.22	0.54	0.64	0.66	0.64	0.64
	0.5	−47.68	−7.55	−1.61	−0.02	0.48	0.63	0.65	0.62	0.59
	0.6	−68.93	−11.13	−2.56	−0.28	0.45	0.67	0.69	0.65	0.58
	0.7	−94.00	−15.31	−3.65	−0.55	0.44	0.74	0.77	0.71	0.61
	0.8	−122.90	−20.12	−4.88	−0.83	0.46	0.85	0.90	0.81	0.68
	0.9	−155.63	−25.54	−6.25	−1.12	0.51	1.00	1.06	0.94	0.77
	1.0	−192.18	−31.58	−7.77	−1.43	0.59	1.19	1.26	1.12	0.90
0.6	0.2	−5.12	−0.10	0.62	0.79	0.85	0.87	0.90	0.95	1.11
	0.3	−13.00	−1.49	0.18	0.61	0.75	0.79	0.82	0.86	1.02
	0.4	−24.31	−3.55	−0.50	0.30	0.55	0.62	0.63	0.62	0.63
	0.5	−38.41	−5.94	−1.16	0.09	0.48	0.59	0.60	0.57	0.55
	0.6	−55.58	−8.80	−1.92	−0.12	0.45	0.61	0.62	0.57	0.52
	0.7	−75.83	−12.16	−2.79	−0.33	0.44	0.66	0.67	0.60	0.52
	0.8	−99.17	−16.00	−3.76	−0.54	0.46	0.74	0.76	0.67	0.56
	0.9	−125.60	−20.33	−4.83	−0.76	0.51	0.86	0.88	0.77	0.62
	1.0	−155.12	−25.14	−6.02	−0.99	0.58	1.02	1.04	0.90	0.71
0.7	0.2	−4.24	0.05	0.65	0.80	0.85	0.87	0.89	0.94	1.12
	0.3	−11.00	−1.15	0.27	0.63	0.75	0.79	0.82	0.87	1.06
	0.4	−20.82	−3.00	−0.38	0.31	0.52	0.59	0.60	0.59	0.61
	0.5	−32.99	−5.09	−0.98	0.10	0.43	0.53	0.54	0.52	0.51
	0.6	−47.78	−7.58	−1.67	−0.11	0.38	0.52	0.53	0.49	0.45
	0.7	−65.22	−10.50	−2.44	−0.32	0.34	0.53	0.54	0.49	0.43
	0.8	−85.32	−13.83	−3.30	−0.53	0.33	0.58	0.59	0.52	0.43
	0.9	−108.07	−17.58	−4.26	−0.75	0.34	0.66	0.67	0.58	0.46
	1.0	−133.48	−21.76	−5.30	−0.97	0.38	0.76	0.78	0.67	0.51

ED5-1 Wye, 30 Degree, Converging (*Continued*)

		C_b Values (*Concluded*)								
		Q_b/Q_c								
A_s/A_c	A_b/A_c	**0.1**	**0.2**	**0.3**	**0.4**	**0.5**	**0.6**	**0.7**	**0.8**	**0.9**
0.8	0.2	−3.75	0.11	0.65	0.79	0.84	0.86	0.88	0.94	1.12
	0.3	−9.88	−0.99	0.29	0.63	0.74	0.78	0.81	0.87	1.09
	0.4	−18.88	−2.75	−0.36	0.28	0.48	0.55	0.56	0.57	0.61
	0.5	−29.98	−4.71	−0.96	0.04	0.36	0.46	0.47	0.46	0.47
	0.6	−43.46	−7.05	−1.64	−0.20	0.26	0.41	0.43	0.41	0.39
	0.7	−59.34	−9.77	−2.40	−0.44	0.19	0.38	0.41	0.38	0.34
	0.8	−77.64	−12.88	−3.26	−0.69	0.13	0.38	0.42	0.37	0.31
	0.9	−98.35	−16.38	−4.20	−0.95	0.09	0.40	0.45	0.39	0.30
	1.0	−121.48	−20.27	−5.24	−1.23	0.06	0.45	0.51	0.43	0.31
0.9	0.2	−3.52	0.12	0.64	0.78	0.82	0.85	0.88	0.93	1.12
	0.3	−9.34	−0.95	0.28	0.60	0.71	0.76	0.80	0.87	1.10
	0.4	−17.96	−2.70	−0.40	0.22	0.43	0.50	0.53	0.54	0.60
	0.5	−28.58	−4.65	−1.05	−0.07	0.26	0.37	0.40	0.41	0.42
	0.6	−41.45	−6.97	−1.77	−0.35	0.12	0.28	0.32	0.32	0.32
	0.7	−56.61	−9.66	−2.58	−0.65	0.00	0.21	0.27	0.26	0.24
	0.8	−74.08	−12.74	−3.49	−0.97	−0.12	0.16	0.23	0.22	0.18
	0.9	−93.84	−16.21	−4.50	−1.30	−0.23	0.13	0.21	0.19	0.14
	1.0	−115.92	−20.06	−5.61	−1.66	−0.34	0.11	0.21	0.18	0.11
1.0	0.2	−3.48	0.10	0.62	0.76	0.81	0.84	0.87	0.92	1.11
	0.3	−9.22	−1.00	0.23	0.56	0.68	0.74	0.78	0.86	1.11
	0.4	−17.76	−2.79	−0.50	0.14	0.37	0.45	0.49	0.52	0.60
	0.5	−28.31	−4.82	−1.21	−0.20	0.15	0.28	0.33	0.35	0.38
	0.6	−41.06	−7.21	−2.01	−0.55	−0.04	0.15	0.22	0.23	0.25
	0.7	−56.09	−9.99	−2.91	−0.92	−0.23	0.03	0.12	0.14	0.15
	0.8	−73.39	−13.17	−3.92	−1.32	−0.41	−0.07	0.04	0.06	0.06
	0.9	−92.98	−16.75	−5.04	−1.75	−0.60	−0.17	−0.03	−0.01	−0.02
	1.0	−114.85	−20.74	−6.28	−2.21	−0.79	−0.26	−0.09	−0.07	−0.09
		C_s Values								
		Q_s/Q_c								
A_s/A_c	A_b/A_c	**0.1**	**0.2**	**0.3**	**0.4**	**0.5**	**0.6**	**0.7**	**0.8**	**0.9**
0.2	0.2	−16.02	−3.15	−0.80	0.04	0.45	0.69	0.86	0.99	1.10
	0.3	−11.65	−1.94	−0.26	0.32	0.60	0.77	0.90	1.01	1.10
	0.4	−8.56	−1.20	0.05	0.47	0.68	0.82	0.92	1.02	1.11
	0.5	−6.41	−0.71	0.25	0.57	0.73	0.84	0.93	1.02	1.11
	0.6	−4.85	−0.36	0.38	0.63	0.76	0.86	0.94	1.02	1.11
	0.7	−3.68	−0.10	0.48	0.68	0.79	0.87	0.95	1.03	1.11
	0.8	−2.77	0.10	0.56	0.71	0.81	0.88	0.95	1.03	1.11
	0.9	−2.04	0.26	0.62	0.74	0.82	0.89	0.95	1.03	1.11
	1.0	−1.45	0.38	0.66	0.76	0.83	0.89	0.96	1.03	1.11
0.3	0.2	−36.37	−7.59	−2.48	−0.79	−0.06	0.29	0.47	0.57	0.61
	0.3	−26.79	−5.07	−1.42	−0.27	0.21	0.42	0.53	0.59	0.61
	0.4	−19.94	−3.49	−0.80	0.02	0.35	0.49	0.56	0.60	0.62
	0.5	−15.18	−2.44	−0.41	0.20	0.43	0.54	0.58	0.61	0.62
	0.6	−11.73	−1.70	−0.13	0.32	0.49	0.56	0.60	0.61	0.62
	0.7	−9.13	−1.14	0.07	0.41	0.53	0.58	0.60	0.61	0.62
	0.8	−7.11	−0.72	0.23	0.48	0.57	0.60	0.61	0.62	0.62
	0.9	−5.49	−0.38	0.35	0.53	0.59	0.61	0.62	0.62	0.62
	1.0	−4.17	−0.11	0.45	0.58	0.61	0.62	0.62	0.62	0.62
0.4	0.2	−64.82	−13.76	−4.74	−1.81	−0.59	−0.02	0.24	0.36	0.39
	0.3	−47.92	−9.38	−2.93	−0.94	−0.16	0.19	0.34	0.39	0.40
	0.4	−35.81	−6.62	−1.88	−0.46	0.07	0.30	0.38	0.41	0.40
	0.5	−27.39	−4.78	−1.20	−0.16	0.22	0.36	0.41	0.42	0.41
	0.6	−21.28	−3.48	−0.73	0.04	0.31	0.41	0.43	0.43	0.41
	0.7	−16.68	−2.51	−0.38	0.20	0.38	0.44	0.45	0.43	0.41
	0.8	−13.10	−1.77	−0.12	0.31	0.44	0.46	0.46	0.44	0.41
	0.9	−10.24	−1.18	0.09	0.40	0.48	0.48	0.46	0.44	0.41
	1.0	−7.90	−0.69	0.26	0.47	0.51	0.50	0.47	0.44	0.41

ED5-1 Wye, 30 Degree, Converging (*Concluded*)

		C_s Values (*Concluded*)								
		Q_s/Q_c								
A_s/A_c	A_b/A_c	0.1	0.2	0.3	0.4	0.5	0.6	0.7	0.8	0.9
0.5	0.2	−101.39	−21.64	−7.61	−3.07	−1.19	−0.34	0.05	0.22	0.26
	0.3	−75.05	−14.87	−4.83	−1.75	−0.54	−0.03	0.19	0.26	0.27
	0.4	−56.18	−10.59	−3.21	−1.02	−0.20	0.13	0.26	0.29	0.27
	0.5	−43.04	−7.74	−2.16	−0.56	0.02	0.23	0.30	0.30	0.27
	0.6	−33.51	−5.72	−1.43	−0.24	0.16	0.30	0.33	0.31	0.28
	0.7	−26.34	−4.22	−0.90	−0.01	0.27	0.35	0.35	0.32	0.28
	0.8	−20.75	−3.06	−0.49	0.16	0.35	0.39	0.37	0.33	0.28
	0.9	−16.29	−2.14	−0.17	0.30	0.41	0.41	0.38	0.33	0.28
	1.0	−12.64	−1.39	0.10	0.41	0.46	0.44	0.39	0.33	0.28
0.6	0.2	−146.06	−31.26	−11.09	−4.56	−1.89	−0.68	−0.12	0.10	0.16
	0.3	−108.19	−21.55	−7.12	−2.69	−0.97	−0.24	0.07	0.17	0.17
	0.4	−81.04	−15.40	−4.80	−1.65	−0.48	−0.01	0.17	0.20	0.18
	0.5	−62.13	−11.31	−3.30	−0.99	−0.17	0.13	0.22	0.22	0.18
	0.6	−48.43	−8.41	−2.25	−0.54	0.03	0.22	0.26	0.24	0.18
	0.7	−38.10	−6.25	−1.49	−0.22	0.18	0.29	0.29	0.25	0.19
	0.8	−30.07	−4.59	−0.90	0.03	0.30	0.34	0.31	0.25	0.19
	0.9	−23.64	−3.27	−0.44	0.23	0.39	0.38	0.33	0.26	0.19
	1.0	−18.39	−2.20	−0.06	0.39	0.46	0.42	0.34	0.27	0.19
0.7	0.2	−198.85	−42.62	−15.17	−6.31	−2.68	−1.04	−0.29	0.01	0.08
	0.3	−147.33	−29.41	−9.78	−3.77	−1.44	−0.45	−0.04	0.10	0.10
	0.4	−110.40	−21.07	−6.64	−2.36	−0.77	−0.14	0.09	0.15	0.11
	0.5	−84.67	−15.50	−4.60	−1.48	−0.36	0.05	0.17	0.17	0.11
	0.6	−66.02	−11.56	−3.19	−0.86	−0.08	0.18	0.23	0.19	0.12
	0.7	−51.97	−8.63	−2.15	−0.42	0.12	0.27	0.27	0.20	0.12
	0.8	−41.04	−6.37	−1.35	−0.08	0.27	0.34	0.29	0.21	0.12
	0.9	−32.30	−4.58	−0.72	0.19	0.39	0.39	0.32	0.22	0.12
	1.0	−25.16	−3.12	−0.21	0.40	0.49	0.43	0.33	0.23	0.13
0.8	0.2	−259.75	−55.70	−19.86	−8.29	−3.56	−1.43	−0.46	−0.06	0.03
	0.3	−192.48	−38.47	−12.84	−4.99	−1.95	−0.66	−0.12	0.05	0.05
	0.4	−144.25	−27.58	−8.74	−3.16	−1.09	−0.26	0.05	0.11	0.06
	0.5	−110.65	−20.32	−6.08	−2.00	−0.55	−0.01	0.15	0.15	0.07
	0.6	−86.30	−15.17	−4.24	−1.20	−0.19	0.15	0.22	0.17	0.08
	0.7	−67.95	−11.34	−2.88	−0.62	0.08	0.27	0.27	0.19	0.08
	0.8	−53.67	−8.40	−1.84	−0.18	0.28	0.36	0.30	0.20	0.08
	0.9	−42.26	−6.05	−1.02	0.16	0.44	0.43	0.33	0.21	0.08
	1.0	−32.93	−4.15	−0.35	0.44	0.56	0.49	0.36	0.22	0.09
0.9	0.2	−328.76	−70.51	−25.16	−10.53	−4.54	−1.84	−0.62	−0.12	0.00
	0.3	−243.63	−48.72	−16.28	−6.35	−2.50	−0.87	−0.20	0.03	0.03
	0.4	−182.60	−34.94	−11.09	−4.03	−1.41	−0.37	0.02	0.10	0.04
	0.5	−140.07	−25.75	−7.74	−2.57	−0.74	−0.06	0.15	0.14	0.05
	0.6	−109.25	−19.24	−5.40	−1.56	−0.28	0.15	0.23	0.17	0.05
	0.7	−86.04	−14.40	−3.68	−0.83	0.06	0.30	0.30	0.20	0.06
	0.8	−67.96	−10.66	−2.37	−0.27	0.31	0.41	0.34	0.21	0.06
	0.9	−53.52	−7.70	−1.33	0.17	0.51	0.50	0.38	0.22	0.06
	1.0	−41.71	−5.29	−0.49	0.52	0.67	0.57	0.41	0.23	0.07
1.0	0.2	−405.88	−87.06	−31.07	−13.01	−5.62	−2.29	−0.77	−0.16	−0.02
	0.3	−300.78	−60.15	−20.11	−7.85	−3.10	−1.09	−0.26	0.02	0.02
	0.4	−225.44	−43.14	−13.70	−4.99	−1.76	−0.47	0.01	0.11	0.04
	0.5	−172.93	−31.80	−9.56	−3.18	−0.92	−0.09	0.17	0.17	0.05
	0.6	−134.89	−23.76	−6.68	−1.94	−0.35	0.17	0.28	0.20	0.06
	0.7	−106.23	−17.78	−4.56	−1.04	0.06	0.36	0.35	0.23	0.06
	0.8	−83.92	−13.18	−2.93	−0.35	0.37	0.50	0.41	0.25	0.06
	0.9	−66.08	−9.52	−1.65	0.19	0.62	0.61	0.46	0.26	0.07
	1.0	−51.51	−6.54	−0.61	0.63	0.81	0.70	0.49	0.28	0.07

ED5-2 Wye, 45 Degree, Converging

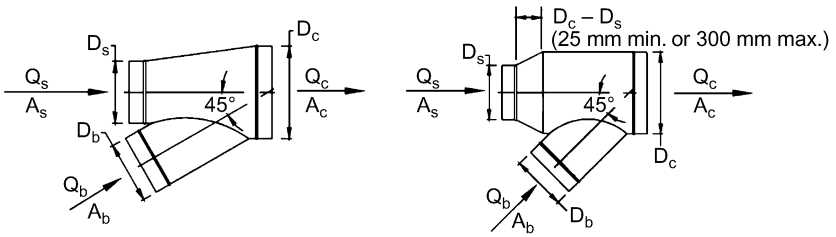

		C_b Values								
		Q_b/Q_c								
A_s/A_c	A_b/A_c	0.1	0.2	0.3	0.4	0.5	0.6	0.7	0.8	0.9
0.2	0.2	−25.19	−3.97	−0.64	0.32	0.67	0.82	0.90	0.96	1.08
	0.3	−58.03	−10.14	−2.63	−0.45	0.36	0.69	0.84	0.93	1.08
	0.4	−104.08	−18.80	−5.40	−1.51	−0.07	0.52	0.77	0.88	1.01
	0.5	−163.36	−29.97	−8.97	−2.87	−0.62	0.29	0.67	0.80	0.84
	0.6	−235.59	−43.47	−13.22	−4.44	−1.20	0.12	0.65	0.83	0.85
	0.7	−320.90	−59.38	−18.21	−6.25	−1.84	−0.04	0.68	0.91	0.93
	0.8	−419.32	−77.73	−23.95	−8.33	−2.56	−0.22	0.72	1.02	1.02
	0.9	−530.86	−98.50	−30.44	−10.66	−3.36	−0.40	0.79	1.16	1.14
	1.0	−655.51	−121.72	−37.68	−13.26	−4.25	−0.59	0.87	1.33	1.28
0.3	0.2	−14.27	−1.77	0.13	0.66	0.85	0.93	0.97	1.03	1.21
	0.3	−33.62	−5.28	−0.95	0.27	0.70	0.87	0.94	1.01	1.19
	0.4	−60.85	−10.26	−2.48	−0.30	0.47	0.77	0.88	0.93	1.04
	0.5	−95.87	−16.64	−4.44	−1.00	0.21	0.66	0.82	0.84	0.84
	0.6	−138.38	−24.26	−6.68	−1.73	0.01	0.66	0.88	0.91	0.88
	0.7	−188.60	−33.25	−9.32	−2.58	−0.20	0.68	0.98	1.02	0.95
	0.8	−246.54	−43.60	−12.34	−3.54	−0.43	0.72	1.11	1.15	1.03
	0.9	−312.21	−55.33	−15.76	−4.61	−0.68	0.78	1.26	1.31	1.13
	1.0	−385.59	−68.43	−19.56	−5.79	−0.94	0.86	1.45	1.49	1.24
0.4	0.2	−8.77	−0.64	0.54	0.85	0.95	0.99	1.03	1.09	1.31
	0.3	−21.41	−2.85	−0.10	0.63	0.87	0.96	1.00	1.06	1.26
	0.4	−39.30	−6.02	−1.05	0.28	0.72	0.87	0.91	0.92	1.00
	0.5	−62.10	−9.96	−2.16	−0.06	0.63	0.85	0.90	0.88	0.86
	0.6	−89.77	−14.65	−3.42	−0.38	0.61	0.93	0.99	0.95	0.90
	0.7	−122.46	−20.19	−4.88	−0.74	0.61	1.04	1.12	1.06	0.95
	0.8	−160.18	−26.56	−6.55	−1.15	0.62	1.18	1.29	1.19	1.01
	0.9	−202.93	−33.77	−8.44	−1.60	0.64	1.36	1.48	1.35	1.07
	1.0	−250.70	−41.83	−10.54	−2.09	0.68	1.56	1.71	1.53	1.15
0.5	0.2	−5.45	0.04	0.79	0.97	1.02	1.04	1.07	1.14	1.39
	0.3	−14.10	−1.39	0.40	0.84	0.97	1.00	1.02	1.07	1.28
	0.4	−26.48	−3.53	−0.24	0.59	0.83	0.89	0.88	0.85	0.86
	0.5	−41.84	−5.96	−0.80	0.51	0.88	0.97	0.95	0.90	0.87
	0.6	−60.61	−8.90	−1.46	0.43	0.97	1.09	1.06	0.97	0.90
	0.7	−82.80	−12.36	−2.22	0.35	1.09	1.25	1.20	1.08	0.93
	0.8	−108.39	−16.35	−3.09	0.27	1.24	1.45	1.38	1.20	0.96
	0.9	−137.41	−20.86	−4.07	0.19	1.42	1.68	1.59	1.35	0.99
	1.0	−169.84	−25.90	−5.15	0.11	1.63	1.95	1.83	1.52	1.02
0.6	0.2	−5.54	−0.08	0.70	0.91	0.98	1.01	1.05	1.14	1.42
	0.3	−14.48	−1.75	0.13	0.64	0.81	0.88	0.92	0.98	1.19
	0.4	−27.10	−4.14	−0.68	0.26	0.57	0.68	0.71	0.72	0.76
	0.5	−42.84	−6.91	−1.50	−0.02	0.47	0.64	0.68	0.69	0.70
	0.6	−62.07	−10.28	−2.48	−0.34	0.37	0.61	0.67	0.66	0.63
	0.7	−84.79	−14.26	−3.62	−0.71	0.27	0.59	0.67	0.63	0.54
	0.8	−111.02	−18.84	−4.92	−1.12	0.16	0.58	0.67	0.61	0.44
	0.9	−140.76	−24.03	−6.40	−1.57	0.04	0.58	0.68	0.59	0.31
	1.0	−174.01	−29.83	−8.04	−2.07	−0.08	0.58	0.70	0.56	0.15
0.7	0.2	−3.96	0.25	0.83	0.97	1.01	1.04	1.08	1.17	1.47
	0.3	−11.07	−1.10	0.34	0.71	0.83	0.87	0.90	0.95	1.13
	0.4	−20.92	−2.92	−0.27	0.43	0.65	0.72	0.73	0.73	0.77
	0.5	−33.20	−5.01	−0.85	0.24	0.59	0.69	0.71	0.69	0.70
	0.6	−48.21	−7.55	−1.55	0.03	0.53	0.68	0.69	0.65	0.61
	0.7	−65.95	−10.56	−2.37	−0.20	0.48	0.68	0.69	0.62	0.49
	0.8	−86.42	−14.01	−3.30	−0.46	0.43	0.68	0.69	0.58	0.35
	0.9	−109.65	−17.93	−4.35	−0.75	0.38	0.70	0.70	0.53	0.18
	1.0	−135.63	−22.32	−5.53	−1.07	0.33	0.72	0.71	0.48	−0.03

ED5-2 Wye, 45 Degree, Converging (*Continued*)

		C_b Values (*Concluded*)								
		Q_b/Q_c								
A_s/A_c	A_b/A_c	0.1	0.2	0.3	0.4	0.5	0.6	0.7	0.8	0.9
0.8	0.2	−2.78	0.50	0.91	1.01	1.03	1.05	1.09	1.18	1.49
	0.3	−8.58	−0.65	0.47	0.74	0.82	0.85	0.86	0.89	1.02
	0.4	−16.29	−2.00	0.05	0.56	0.71	0.75	0.74	0.74	0.78
	0.5	−25.98	−3.59	−0.37	0.44	0.68	0.73	0.72	0.69	0.69
	0.6	−37.82	−5.52	−0.87	0.31	0.65	0.72	0.70	0.64	0.58
	0.7	−51.83	−7.79	−1.44	0.17	0.63	0.73	0.69	0.59	0.43
	0.8	−68.01	−10.42	−2.10	0.01	0.62	0.75	0.69	0.53	0.25
	0.9	−86.37	−13.39	−2.84	−0.16	0.61	0.77	0.68	0.47	0.03
	1.0	−106.91	−16.73	−3.68	−0.35	0.61	0.79	0.68	0.38	−0.25
0.9	0.2	−1.87	0.68	0.98	1.03	1.05	1.06	1.09	1.18	1.49
	0.3	−6.70	−0.33	0.54	0.74	0.79	0.80	0.80	0.81	0.87
	0.4	−12.69	−1.29	0.29	0.66	0.76	0.77	0.75	0.74	0.78
	0.5	−20.37	−2.48	0.00	0.59	0.74	0.75	0.72	0.69	0.67
	0.6	−29.77	−3.94	−0.34	0.52	0.73	0.75	0.70	0.63	0.54
	0.7	−40.89	−5.66	−0.73	0.45	0.74	0.76	0.68	0.56	0.36
	0.8	−53.74	−7.64	−1.18	0.37	0.76	0.78	0.67	0.48	0.13
	0.9	−68.32	−9.89	−1.69	0.28	0.77	0.80	0.65	0.38	−0.15
	1.0	−84.66	−12.42	−2.27	0.18	0.80	0.83	0.62	0.26	−0.49
1.0	0.2	−1.17	0.81	1.02	1.05	1.05	1.06	1.09	1.18	1.48
	0.3	−5.09	−0.02	0.64	0.78	0.81	0.81	0.80	0.80	0.86
	0.4	−9.81	−0.72	0.48	0.74	0.79	0.78	0.76	0.74	0.77
	0.5	−15.89	−1.61	0.29	0.71	0.79	0.77	0.72	0.68	0.65
	0.6	−23.34	−2.69	0.07	0.68	0.80	0.77	0.69	0.60	0.49
	0.7	−32.15	−3.96	−0.18	0.66	0.82	0.78	0.67	0.51	0.27
	0.8	−42.35	−5.44	−0.47	0.64	0.85	0.79	0.63	0.41	0.00
	0.9	−53.94	−7.12	−0.80	0.61	0.88	0.81	0.60	0.28	−0.34
	1.0	−66.93	−9.01	−1.17	0.58	0.92	0.82	0.55	0.13	−0.75
		C_s Values								
		Q_s/Q_c								
A_s/A_c	A_b/A_c	0.1	0.2	0.3	0.4	0.5	0.6	0.7	0.8	0.9
0.2	0.2	−10.16	−2.08	−0.43	0.24	0.62	0.88	1.10	1.29	1.46
	0.3	−7.83	−1.20	0.03	0.50	0.77	0.97	1.14	1.30	1.46
	0.4	−5.62	−0.59	0.30	0.65	0.85	1.01	1.16	1.31	1.46
	0.5	−3.96	−0.18	0.48	0.74	0.90	1.04	1.18	1.32	1.47
	0.6	−2.71	0.12	0.60	0.80	0.94	1.06	1.19	1.32	1.47
	0.7	−1.75	0.34	0.70	0.85	0.96	1.07	1.19	1.32	1.47
	0.8	−0.99	0.52	0.77	0.88	0.98	1.08	1.20	1.32	1.47
	0.9	−0.38	0.66	0.82	0.91	0.99	1.09	1.20	1.33	1.47
	1.0	0.13	0.77	0.87	0.93	1.00	1.10	1.20	1.33	1.47
0.3	0.2	−23.33	−5.14	−1.67	−0.44	0.12	0.42	0.58	0.67	0.72
	0.3	−18.44	−3.44	−0.84	0.00	0.36	0.54	0.64	0.69	0.73
	0.4	−13.64	−2.22	−0.34	0.25	0.49	0.60	0.67	0.70	0.73
	0.5	−10.00	−1.37	0.00	0.41	0.57	0.64	0.69	0.71	0.73
	0.6	−7.26	−0.75	0.24	0.52	0.62	0.67	0.70	0.72	0.73
	0.7	−5.15	−0.29	0.41	0.60	0.66	0.69	0.71	0.72	0.73
	0.8	−3.48	0.07	0.55	0.66	0.69	0.70	0.71	0.72	0.73
	0.9	−2.14	0.36	0.65	0.71	0.72	0.72	0.72	0.72	0.73
	1.0	−1.03	0.60	0.74	0.75	0.73	0.73	0.72	0.72	0.73
0.4	0.2	−42.17	−9.48	−3.34	−1.23	−0.31	0.12	0.33	0.42	0.44
	0.3	−33.68	−6.60	−1.98	−0.53	0.05	0.31	0.41	0.45	0.45
	0.4	−25.24	−4.51	−1.13	−0.13	0.25	0.40	0.46	0.47	0.45
	0.5	−18.83	−3.04	−0.57	0.13	0.37	0.46	0.48	0.48	0.46
	0.6	−13.99	−1.97	−0.17	0.31	0.46	0.50	0.50	0.48	0.46
	0.7	−10.27	−1.17	0.12	0.44	0.52	0.53	0.51	0.49	0.46
	0.8	−7.32	−0.54	0.35	0.54	0.57	0.55	0.52	0.49	0.46
	0.9	−4.94	−0.04	0.53	0.62	0.61	0.57	0.53	0.49	0.46
	1.0	−2.98	0.37	0.68	0.68	0.64	0.58	0.54	0.50	0.46
0.5	0.2	−66.95	−15.18	−5.49	−2.21	−0.81	−0.16	0.14	0.26	0.28
	0.3	−53.80	−10.77	−3.45	−1.17	−0.27	0.11	0.26	0.30	0.29
	0.4	−40.66	−7.54	−2.16	−0.57	0.02	0.25	0.32	0.33	0.30
	0.5	−30.68	−5.27	−1.30	−0.18	0.21	0.33	0.36	0.34	0.30
	0.6	−23.15	−3.62	−0.69	0.09	0.33	0.39	0.38	0.35	0.30
	0.7	−17.34	−2.38	−0.24	0.29	0.42	0.43	0.40	0.35	0.30
	0.8	−12.75	−1.41	0.11	0.44	0.49	0.47	0.41	0.36	0.30
	0.9	−9.04	−0.64	0.39	0.56	0.55	0.49	0.43	0.36	0.30
	1.0	−5.99	0.00	0.61	0.65	0.59	0.51	0.43	0.36	0.30

ED5-2 Wye, 45 Degree, Converging (*Concluded*)

		C_s Values (*Concluded*)								
		Q_s/Q_c								
A_s/A_c	A_b/A_c	0.1	0.2	0.3	0.4	0.5	0.6	0.7	0.8	0.9
0.6	0.2	−97.90	−22.29	−8.18	−3.41	−1.39	−0.46	−0.03	0.13	0.16
	0.3	−79.03	−15.99	−5.28	−1.94	−0.64	−0.09	0.13	0.19	0.17
	0.4	−60.15	−11.37	−3.44	−1.09	−0.23	0.10	0.21	0.22	0.18
	0.5	−45.80	−8.13	−2.22	−0.55	0.03	0.22	0.26	0.24	0.18
	0.6	−34.97	−5.77	−1.35	−0.17	0.20	0.30	0.30	0.25	0.18
	0.7	−26.62	−3.98	−0.71	0.11	0.33	0.36	0.32	0.26	0.19
	0.8	−20.02	−2.59	−0.21	0.33	0.43	0.41	0.34	0.26	0.19
	0.9	−14.68	−1.48	0.18	0.49	0.51	0.44	0.35	0.27	0.19
	1.0	−10.29	−0.57	0.51	0.63	0.57	0.47	0.37	0.27	0.19
0.7	0.2	−135.28	−30.88	−11.42	−4.85	−2.08	−0.80	−0.21	0.02	0.06
	0.3	−109.64	−22.35	−7.50	−2.88	−1.07	−0.31	0.00	0.09	0.07
	0.4	−83.96	−16.08	−5.02	−1.73	−0.52	−0.05	0.11	0.13	0.08
	0.5	−64.44	−11.67	−3.36	−0.99	−0.17	0.11	0.18	0.15	0.09
	0.6	−49.71	−8.47	−2.19	−0.48	0.06	0.22	0.22	0.17	0.09
	0.7	−38.35	−6.04	−1.31	−0.10	0.24	0.30	0.26	0.18	0.09
	0.8	−29.37	−4.16	−0.64	0.18	0.37	0.36	0.28	0.19	0.09
	0.9	−22.12	−2.65	−0.10	0.41	0.47	0.40	0.30	0.19	0.09
	1.0	−16.14	−1.41	0.33	0.60	0.55	0.44	0.32	0.20	0.09
0.8	0.2	−179.32	−41.01	−15.25	−6.55	−2.88	−1.19	−0.41	−0.10	−0.04
	0.3	−145.86	−29.89	−10.14	−3.99	−1.58	−0.55	−0.13	0.00	−0.02
	0.4	−112.34	−21.71	−6.91	−2.50	−0.86	−0.22	0.01	0.05	−0.01
	0.5	−86.85	−15.96	−4.75	−1.54	−0.41	−0.01	0.10	0.08	0.00
	0.6	−67.62	−11.78	−3.22	−0.87	−0.10	0.13	0.16	0.10	0.00
	0.7	−52.79	−8.62	−2.08	−0.38	0.12	0.23	0.20	0.11	0.00
	0.8	−41.06	−6.16	−1.20	0.00	0.29	0.31	0.23	0.12	0.01
	0.9	−31.59	−4.19	−0.51	0.29	0.43	0.37	0.26	0.13	0.01
	1.0	−23.78	−2.58	0.06	0.53	0.54	0.42	0.28	0.14	0.01
0.9	0.2	−230.27	−52.75	−19.69	−8.53	−3.81	−1.63	−0.63	−0.22	−0.13
	0.3	−187.95	−38.69	−13.24	−5.29	−2.16	−0.83	−0.28	−0.10	−0.10
	0.4	−145.53	−28.34	−9.15	−3.41	−1.26	−0.41	−0.10	−0.04	−0.09
	0.5	−113.27	−21.07	−6.42	−2.19	−0.69	−0.15	0.01	0.00	−0.09
	0.6	−88.94	−15.78	−4.48	−1.35	−0.30	0.03	0.09	0.03	−0.08
	0.7	−70.16	−11.78	−3.04	−0.73	−0.02	0.16	0.14	0.04	−0.08
	0.8	−55.33	−8.67	−1.93	−0.25	0.20	0.26	0.18	0.06	−0.07
	0.9	−43.33	−6.18	−1.05	0.12	0.37	0.33	0.21	0.07	−0.07
	1.0	−33.46	−4.14	−0.34	0.42	0.50	0.39	0.24	0.08	−0.07
1.0	0.2	−288.39	−66.15	−24.77	−10.80	−4.88	−2.14	−0.87	−0.35	−0.22
	0.3	−236.14	−48.79	−16.81	−6.80	−2.85	−1.15	−0.44	−0.20	−0.19
	0.4	−183.77	−36.02	−11.76	−4.47	−1.73	−0.63	−0.22	−0.12	−0.18
	0.5	−143.95	−27.05	−8.39	−2.98	−1.03	−0.31	−0.08	−0.08	−0.17
	0.6	−113.91	−20.52	−6.00	−1.93	−0.55	−0.09	0.01	−0.04	−0.16
	0.7	−90.73	−15.58	−4.23	−1.17	−0.20	0.07	0.08	−0.02	−0.16
	0.8	−72.41	−11.74	−2.86	−0.58	0.06	0.19	0.13	−0.01	−0.16
	0.9	−57.61	−8.66	−1.77	−0.12	0.27	0.28	0.16	0.01	−0.15
	1.0	−45.42	−6.15	−0.88	0.25	0.44	0.36	0.20	0.02	−0.15

ED5-3 Tee, D_c < or = 250 mm, Converging

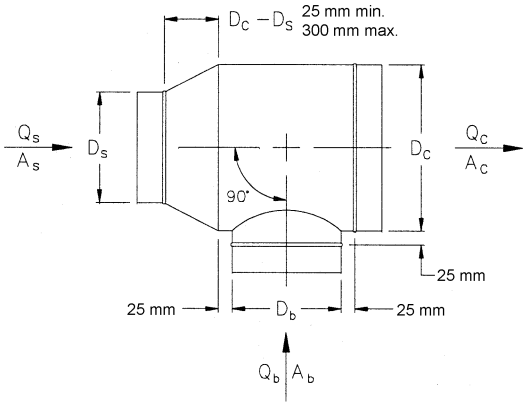

		C_b Values								
		Q_b/Q_c								
A_s/A_c	A_b/A_c	0.1	0.2	0.3	0.4	0.5	0.6	0.7	0.8	0.9
0.2	0.2	–24.56	–3.63	–0.36	0.59	0.93	1.08	1.14	1.19	1.27
	0.3	–56.72	–9.54	–2.15	–0.01	0.78	1.10	1.23	1.30	1.39
	0.4	–101.83	–17.86	–4.68	–0.87	0.52	1.09	1.32	1.41	1.48
	0.5	–159.91	–28.59	–7.98	–2.02	0.17	1.05	1.40	1.51	1.51
	0.6	–230.83	–41.68	–11.98	–3.39	–0.24	1.03	1.53	1.66	1.61
	0.7	–314.56	–57.10	–16.68	–4.98	–0.69	1.04	1.71	1.90	1.82
	0.8	–411.18	–74.90	–22.10	–6.82	–1.21	1.04	1.92	2.16	2.05
	0.9	–520.69	–95.08	–28.25	–8.90	–1.81	1.04	2.15	2.45	2.31
	1.0	–643.09	–117.63	–35.12	–11.24	–2.47	1.04	2.41	2.78	2.58
0.3	0.2	–14.05	–1.55	0.36	0.89	1.08	1.16	1.19	1.23	1.34
	0.3	–33.18	–4.91	–0.58	0.64	1.07	1.23	1.30	1.34	1.44
	0.4	–60.09	–9.68	–1.94	0.24	1.00	1.29	1.39	1.42	1.47
	0.5	–94.80	–15.89	–3.74	–0.33	0.87	1.32	1.46	1.46	1.38
	0.6	–136.97	–23.33	–5.84	–0.92	0.81	1.45	1.65	1.66	1.53
	0.7	–186.81	–32.14	–8.32	–1.62	0.74	1.61	1.88	1.88	1.70
	0.8	–244.33	–42.30	–11.19	–2.43	0.65	1.78	2.14	2.13	1.88
	0.9	–309.54	–53.82	–14.44	–3.35	0.54	1.98	2.42	2.41	2.08
	1.0	–382.43	–66.70	–18.08	–4.39	0.42	2.19	2.74	2.72	2.29
0.4	0.2	–8.95	–0.54	0.71	1.04	1.15	1.20	1.22	1.26	1.40
	0.3	–21.82	–2.70	0.16	0.94	1.19	1.29	1.32	1.35	1.47
	0.4	–39.99	–5.81	–0.67	0.73	1.19	1.35	1.39	1.39	1.41
	0.5	–63.37	–9.82	–1.75	0.45	1.18	1.42	1.47	1.43	1.32
	0.6	–91.72	–14.59	–2.97	0.20	1.26	1.60	1.67	1.60	1.43
	0.7	–125.23	–20.24	–4.41	–0.10	1.34	1.81	1.90	1.81	1.56
	0.8	–163.91	–26.77	–6.09	–0.45	1.43	2.04	2.16	2.03	1.69
	0.9	–207.76	–34.17	–7.99	–0.85	1.53	2.30	2.44	2.28	1.82
	1.0	–256.79	–42.45	–10.12	–1.30	1.63	2.58	2.75	2.54	1.95
0.5	0.2	–6.03	0.04	0.91	1.13	1.20	1.22	1.24	1.29	1.44
	0.3	–15.35	–1.46	0.56	1.09	1.25	1.30	1.32	1.35	1.46
	0.4	–28.59	–3.67	–0.01	0.96	1.26	1.34	1.35	1.32	1.29
	0.5	–45.45	–6.42	–0.66	0.85	1.33	1.45	1.45	1.38	1.24
	0.6	–65.92	–9.70	–1.41	0.78	1.46	1.64	1.63	1.53	1.32
	0.7	–90.12	–13.58	–2.29	0.69	1.61	1.86	1.85	1.70	1.39
	0.8	–118.07	–18.07	–3.32	0.57	1.78	2.11	2.09	1.89	1.46
	0.9	–149.75	–23.18	–4.49	0.43	1.96	2.38	2.35	2.09	1.53
	1.0	–185.19	–28.89	–5.81	0.27	2.16	2.67	2.63	2.31	1.57
0.6	0.2	–4.20	0.39	1.03	1.18	1.22	1.24	1.26	1.30	1.47
	0.3	–11.33	–0.72	0.79	1.16	1.27	1.30	1.31	1.33	1.43
	0.4	–21.57	–2.42	0.35	1.05	1.25	1.29	1.27	1.22	1.12
	0.5	–34.29	–4.35	–0.03	1.07	1.38	1.44	1.41	1.32	1.16
	0.6	–49.85	–6.73	–0.50	1.08	1.54	1.63	1.57	1.45	1.19
	0.7	–68.26	–9.55	–1.06	1.09	1.71	1.83	1.76	1.58	1.21
	0.8	–89.52	–12.81	–1.72	1.10	1.91	2.07	1.97	1.73	1.22
	0.9	–113.64	–16.52	–2.47	1.10	2.12	2.32	2.20	1.88	1.21
	1.0	–140.62	–20.68	–3.33	1.09	2.35	2.60	2.44	2.03	1.16

ED5-3 Tee, D_c < or = 250 mm, Converging (*Continued*)

		C_b Values (*Concluded*)								
		Q_b/Q_c								
A_s/A_c	A_b/A_c	0.1	0.2	0.3	0.4	0.5	0.6	0.7	0.8	0.9
0.7	0.2	–3.00	0.62	1.10	1.21	1.23	1.24	1.26	1.31	1.49
	0.3	–8.74	–0.27	0.91	1.19	1.26	1.27	1.27	1.28	1.36
	0.4	–16.90	–1.59	0.58	1.11	1.25	1.27	1.24	1.18	1.06
	0.5	–26.99	–3.06	0.33	1.17	1.38	1.41	1.36	1.26	1.06
	0.6	–39.35	–4.86	0.02	1.22	1.54	1.57	1.50	1.35	1.05
	0.7	–53.97	–7.01	–0.35	1.29	1.72	1.76	1.65	1.45	1.02
	0.8	–70.87	–9.50	–0.79	1.35	1.91	1.97	1.82	1.54	0.96
	0.9	–90.04	–12.34	–1.31	1.41	2.12	2.19	2.00	1.64	0.86
	1.0	–111.50	–15.53	–1.89	1.46	2.34	2.43	2.19	1.73	0.72
0.8	0.2	–2.20	0.76	1.14	1.22	1.24	1.24	1.26	1.31	1.49
	0.3	–7.04	–0.01	0.95	1.18	1.23	1.23	1.23	1.22	1.27
	0.4	–13.77	–1.06	0.71	1.13	1.24	1.24	1.20	1.13	1.00
	0.5	–22.11	–2.24	0.54	1.20	1.36	1.36	1.30	1.19	0.97
	0.6	–32.33	–3.69	0.31	1.27	1.50	1.50	1.41	1.25	0.90
	0.7	–44.42	–5.41	0.04	1.34	1.66	1.65	1.53	1.30	0.81
	0.8	–58.40	–7.42	–0.29	1.42	1.83	1.83	1.65	1.35	0.67
	0.9	–74.28	–9.72	–0.67	1.49	2.01	2.01	1.78	1.38	0.49
	1.0	–92.06	–12.30	–1.12	1.56	2.21	2.20	1.92	1.40	0.24
0.9	0.2	–1.67	0.85	1.16	1.22	1.23	1.24	1.25	1.30	1.48
	0.3	–5.95	0.12	0.95	1.14	1.18	1.18	1.16	1.15	1.14
	0.4	–11.68	–0.74	0.77	1.12	1.20	1.20	1.16	1.08	0.93
	0.5	–18.85	–1.74	0.63	1.18	1.31	1.30	1.23	1.11	0.86
	0.6	–27.63	–2.98	0.44	1.24	1.42	1.41	1.31	1.13	0.75
	0.7	–38.04	–4.45	0.21	1.30	1.55	1.53	1.39	1.14	0.58
	0.8	–50.07	–6.17	–0.07	1.36	1.69	1.66	1.47	1.13	0.37
	0.9	–63.75	–8.14	–0.40	1.42	1.83	1.79	1.54	1.11	0.09
	1.0	–79.08	–10.36	–0.79	1.46	1.98	1.92	1.61	1.06	–0.26
1.0	0.2	–1.33	0.89	1.16	1.21	1.22	1.22	1.24	1.29	1.46
	0.3	–5.30	0.15	0.90	1.08	1.11	1.11	1.09	1.06	0.99
	0.4	–10.31	–0.57	0.78	1.09	1.16	1.15	1.11	1.03	0.86
	0.5	–16.71	–1.47	0.64	1.13	1.24	1.22	1.15	1.03	0.74
	0.6	–24.56	–2.59	0.46	1.17	1.32	1.30	1.20	1.01	0.57
	0.7	–33.87	–3.93	0.23	1.20	1.41	1.38	1.24	0.97	0.34
	0.8	–44.64	–5.49	–0.05	1.22	1.51	1.46	1.27	0.91	0.05
	0.9	–56.89	–7.29	–0.38	1.24	1.59	1.54	1.28	0.82	–0.33
	1.0	–70.62	–9.32	–0.77	1.24	1.68	1.61	1.28	0.69	–0.80

ED5–3 Tee, D_c < or = 250 mm, Converging

		C_s Values								
		Q_s/Q_c								
A_s/A_c	A_b/A_c	0.1	0.2	0.3	0.4	0.5	0.6	0.7	0.8	0.9
0.2	0.2	18.11	3.42	1.62	1.11	0.90	0.80	0.74	0.70	0.68
	0.3	12.67	2.79	1.45	1.04	0.87	0.78	0.73	0.70	0.68
	0.4	9.98	2.47	1.36	1.01	0.85	0.77	0.72	0.69	0.67
	0.5	8.39	2.27	1.30	0.98	0.84	0.76	0.72	0.69	0.67
	0.6	7.34	2.13	1.26	0.96	0.83	0.76	0.72	0.69	0.67
	0.7	6.61	2.02	1.22	0.95	0.82	0.75	0.71	0.69	0.67
	0.8	6.08	1.94	1.19	0.93	0.81	0.75	0.71	0.68	0.67
	0.9	5.68	1.87	1.17	0.92	0.80	0.74	0.70	0.68	0.66
	1.0	4.55	1.61	1.05	0.86	0.76	0.71	0.68	0.66	0.65
0.3	0.2	44.33	7.19	2.80	1.57	1.08	0.84	0.71	0.63	0.57
	0.3	29.24	5.46	2.33	1.40	1.00	0.80	0.69	0.62	0.57
	0.4	21.88	4.59	2.09	1.30	0.96	0.78	0.67	0.61	0.56
	0.5	17.62	4.06	1.93	1.24	0.92	0.76	0.66	0.60	0.56
	0.6	14.90	3.71	1.82	1.19	0.90	0.74	0.65	0.59	0.55
	0.7	13.06	3.45	1.74	1.15	0.88	0.73	0.64	0.59	0.55
	0.8	11.78	3.26	1.67	1.12	0.86	0.72	0.63	0.58	0.54
	0.9	9.02	2.64	1.41	0.97	0.77	0.66	0.59	0.54	0.51
	1.0	8.36	2.52	1.36	0.95	0.75	0.65	0.58	0.54	0.51

ED5–3 Tee, D_c < or = 250 mm, Converging (*Continued*)

		C_s Values (*Concluded*)								
		Q_s/Q_c								
A_s/A_c	A_b/A_c	0.1	0.2	0.3	0.4	0.5	0.6	0.7	0.8	0.9
0.4	0.2	78.99	12.25	4.42	2.26	1.39	0.97	0.74	0.60	0.50
	0.3	50.14	8.96	3.54	1.92	1.24	0.90	0.70	0.57	0.49
	0.4	36.26	7.32	3.08	1.74	1.16	0.85	0.67	0.56	0.48
	0.5	28.38	6.35	2.80	1.63	1.10	0.82	0.65	0.54	0.47
	0.6	23.50	5.72	2.61	1.54	1.05	0.79	0.63	0.53	0.46
	0.7	20.32	5.27	2.46	1.47	1.02	0.77	0.62	0.52	0.45
	0.8	14.94	4.13	1.98	1.21	0.85	0.65	0.53	0.46	0.40
	0.9	13.55	3.88	1.89	1.16	0.82	0.63	0.52	0.45	0.39
	1.0	12.66	3.69	1.80	1.12	0.79	0.62	0.51	0.44	0.39
0.5	0.2	114.73	17.76	6.27	3.07	1.79	1.16	0.81	0.60	0.46
	0.3	70.56	12.71	4.92	2.56	1.56	1.05	0.75	0.56	0.44
	0.4	49.68	10.24	4.23	2.29	1.43	0.98	0.71	0.54	0.42
	0.5	38.12	8.81	3.81	2.11	1.34	0.93	0.68	0.52	0.41
	0.6	31.23	7.90	3.53	1.99	1.27	0.88	0.65	0.50	0.39
	0.7	21.87	6.00	2.75	1.57	1.01	0.71	0.52	0.40	0.32
	0.8	19.30	5.57	2.59	1.49	0.96	0.67	0.50	0.38	0.30
	0.9	17.84	5.27	2.46	1.42	0.92	0.65	0.48	0.37	0.29
	1.0	17.16	5.05	2.36	1.36	0.88	0.62	0.46	0.35	0.28
0.6	0.2	142.32	22.64	8.06	3.91	2.23	1.39	0.92	0.63	0.44
	0.3	84.89	16.05	6.28	3.24	1.92	1.23	0.83	0.58	0.41
	0.4	58.43	12.90	5.39	2.88	1.75	1.14	0.78	0.55	0.39
	0.5	44.34	11.13	4.86	2.66	1.63	1.07	0.74	0.52	0.37
	0.6	29.06	8.20	3.69	2.04	1.25	0.81	0.55	0.38	0.26
	0.7	24.71	7.51	3.44	1.91	1.18	0.77	0.52	0.35	0.24
	0.8	22.56	7.06	3.26	1.81	1.11	0.72	0.48	0.33	0.22
	0.9	21.89	6.78	3.12	1.73	1.06	0.68	0.45	0.30	0.20
	1.0	22.24	6.61	3.00	1.65	1.00	0.65	0.43	0.28	0.18
0.7	0.2	152.32	25.82	9.48	4.66	2.65	1.63	1.04	0.68	0.44
	0.3	87.85	18.38	7.46	3.88	2.29	1.44	0.94	0.62	0.40
	0.4	59.34	14.92	6.47	3.48	2.09	1.33	0.87	0.58	0.37
	0.5	35.18	10.56	4.78	2.60	1.55	0.97	0.62	0.38	0.22
	0.6	28.26	9.51	4.41	2.42	1.45	0.90	0.57	0.35	0.19
	0.7	25.45	8.91	4.16	2.28	1.36	0.85	0.53	0.32	0.17
	0.8	25.21	8.60	3.99	2.18	1.29	0.79	0.49	0.28	0.14
	0.9	26.68	8.48	3.86	2.08	1.22	0.74	0.45	0.25	0.12
	1.0	29.34	8.49	3.77	2.01	1.16	0.70	0.41	0.22	0.10
0.8	0.2	136.74	26.38	10.30	5.22	3.01	1.85	1.17	0.74	0.45
	0.3	75.52	19.20	8.32	4.45	2.64	1.66	1.06	0.67	0.41
	0.4	37.55	12.79	5.92	3.23	1.91	1.17	0.72	0.42	0.21
	0.5	27.25	11.28	5.41	2.98	1.77	1.08	0.66	0.37	0.18
	0.6	24.23	10.57	5.10	2.81	1.66	1.01	0.60	0.33	0.14
	0.7	25.36	10.32	4.91	2.69	1.57	0.94	0.55	0.29	0.11
	0.8	29.09	10.37	4.80	2.59	1.50	0.88	0.50	0.25	0.08
	0.9	34.55	10.60	4.74	2.50	1.42	0.82	0.46	0.21	0.05
	1.0	41.23	10.98	4.71	2.43	1.36	0.77	0.41	0.18	0.01
0.9	0.2	90.70	23.73	10.34	5.54	3.28	2.05	1.30	0.81	0.47
	0.3	29.93	14.20	6.95	3.86	2.30	1.41	0.85	0.48	0.22
	0.4	16.27	12.21	6.28	3.55	2.12	1.29	0.77	0.42	0.18
	0.5	14.80	11.58	5.96	3.35	1.99	1.20	0.70	0.37	0.14
	0.6	19.43	11.62	5.81	3.23	1.89	1.13	0.64	0.32	0.10
	0.7	27.55	12.06	5.77	3.14	1.81	1.06	0.59	0.27	0.06
	0.8	37.84	12.73	5.79	3.07	1.74	0.99	0.53	0.23	0.02
	0.9	49.59	13.57	5.85	3.01	1.67	0.93	0.48	0.18	–0.02
	1.0	62.35	14.52	5.94	2.97	1.61	0.87	0.42	0.14	–0.06
1.0	0.2	–6.40	12.70	7.32	4.31	2.64	1.64	1.00	0.56	0.25
	0.3	–17.35	10.90	6.66	3.97	2.44	1.51	0.90	0.49	0.20
	0.4	–11.05	11.02	6.50	3.82	2.32	1.41	0.83	0.43	0.15
	0.5	2.15	11.91	6.54	3.74	2.23	1.33	0.76	0.38	0.10
	0.6	18.80	13.18	6.67	3.70	2.16	1.26	0.70	0.32	0.06
	0.7	37.42	14.67	6.86	3.68	2.09	1.19	0.63	0.26	0.01
	0.8	57.27	16.30	7.09	3.67	2.03	1.12	0.57	0.21	–0.04
	0.9	77.95	18.02	7.35	3.66	1.97	1.06	0.51	0.15	–0.09
	1.0	99.20	19.80	7.61	3.67	1.92	1.00	0.45	0.10	–0.14

ED5–3 Tee, D_c > 250 mm, Converging *(Continued)*

		C_b Values								
		Q_b/Q_c								
A_s/A_c	A_b/A_c	0.1	0.2	0.3	0.4	0.5	0.6	0.7	0.8	0.9
0.2	0.2	–26.08	–4.19	–0.70	0.33	0.71	0.87	0.93	0.95	0.93
	0.3	–59.71	–10.53	–2.72	–0.43	0.43	0.78	0.91	0.95	0.91
	0.4	–106.78	–19.39	–5.53	–1.46	0.05	0.67	0.91	0.97	0.91
	0.5	–167.36	–30.77	–9.12	–2.78	–0.42	0.55	0.93	1.02	0.93
	0.6	–241.50	–44.68	–13.50	–4.37	–0.97	0.42	0.96	1.10	0.98
	0.7	–329.25	–61.15	–18.68	–6.25	–1.62	0.27	1.02	1.21	1.06
	0.8	–430.67	–80.18	–24.67	–8.42	–2.37	0.10	1.09	1.35	1.17
	0.9	–545.81	–101.78	–31.47	–10.89	–3.22	–0.08	1.17	1.52	1.31
	1.0	–674.72	–125.98	–39.08	–13.64	–4.17	–0.28	1.28	1.72	1.48
0.3	0.2	–15.50	–2.16	–0.04	0.58	0.81	0.90	0.93	0.94	0.91
	0.3	–35.76	–5.90	–1.20	0.16	0.66	0.85	0.92	0.92	0.88
	0.4	–64.09	–11.09	–2.78	–0.38	0.48	0.82	0.93	0.94	0.86
	0.5	–100.54	–17.73	–4.78	–1.06	0.29	0.80	0.97	0.98	0.87
	0.6	–145.16	–25.85	–7.21	–1.86	0.06	0.80	1.05	1.05	0.90
	0.7	–198.01	–35.46	–10.08	–2.81	–0.19	0.82	1.15	1.16	0.96
	0.8	–259.13	–46.56	–13.39	–3.89	–0.47	0.85	1.28	1.30	1.05
	0.9	–328.59	–59.18	–17.15	–5.11	–0.78	0.89	1.44	1.47	1.17
	1.0	–406.44	–73.33	–21.37	–6.48	–1.12	0.94	1.63	1.68	1.32
0.4	0.2	–10.31	–1.18	0.26	0.69	0.84	0.91	0.93	0.93	0.90
	0.3	–23.96	–3.65	–0.48	0.43	0.75	0.88	0.91	0.91	0.86
	0.4	–42.98	–7.03	–1.46	0.11	0.67	0.87	0.93	0.91	0.84
	0.5	–67.44	–11.35	–2.69	–0.26	0.59	0.90	0.97	0.94	0.84
	0.6	–97.39	–16.60	–4.17	–0.69	0.52	0.95	1.06	1.01	0.87
	0.7	–132.88	–22.81	–5.91	–1.17	0.46	1.03	1.17	1.11	0.92
	0.8	–173.96	–29.99	–7.90	–1.73	0.40	1.15	1.33	1.24	1.00
	0.9	–220.69	–38.15	–10.16	–2.35	0.35	1.29	1.51	1.40	1.11
	1.0	–273.12	–47.31	–12.70	–3.04	0.29	1.45	1.74	1.61	1.26
0.5	0.2	–7.26	–0.62	0.43	0.75	0.86	0.91	0.93	0.93	0.90
	0.3	–16.99	–2.35	–0.07	0.57	0.80	0.89	0.91	0.90	0.87
	0.4	–30.49	–4.67	–0.72	0.38	0.76	0.89	0.92	0.90	0.85
	0.5	–47.82	–7.61	–1.50	0.19	0.75	0.93	0.97	0.93	0.85
	0.6	–69.03	–11.17	–2.42	–0.03	0.76	1.01	1.05	0.98	0.88
	0.7	–94.17	–15.37	–3.49	–0.26	0.80	1.13	1.17	1.07	0.93
	0.8	–123.30	–20.22	–4.71	–0.50	0.87	1.29	1.33	1.20	1.02
	0.9	–156.48	–25.73	–6.09	–0.77	0.96	1.48	1.53	1.36	1.13
	1.0	–193.74	–31.92	–7.63	–1.07	1.06	1.71	1.77	1.56	1.28
0.6	0.2	–5.28	–0.27	0.54	0.78	0.88	0.91	0.93	0.93	0.91
	0.3	–12.43	–1.51	0.18	0.66	0.83	0.89	0.91	0.91	0.89
	0.4	–22.29	–3.15	–0.25	0.55	0.82	0.90	0.92	0.91	0.88
	0.5	–34.92	–5.19	–0.74	0.46	0.84	0.95	0.96	0.93	0.89
	0.6	–50.35	–7.64	–1.30	0.38	0.91	1.05	1.04	0.98	0.93
	0.7	–68.66	–10.52	–1.94	0.32	1.01	1.18	1.16	1.07	0.99
	0.8	–89.89	–13.83	–2.65	0.26	1.15	1.36	1.33	1.19	1.08
	0.9	–114.09	–17.61	–3.46	0.22	1.32	1.59	1.53	1.35	1.21
	1.0	–141.33	–21.84	–4.35	0.18	1.54	1.85	1.77	1.54	1.37
0.7	0.2	–3.90	–0.03	0.61	0.81	0.89	0.92	0.94	0.94	0.93
	0.3	–9.25	–0.94	0.35	0.72	0.85	0.90	0.92	0.92	0.92
	0.4	–16.54	–2.10	0.07	0.66	0.85	0.91	0.93	0.92	0.92
	0.5	–25.85	–3.51	–0.22	0.64	0.90	0.97	0.97	0.94	0.95
	0.6	–37.21	–5.18	–0.54	0.65	1.00	1.07	1.05	1.00	1.00
	0.7	–50.68	–7.13	–0.87	0.70	1.14	1.22	1.17	1.08	1.08
	0.8	–66.31	–9.37	–1.24	0.78	1.33	1.41	1.33	1.21	1.20
	0.9	–84.17	–11.92	–1.64	0.89	1.56	1.65	1.53	1.36	1.34
	1.0	–104.29	–14.78	–2.09	1.03	1.84	1.94	1.78	1.56	1.52
0.8	0.2	–2.90	0.15	0.67	0.83	0.90	0.93	0.94	0.95	0.96
	0.3	–6.91	–0.53	0.47	0.76	0.87	0.91	0.93	0.94	0.96
	0.4	–12.31	–1.34	0.30	0.74	0.88	0.93	0.94	0.95	0.98
	0.5	–19.16	–2.29	0.15	0.77	0.94	0.99	0.98	0.98	1.03
	0.6	–27.50	–3.39	0.01	0.84	1.06	1.09	1.06	1.03	1.11
	0.7	–37.38	–4.66	–0.11	0.97	1.23	1.24	1.18	1.12	1.21
	0.8	–48.87	–6.11	–0.22	1.15	1.46	1.45	1.35	1.25	1.35
	0.9	–62.01	–7.75	–0.33	1.37	1.73	1.70	1.55	1.41	1.52
	1.0	–76.85	–9.59	–0.44	1.63	2.06	2.00	1.80	1.61	1.73

ED5–3 Tee, D_c > 250 mm, Converging *(Continued)*

		C_b Values (*Concluded*)								
		Q_b/Q_c								
A_s/A_c	A_b/A_c	0.1	0.2	0.3	0.4	0.5	0.6	0.7	0.8	0.9
0.9	0.2	–2.14	0.28	0.71	0.85	0.91	0.94	0.96	0.97	0.99
	0.3	–5.14	–0.21	0.57	0.80	0.88	0.92	0.95	0.97	1.02
	0.4	–9.09	–0.76	0.47	0.80	0.91	0.94	0.96	0.98	1.06
	0.5	–14.06	–1.36	0.42	0.86	0.98	1.01	1.01	1.02	1.14
	0.6	–20.08	–2.04	0.42	0.99	1.11	1.12	1.09	1.09	1.24
	0.7	–27.21	–2.79	0.47	1.17	1.30	1.27	1.21	1.19	1.38
	0.8	–35.50	–3.63	0.55	1.42	1.55	1.49	1.38	1.32	1.55
	0.9	–45.01	–4.57	0.66	1.72	1.86	1.75	1.59	1.49	1.75
	1.0	–55.79	–5.64	0.80	2.08	2.22	2.06	1.84	1.69	1.99
1.0	0.2	–1.54	0.39	0.74	0.87	0.92	0.95	0.97	0.99	1.03
	0.3	–3.75	0.03	0.64	0.83	0.90	0.94	0.97	1.00	1.08
	0.4	–6.57	–0.32	0.61	0.85	0.93	0.97	0.99	1.03	1.16
	0.5	–10.05	–0.65	0.64	0.94	1.02	1.03	1.04	1.08	1.26
	0.6	–14.24	–0.98	0.74	1.10	1.16	1.15	1.13	1.16	1.40
	0.7	–19.20	–1.32	0.91	1.33	1.37	1.31	1.26	1.27	1.57
	0.8	–24.98	–1.69	1.14	1.63	1.63	1.53	1.43	1.41	1.78
	0.9	–31.62	–2.10	1.42	2.00	1.96	1.80	1.64	1.59	2.02
	1.0	–39.19	–2.55	1.76	2.43	2.35	2.12	1.90	1.81	2.30

ED5–3 Tee, D_c > 250 mm, Converging

		C_s Values								
		Q_s/Q_c								
A_s/A_c	A_b/A_c	0.1	0.2	0.3	0.4	0.5	0.6	0.7	0.8	0.9
0.2	0.2	20.43	3.28	1.45	0.98	0.81	0.73	0.69	0.66	0.64
	0.3	12.53	2.40	1.22	0.90	0.77	0.71	0.68	0.66	0.64
	0.4	8.78	1.98	1.12	0.86	0.76	0.70	0.67	0.66	0.64
	0.5	6.69	1.75	1.06	0.84	0.75	0.70	0.67	0.65	0.64
	0.6	5.43	1.61	1.02	0.83	0.74	0.70	0.67	0.65	0.64
	0.7	4.64	1.52	1.00	0.82	0.74	0.70	0.67	0.65	0.64
	0.8	4.15	1.47	0.98	0.81	0.74	0.69	0.67	0.65	0.64
	0.9	3.86	1.43	0.97	0.81	0.74	0.69	0.67	0.65	0.64
	1.0	3.71	1.42	0.97	0.81	0.73	0.69	0.67	0.65	0.64
0.3	0.2	51.24	7.11	2.49	1.33	0.90	0.70	0.60	0.54	0.50
	0.3	29.57	4.70	1.87	1.10	0.80	0.66	0.58	0.53	0.50
	0.4	19.40	3.57	1.58	1.00	0.76	0.64	0.57	0.52	0.50
	0.5	13.84	2.96	1.42	0.94	0.73	0.62	0.56	0.52	0.50
	0.6	10.58	2.59	1.32	0.90	0.72	0.62	0.56	0.52	0.49
	0.7	8.64	2.38	1.27	0.88	0.71	0.61	0.56	0.52	0.49
	0.8	7.52	2.25	1.23	0.87	0.70	0.61	0.56	0.52	0.49
	0.9	6.95	2.19	1.22	0.87	0.70	0.61	0.56	0.52	0.49
	1.0	6.76	2.17	1.21	0.86	0.70	0.61	0.55	0.52	0.49
0.4	0.2	90.30	12.10	3.91	1.85	1.08	0.74	0.55	0.45	0.38
	0.3	49.68	7.59	2.74	1.42	0.90	0.65	0.51	0.43	0.37
	0.4	30.96	5.51	2.21	1.23	0.82	0.61	0.49	0.42	0.37
	0.5	21.00	4.40	1.92	1.13	0.78	0.59	0.48	0.42	0.37
	0.6	15.43	3.78	1.76	1.07	0.75	0.58	0.48	0.41	0.37
	0.7	12.36	3.44	1.67	1.04	0.74	0.57	0.48	0.41	0.37
	0.8	10.86	3.27	1.63	1.02	0.73	0.57	0.47	0.41	0.37
	0.9	10.40	3.22	1.61	1.01	0.73	0.57	0.47	0.41	0.37
	1.0	10.67	3.25	1.62	1.02	0.73	0.57	0.47	0.41	0.37
0.5	0.2	126.36	16.99	5.39	2.42	1.32	0.81	0.54	0.38	0.28
	0.3	65.94	10.28	3.65	1.79	1.05	0.68	0.48	0.35	0.27
	0.4	38.84	7.27	2.87	1.51	0.93	0.63	0.45	0.34	0.27
	0.5	25.07	5.74	2.47	1.37	0.87	0.60	0.44	0.33	0.26
	0.6	17.98	4.95	2.27	1.29	0.84	0.58	0.43	0.33	0.26
	0.7	14.69	4.58	2.17	1.26	0.82	0.58	0.43	0.33	0.26
	0.8	13.78	4.48	2.15	1.25	0.82	0.57	0.43	0.33	0.26
	0.9	14.45	4.56	2.17	1.26	0.82	0.58	0.43	0.33	0.26
	1.0	16.24	4.76	2.22	1.28	0.83	0.58	0.43	0.33	0.26

ED5–3 Tee, D_c > 250 mm, Converging (*Continued*)

		C_s Values (*Concluded*)								
		Q_s/Q_c								
A_s/A_c	A_b/A_c	**0.1**	**0.2**	**0.3**	**0.4**	**0.5**	**0.6**	**0.7**	**0.8**	**0.9**
0.6	0.2	146.22	20.32	6.54	2.92	1.54	0.89	0.54	0.33	0.20
	0.3	70.93	11.95	4.37	2.13	1.20	0.73	0.46	0.30	0.18
	0.4	38.66	8.37	3.44	1.80	1.06	0.67	0.43	0.28	0.18
	0.5	23.61	6.70	3.00	1.64	0.99	0.64	0.42	0.28	0.18
	0.6	17.17	5.98	2.82	1.57	0.97	0.62	0.41	0.27	0.18
	0.7	15.64	5.81	2.77	1.56	0.96	0.62	0.41	0.27	0.18
	0.8	17.19	5.98	2.82	1.57	0.97	0.62	0.41	0.27	0.18
	0.9	20.79	6.38	2.92	1.61	0.98	0.63	0.42	0.27	0.18
	1.0	25.82	6.94	3.07	1.66	1.00	0.64	0.42	0.28	0.18
0.7	0.2	137.78	20.74	7.01	3.21	1.70	0.96	0.54	0.29	0.13
	0.3	58.74	11.96	4.73	2.39	1.34	0.79	0.47	0.26	0.12
	0.4	27.78	8.52	3.84	2.06	1.21	0.73	0.44	0.24	0.11
	0.5	16.04	7.21	3.50	1.94	1.15	0.71	0.43	0.24	0.11
	0.6	13.91	6.97	3.44	1.92	1.14	0.70	0.42	0.24	0.11
	0.7	17.28	7.35	3.54	1.95	1.16	0.71	0.43	0.24	0.11
	0.8	24.08	8.10	3.73	2.02	1.19	0.72	0.43	0.24	0.11
	0.9	33.17	9.11	3.99	2.12	1.23	0.74	0.44	0.25	0.11
	1.0	43.86	10.30	4.30	2.23	1.28	0.76	0.45	0.25	0.11
0.8	0.2	92.97	17.35	6.57	3.21	1.75	0.99	0.55	0.27	0.08
	0.3	26.98	10.02	4.67	2.52	1.46	0.86	0.48	0.24	0.07
	0.4	6.75	7.77	4.09	2.31	1.37	0.81	0.46	0.23	0.06
	0.5	4.83	7.56	4.03	2.29	1.36	0.81	0.46	0.23	0.06
	0.6	12.05	8.36	4.24	2.37	1.39	0.83	0.47	0.23	0.07
	0.7	24.51	9.75	4.60	2.49	1.45	0.85	0.48	0.24	0.07
	0.8	40.23	11.49	5.05	2.66	1.52	0.88	0.50	0.24	0.07
	0.9	58.13	13.48	5.57	2.85	1.60	0.92	0.51	0.25	0.07
	1.0	77.56	15.64	6.13	3.05	1.68	0.96	0.53	0.26	0.08
0.9	0.2	10.77	10.05	5.20	2.91	1.70	0.99	0.55	0.25	0.04
	0.3	–21.27	6.49	4.28	2.57	1.56	0.93	0.52	0.24	0.04
	0.4	–19.11	6.73	4.34	2.60	1.57	0.93	0.52	0.24	0.04
	0.5	–3.28	8.49	4.80	2.76	1.64	0.97	0.54	0.24	0.04
	0.6	19.39	11.01	5.45	3.00	1.74	1.01	0.56	0.25	0.04
	0.7	45.97	13.96	6.21	3.27	1.86	1.07	0.58	0.27	0.05
	0.8	74.99	17.18	7.05	3.58	1.98	1.13	0.61	0.28	0.05
	0.9	105.64	20.59	7.93	3.89	2.12	1.19	0.64	0.29	0.06
	1.0	137.43	24.12	8.85	4.23	2.26	1.26	0.67	0.31	0.06
1.0	0.2	–99.78	–0.17	3.15	2.40	1.58	0.98	0.56	0.25	0.02
	0.3	–75.42	2.54	3.85	2.65	1.69	1.03	0.58	0.26	0.03
	0.4	–38.31	6.66	4.92	3.04	1.86	1.11	0.62	0.28	0.03
	0.5	3.90	11.35	6.14	3.48	2.04	1.20	0.66	0.29	0.04
	0.6	48.66	16.32	7.43	3.94	2.24	1.29	0.70	0.31	0.04
	0.7	94.88	21.46	8.76	4.43	2.45	1.38	0.75	0.33	0.05
	0.8	142.01	26.70	10.12	4.92	2.66	1.48	0.79	0.35	0.06
	0.9	189.74	32.00	11.49	5.41	2.87	1.58	0.84	0.37	0.07
	1.0	237.90	37.35	12.88	5.92	3.08	1.68	0.88	0.39	0.07

ED5-6 Capped Wye, Branch with 45-Degree Elbow, Branch 90 Degrees to Main, Converging, r/D_b = 1.5

A_b/A_c	0.1	0.2	0.3	0.4	0.5	0.6	0.7	0.8	0.9	1.0
C_b	1.26	1.07	0.94	0.86	0.81	0.76	0.71	0.67	0.64	0.64

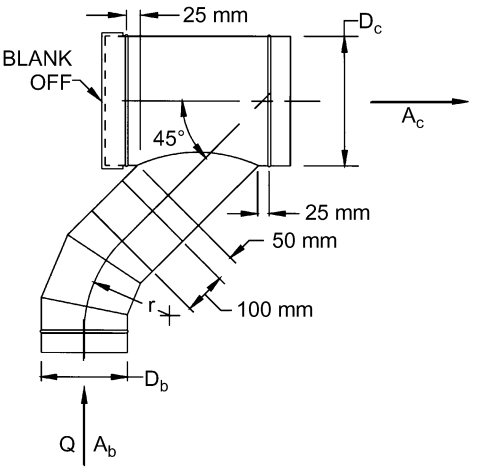

ED5-9 Symmetrical Wye, 60 Degree, $D_{b1} \geq D_{b2}$, Converging

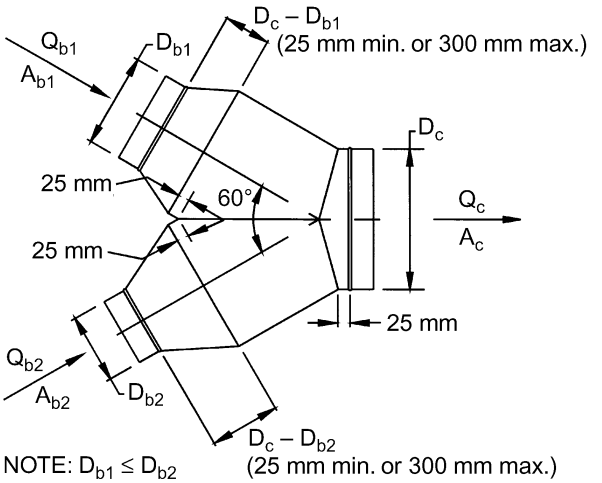

		C_{b1} Values								
		Q_{b1}/Q_c								
A_{b1}/A_c	A_{b2}/A_c	0.1	0.2	0.3	0.4	0.5	0.6	0.7	0.8	0.9
0.2	0.2	−11.95	−1.89	−0.09	0.41	0.62	0.74	0.80	0.80	0.79
	0.3	−11.95	−1.89	−0.09	0.41	0.62	0.74	0.80	0.80	0.79
0.3	0.2	−45.45	−9.39	−2.44	−0.41	0.33	0.68	0.89	1.03	1.13
	0.3	−16.88	−2.92	−0.09	0.59	0.86	1.02	1.09	1.10	1.08
0.4	0.2	−72.04	−14.00	−4.26	−1.24	−0.10	0.33	0.50	0.57	0.63
	0.3	−52.95	−9.91	−2.86	−0.69	0.07	0.30	0.40	0.49	0.62
	0.4	−28.86	−6.22	−2.15	−0.57	0.19	0.55	0.72	0.79	0.85
0.5	0.2	−126.04	−23.80	−7.44	−2.64	−0.85	−0.13	0.16	0.26	0.28
	0.3	−91.07	−16.91	−5.16	−1.73	−0.46	0.04	0.23	0.29	0.28
	0.4	−56.41	−10.07	−2.90	−0.82	−0.07	0.21	0.30	0.31	0.29
	0.5	−30.58	−5.23	−1.06	0.00	0.32	0.43	0.47	0.47	0.41
0.6	0.2	−209.81	−39.31	−12.13	−4.35	−1.54	−0.40	0.06	0.22	0.23
	0.3	−147.43	−27.69	−8.75	−3.20	−1.13	−0.29	0.05	0.17	0.18
	0.4	−85.06	−16.07	−5.38	−2.04	−0.71	−0.17	0.04	0.12	0.13
	0.5	−58.22	−11.03	−3.84	−1.49	−0.50	−0.09	0.07	0.11	0.12
	0.6	−40.57	−7.86	−2.60	−0.99	−0.26	0.00	0.14	0.21	0.25
0.7	0.2	−291.57	−54.52	−17.03	−6.21	−2.27	−0.68	−0.04	0.19	0.21
	0.3	−197.37	−38.02	−12.54	−4.92	−2.01	−0.76	−0.22	0.01	0.08
	0.4	−102.97	−21.41	−8.05	−3.64	−1.75	−0.84	−0.40	−0.17	−0.05
	0.5	−65.15	−14.75	−6.16	−3.07	−1.61	−0.85	−0.44	−0.22	−0.09
	0.6	−48.24	−11.70	−4.97	−2.59	−1.40	−0.76	−0.37	−0.15	−0.03
	0.7	−73.02	−16.68	−6.90	−3.29	−1.61	−0.80	−0.29	0.02	0.22
0.8	0.2	−373.33	−69.73	−21.93	−8.08	−3.00	−0.95	−0.13	0.15	0.20
	0.3	−247.31	−48.35	−16.32	−6.65	−2.89	−1.24	−0.49	−0.15	−0.02
	0.4	−120.88	−26.76	−10.71	−5.24	−2.78	−1.52	−0.84	−0.45	−0.24

ED5-9 Symmetrical Wye, 60 Degree, $D_{b1} \geq D_{b2}$, Converging (*Continued*)

		C_{b1} Values (*Concluded*)								
		Q_{b1}/Q_c								
A_{b1}/A_c	A_{b2}/A_c	**0.1**	**0.2**	**0.3**	**0.4**	**0.5**	**0.6**	**0.7**	**0.8**	**0.9**
	0.5	−72.08	−18.46	−8.48	−4.65	−2.71	−1.61	−0.95	−0.55	−0.31
	0.6	−55.91	−15.54	−7.35	−4.20	−2.54	−1.53	−0.89	−0.51	−0.30
	0.7	−80.68	−20.52	−9.27	−4.90	−2.75	−1.56	−0.80	−0.34	−0.06
	0.8	−105.46	−25.49	−11.19	−5.59	−2.96	−1.60	−0.72	−0.18	0.19
0.9	0.2	−479.24	−89.56	−28.39	−10.59	−4.04	−1.41	−0.36	0.01	0.09
	0.3	−305.31	−61.27	−21.50	−9.28	−4.39	−2.16	−1.07	−0.54	−0.29
	0.4	−131.17	−32.88	−14.60	−7.98	−4.74	−2.91	−1.79	−1.10	−0.68
	0.5	−67.90	−22.76	−12.17	−7.53	−4.89	−3.19	−2.05	−1.30	−0.81
	0.6	−68.95	−23.08	−12.11	−7.45	−4.84	−3.15	−2.01	−1.26	−0.79
	0.7	−90.48	−27.35	−13.58	−7.95	−4.97	−3.16	−1.96	−1.17	−0.65
	0.8	−112.02	−31.63	−15.05	−8.44	−5.11	−3.18	−1.90	−1.07	−0.51
	0.9	−130.32	−35.19	−16.07	−8.70	−5.18	−3.19	−1.88	−1.08	−0.53
1.0	0.2	−585.16	−109.39	−34.85	−13.11	−5.09	−1.86	−0.59	−0.13	−0.01
	0.3	−363.31	−74.20	−26.68	−11.91	−5.90	−3.08	−1.66	−0.94	−0.56
	0.4	−141.46	−39.00	−18.50	−10.71	−6.71	−4.29	−2.74	−1.74	−1.12
	0.5	−63.71	−27.06	−15.85	−10.41	−7.07	−4.77	−3.16	−2.05	−1.31
	0.6	−81.99	−30.62	−16.87	−10.70	−7.13	−4.77	−3.13	−2.02	−1.28
	0.7	−100.28	−34.19	−17.89	−11.00	−7.19	−4.76	−3.11	−1.99	−1.24
	0.8	−118.58	−37.76	−18.91	−11.29	−7.26	−4.76	−3.09	−1.96	−1.20
	0.9	−136.88	−41.32	−19.93	−11.55	−7.32	−4.77	−3.07	−1.98	−1.23
	1.0	−155.18	−44.89	−20.95	−11.80	−7.39	−4.78	−3.05	−1.99	−1.25
		C_{b2} Values								
		Q_{b2}/Q_c								
A_{b1}/A_c	A_{b2}/A_c	**0.1**	**0.2**	**0.3**	**0.4**	**0.5**	**0.6**	**0.7**	**0.8**	**0.9**
0.2	0.2	−11.95	−1.89	−0.09	0.41	0.62	0.74	0.80	0.80	0.79
	0.3	−11.95	−1.89	−0.09	0.41	0.62	0.74	0.80	0.80	0.79
0.3	0.2	−8.24	−1.18	0.05	0.42	0.61	0.73	0.78	0.77	0.76
	0.3	−16.88	−2.92	−0.09	0.59	0.86	1.02	1.09	1.10	1.08
0.4	0.2	−6.95	−1.00	0.16	0.53	0.67	0.71	0.72	0.72	0.71
	0.3	−16.21	−2.90	−0.44	0.40	0.79	0.98	1.05	1.06	1.05
	0.4	−28.86	−6.22	−2.15	−0.57	0.19	0.55	0.72	0.79	0.85
0.5	0.2	−4.82	−0.01	0.56	0.71	0.82	0.89	0.92	0.90	0.89
	0.3	−12.27	−1.17	0.44	0.88	1.11	1.25	1.29	1.25	1.23
	0.4	−20.76	−2.93	−0.21	0.48	0.73	0.84	0.88	0.87	0.82
	0.5	−30.58	−5.23	−1.06	0.00	0.32	0.43	0.47	0.47	0.41
0.6	0.2	−3.68	0.07	0.77	0.98	1.06	1.08	1.08	1.06	1.04
	0.3	−9.06	−0.55	0.86	1.27	1.42	1.48	1.49	1.46	1.42
	0.4	−17.62	−2.12	0.06	0.60	0.83	0.95	0.98	0.95	0.91
	0.5	−28.00	−4.26	−0.99	−0.16	0.20	0.39	0.45	0.41	0.38
	0.6	−40.57	−7.86	−2.60	−0.99	−0.26	0.00	0.14	0.21	0.25
0.7	0.2	−5.44	−0.40	0.55	0.86	0.98	1.02	1.04	1.03	1.02
	0.3	−9.36	−0.77	0.73	1.20	1.39	1.47	1.49	1.47	1.44
	0.4	−19.57	−3.09	−0.44	0.36	0.71	0.89	0.97	0.98	0.97
	0.5	−31.88	−6.02	−1.90	−0.63	−0.05	0.26	0.40	0.44	0.46
	0.6	−46.44	−9.82	−3.47	−1.41	−0.48	−0.04	0.21	0.36	0.45
	0.7	−73.02	−16.68	−6.90	−3.29	−1.61	−0.80	−0.29	0.02	0.22
0.8	0.2	−7.21	−0.87	0.33	0.73	0.90	0.97	1.00	1.00	0.99
	0.3	−9.67	−0.99	0.60	1.13	1.36	1.45	1.49	1.48	1.46
	0.4	−21.53	−4.06	−0.93	0.11	0.59	0.83	0.96	1.01	1.03
	0.5	−35.77	−7.77	−2.82	−1.09	−0.29	0.13	0.35	0.48	0.55
	0.6	−52.32	−11.78	−4.34	−1.83	−0.70	−0.09	0.28	0.51	0.65
	0.7	−78.89	−18.64	−7.76	−3.71	−1.83	−0.85	−0.22	0.16	0.42
	0.8	−105.46	−25.49	−11.19	−5.59	−2.96	−1.60	−0.72	−0.18	0.19
0.9	0.2	−4.98	−0.34	0.54	0.85	0.97	1.03	1.04	1.03	1.01
	0.3	−9.97	−1.21	0.48	1.06	1.32	1.44	1.49	1.49	1.48
	0.4	−23.54	−4.98	−1.39	−0.12	0.47	0.78	0.95	1.04	1.09
	0.5	−40.14	−9.57	−3.69	−1.56	−0.55	−0.01	0.31	0.51	0.63
	0.6	−58.25	−14.28	−5.64	−2.53	−1.08	−0.30	0.18	0.49	0.70
	0.7	−84.09	−21.02	−8.91	−4.38	−2.22	−1.04	−0.31	0.15	0.46
	0.8	−109.92	−27.77	−12.18	−6.22	−3.35	−1.79	−0.81	−0.19	0.23
	0.9	−130.32	−35.19	−16.07	−8.70	−5.18	−3.19	−1.88	−1.08	−0.53
1.0	0.2	−2.75	0.19	0.76	0.96	1.05	1.08	1.08	1.06	1.04
	0.3	−10.28	−1.43	0.35	0.99	1.29	1.43	1.49	1.50	1.50
	0.4	−25.56	−5.89	−1.86	−0.36	0.35	0.72	0.93	1.07	1.15
	0.5	−44.52	−11.37	−4.56	−2.02	−0.81	−0.14	0.27	0.54	0.72
	0.6	−64.19	−16.77	−6.94	−3.24	−1.47	−0.50	0.09	0.48	0.74
	0.7	−89.28	−23.41	−10.05	−5.05	−2.61	−1.24	−0.40	0.14	0.50
	0.8	−114.38	−30.04	−13.16	−6.86	−3.75	−1.97	−0.89	−0.20	0.27
	0.9	−134.78	−37.47	−17.06	−9.33	−5.57	−3.38	−1.97	−1.09	−0.49
	1.0	−155.18	−44.89	−20.95	−11.80	−7.39	−4.78	−3.05	−1.99	−1.25

ED7-1 Centrifugal Fan Located in Plenum or Cabinet

L/D_o	0.30	0.40	0.50	0.75
C_o	0.80	0.53	0.40	0.22

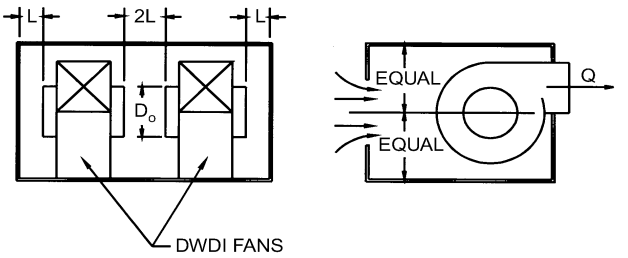

ED7-2 Fan Inlet, Centrifugal, SWSI, with 4 Gore Elbow

	C_o Values			
	L/D_o			
r/D_o	0.0	2.0	5.0	10.0
0.50	1.80	1.00	0.53	0.53
0.75	1.40	0.80	0.40	0.40
1.00	1.20	0.67	0.33	0.33
1.50	1.10	0.60	0.33	0.33
2.00	1.00	0.53	0.33	0.33
3.00	0.67	0.40	0.22	0.22

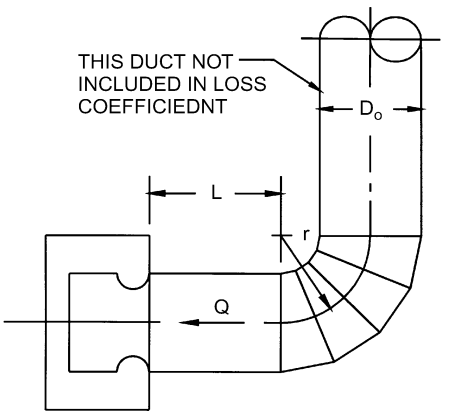

SD1-1 Bellmouth, Plenum to Round, Supply Air Systems

r/D_o	0.00	0.01	0.02	0.03	0.04	0.05	0.06	0.08	0.10	0.12	0.16	0.20	10.00
C_o	0.50	0.44	0.36	0.31	0.26	0.22	0.20	0.15	0.12	0.09	0.06	0.03	0.03

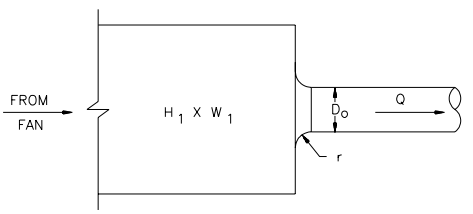

SD1-2 Conical Bellmouth/Sudden Contraction, Plenum to Round, Supply Air Systems

		C_o Values									
		θ									
A_o/A_1	L/D_o	0	10	20	30	45	60	90	120	150	180
0.10	0.025	0.46	0.43	0.42	0.40	0.38	0.37	0.38	0.40	0.43	0.46
	0.050	0.46	0.42	0.38	0.33	0.30	0.28	0.31	0.36	0.41	0.46
	0.075	0.46	0.39	0.32	0.28	0.23	0.21	0.26	0.32	0.39	0.46
	0.100	0.46	0.36	0.30	0.23	0.19	0.17	0.23	0.30	0.38	0.46
	0.150	0.46	0.34	0.25	0.18	0.15	0.14	0.21	0.29	0.37	0.46
	0.300	0.46	0.31	0.22	0.16	0.13	0.13	0.20	0.28	0.37	0.46
	0.600	0.46	0.25	0.17	0.12	0.10	0.11	0.19	0.27	0.36	0.46
0.20	0.025	0.42	0.40	0.38	0.36	0.34	0.34	0.35	0.37	0.39	0.42
	0.050	0.42	0.38	0.35	0.30	0.27	0.25	0.29	0.33	0.37	0.42
	0.075	0.42	0.36	0.30	0.25	0.21	0.19	0.24	0.30	0.36	0.42
	0.100	0.42	0.33	0.27	0.21	0.18	0.15	0.21	0.27	0.35	0.42
	0.150	0.42	0.31	0.23	0.17	0.13	0.13	0.19	0.26	0.34	0.42
	0.300	0.42	0.28	0.20	0.15	0.12	0.12	0.18	0.26	0.34	0.42
	0.600	0.42	0.23	0.15	0.11	0.10	0.10	0.17	0.25	0.33	0.42

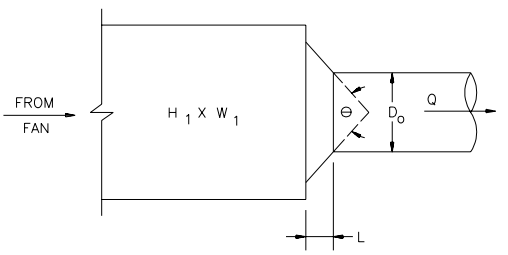

SD1-2 Conical Bellmouth/Sudden Contraction, Plenum to Round, Supply Air Systems (*Continued*)

		C_o Values (*Concluded*)									
		θ									
A_o/A_1	L/D_o	0	10	20	30	45	60	90	120	150	180
0.40	0.025	0.34	0.32	0.31	0.29	0.28	0.27	0.28	0.30	0.32	0.34
	0.050	0.34	0.31	0.28	0.25	0.22	0.20	0.23	0.26	0.30	0.34
	0.075	0.34	0.29	0.24	0.20	0.17	0.16	0.19	0.24	0.29	0.34
	0.100	0.34	0.27	0.22	0.17	0.14	0.12	0.17	0.22	0.28	0.34
	0.150	0.34	0.25	0.18	0.14	0.11	0.10	0.15	0.21	0.27	0.34
	0.300	0.34	0.23	0.16	0.12	0.10	0.10	0.15	0.21	0.27	0.34
	0.600	0.34	0.18	0.12	0.09	0.08	0.08	0.14	0.20	0.27	0.34
0.60	0.025	0.25	0.24	0.23	0.22	0.20	0.20	0.21	0.22	0.23	0.25
	0.050	0.25	0.23	0.21	0.18	0.16	0.15	0.17	0.19	0.22	0.25
	0.075	0.25	0.21	0.18	0.15	0.13	0.12	0.14	0.18	0.21	0.25
	0.100	0.25	0.20	0.16	0.13	0.11	0.09	0.12	0.16	0.21	0.25
	0.150	0.25	0.19	0.14	0.10	0.08	0.08	0.11	0.16	0.20	0.25
	0.300	0.25	0.17	0.12	0.09	0.07	0.07	0.11	0.15	0.20	0.25
	0.600	0.25	0.14	0.09	0.07	0.06	0.06	0.10	0.15	0.20	0.25
0.80	0.025	0.15	0.14	0.13	0.13	0.12	0.12	0.12	0.13	0.14	0.15
	0.050	0.15	0.13	0.12	0.11	0.10	0.09	0.10	0.12	0.13	0.15
	0.075	0.15	0.13	0.10	0.09	0.08	0.07	0.08	0.10	0.13	0.15
	0.100	0.15	0.12	0.10	0.07	0.06	0.05	0.07	0.10	0.12	0.15
	0.150	0.15	0.11	0.08	0.06	0.05	0.04	0.07	0.09	0.12	0.15
	0.300	0.15	0.10	0.07	0.05	0.04	0.04	0.07	0.09	0.12	0.15
	0.600	0.15	0.08	0.05	0.04	0.03	0.04	0.06	0.09	0.12	0.15
0.90	0.025	0.09	0.08	0.08	0.08	0.07	0.07	0.07	0.08	0.08	0.09
	0.050	0.09	0.08	0.07	0.06	0.06	0.05	0.06	0.07	0.08	0.09
	0.075	0.09	0.07	0.06	0.05	0.04	0.04	0.05	0.06	0.08	0.09
	0.100	0.09	0.07	0.06	0.04	0.04	0.03	0.04	0.06	0.07	0.09
	0.150	0.09	0.07	0.05	0.04	0.03	0.03	0.04	0.06	0.07	0.09
	0.300	0.09	0.06	0.04	0.03	0.03	0.02	0.04	0.05	0.07	0.09
	0.600	0.09	0.05	0.03	0.02	0.02	0.02	0.04	0.05	0.07	0.09

SD2-6 Stackhead

D_e/D	0.3	0.4	0.5	0.6	0.7	0.8	0.9	1.0
C_o	129	41.02	16.80	8.10	4.37	2.56	1.60	1.00

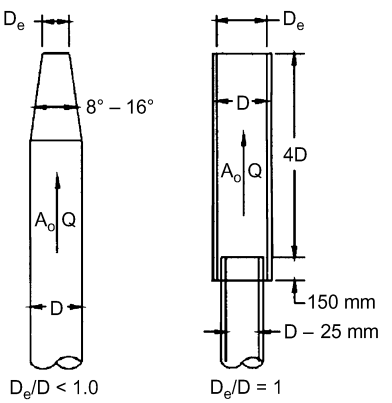

SD4-1 Transition, Round to Round, Supply Air Systems

	C_o Values									
	θ									
A_o/A_1	10	15	20	30	45	60	90	120	150	180
0.10	0.05	0.05	0.05	0.05	0.07	0.08	0.19	0.29	0.37	0.43
0.17	0.05	0.04	0.04	0.04	0.06	0.07	0.18	0.28	0.36	0.42
0.25	0.05	0.04	0.04	0.04	0.06	0.07	0.17	0.27	0.35	0.41
0.50	0.05	0.05	0.05	0.05	0.06	0.06	0.12	0.18	0.24	0.26
1.00	0.00	0.00	0.00	0.00	0.00	0.00	0.00	0.00	0.00	0.00
2.00	0.44	0.52	0.76	1.28	1.32	1.32	1.28	1.24	1.20	1.20
4.00	2.56	3.52	4.80	7.36	9.76	10.88	10.24	10.08	9.92	9.92
10.00	21.00	28.00	38.00	59.00	76.00	80.00	83.00	84.00	83.00	83.00
16.00	53.76	74.24	97.28	153.60	215.04	225.28	225.28	225.28	225.28	225.28

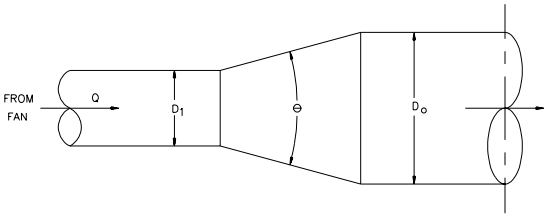

SD4-2 Transition, Rectangular to Round, Supply Air Systems

	C_o Values									
	θ									
A_o/A_1	10	15	20	30	45	60	90	120	150	180
0.10	0.05	0.05	0.05	0.05	0.07	0.08	0.19	0.29	0.37	0.43
0.17	0.05	0.05	0.04	0.04	0.06	0.07	0.18	0.28	0.36	0.42
0.25	0.06	0.05	0.05	0.04	0.06	0.07	0.17	0.27	0.35	0.41
0.50	0.06	0.07	0.07	0.05	0.06	0.06	0.12	0.18	0.24	0.26
1.00	0.00	0.00	0.00	0.00	0.00	0.00	0.00	0.00	0.00	0.00
2.00	0.60	0.84	1.00	1.20	1.32	1.32	1.32	1.28	1.24	1.20
4.00	4.00	5.76	7.20	8.32	9.28	9.92	10.24	10.24	10.24	10.24
10.00	30.00	50.00	53.00	64.00	75.00	84.00	89.00	91.00	91.00	88.00
16.00	76.80	138.24	135.68	166.40	197.12	225.28	243.20	250.88	250.88	238.08

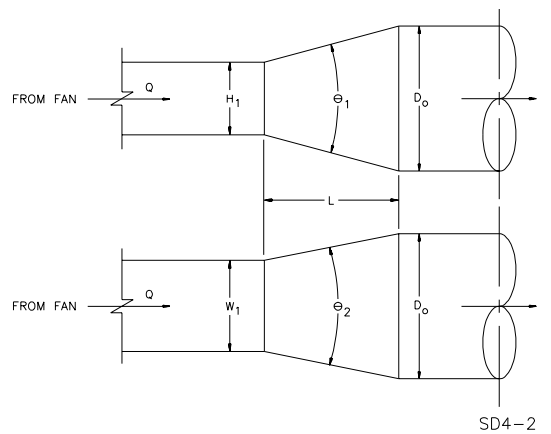

SD5-1 Wye, 45 Degree, Diverging

	C_b Values								
	Q_b/Q_c								
A_b/A_c	0.1	0.2	0.3	0.4	0.5	0.6	0.7	0.8	0.9
0.1	0.38	0.39	0.48						
0.2	2.25	0.38	0.31	0.39	0.46	0.48	0.45		
0.3	6.29	1.02	0.38	0.30	0.33	0.39	0.44	0.48	0.48
0.4	12.41	2.25	0.74	0.38	0.30	0.31	0.35	0.39	0.43
0.5	20.58	4.01	1.37	0.62	0.38	0.30	0.30	0.32	0.36
0.6	30.78	6.29	2.25	1.02	0.56	0.38	0.31	0.30	0.31
0.7	43.02	9.10	3.36	1.57	0.85	0.52	0.38	0.31	0.30
0.8	57.29	12.41	4.71	2.25	1.22	0.74	0.50	0.38	0.32
0.9	73.59	16.24	6.29	3.06	1.69	1.02	0.67	0.48	0.38

	C_s Values								
	Q_s/Q_c								
A_s/A_c	0.1	0.2	0.3	0.4	0.5	0.6	0.7	0.8	0.9
0.1	0.13	0.16							
0.2	0.20	0.13	0.15	0.16	0.28				
0.3	0.90	0.13	0.13	0.14	0.15	0.16	0.20		
0.4	2.88	0.20	0.14	0.13	0.14	0.15	0.15	0.16	0.34
0.5	6.25	0.37	0.17	0.14	0.13	0.14	0.14	0.15	0.15
0.6	11.88	0.90	0.20	0.13	0.14	0.13	0.14	0.14	0.15
0.7	18.62	1.71	0.33	0.18	0.16	0.14	0.13	0.15	0.14
0.8	26.88	2.88	0.50	0.20	0.15	0.14	0.13	0.13	0.14
0.9	36.45	4.46	0.90	0.30	0.19	0.16	0.15	0.14	0.13

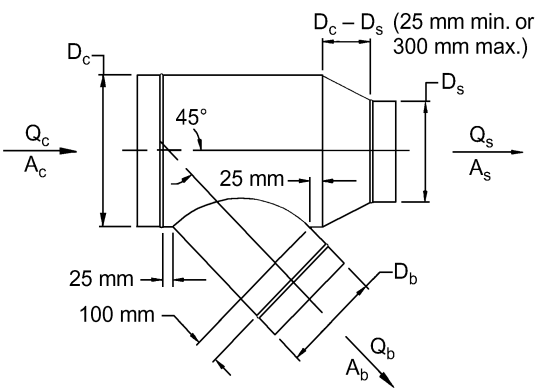

SD5-9 Tee, Diverging

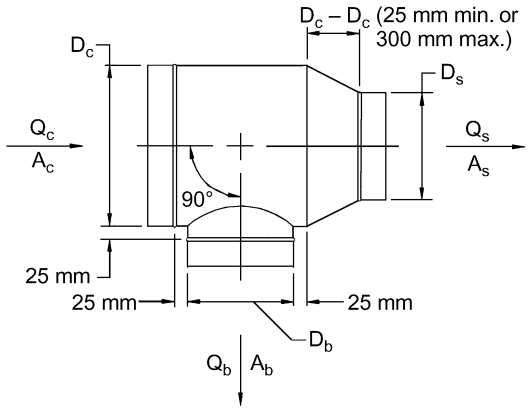

	C_b Values								
	Q_b/Q_c								
A_b/A_c	0.1	0.2	0.3	0.4	0.5	0.6	0.7	0.8	0.9
0.1	1.20	0.62	0.80	1.28	1.99	2.92	4.07	5.44	7.02
0.2	4.10	1.20	0.72	0.62	0.66	0.80	1.01	1.28	1.60
0.3	8.99	2.40	1.20	0.81	0.66	0.62	0.64	0.70	0.80
0.4	15.89	4.10	1.94	1.20	0.88	0.72	0.64	0.62	0.63
0.5	24.80	6.29	2.91	1.74	1.20	0.92	0.77	0.68	0.63
0.6	35.73	8.99	4.10	2.40	1.62	1.20	0.96	0.81	0.72
0.7	48.67	12.19	5.51	3.19	2.12	1.55	1.20	0.99	0.85
0.8	63.63	15.89	7.14	4.10	2.70	1.94	1.49	1.20	1.01
0.9	80.60	20.10	8.99	5.13	3.36	2.40	1.83	1.46	1.20

	C_s Values								
	Q_s/Q_c								
A_s/A_c	0.1	0.2	0.3	0.4	0.5	0.6	0.7	0.8	0.9
0.1	0.13	0.16							
0.2	0.20	0.13	0.15	0.16	0.28				
0.3	0.90	0.13	0.13	0.14	0.15	0.16	0.20		
0.4	2.88	0.20	0.14	0.13	0.14	0.15	0.15	0.16	0.34
0.5	6.25	0.37	0.17	0.14	0.13	0.14	0.14	0.15	0.15
0.6	11.88	0.90	0.20	0.13	0.14	0.13	0.14	0.14	0.15
0.7	18.62	1.71	0.33	0.18	0.16	0.14	0.13	0.15	0.14
0.8	26.88	2.88	0.50	0.20	0.15	0.14	0.13	0.13	0.14
0.9	36.45	4.46	0.90	0.30	0.19	0.16	0.15	0.14	0.13

SD5-10 Tee, Conical Branch Tapered into Body, Diverging

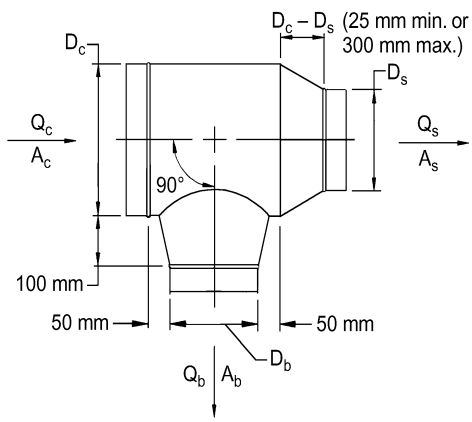

	C_b Values								
	Q_b/Q_c								
A_b/A_c	0.1	0.2	0.3	0.4	0.5	0.6	0.7	0.8	0.9
0.1	0.65	0.24							
0.2	2.98	0.65	0.33	0.24	0.18				
0.3	7.36	1.56	0.65	0.39	0.29	0.24	0.20		
0.4	13.78	2.98	1.20	0.65	0.43	0.33	0.27	0.24	0.21
0.5	22.24	4.92	1.98	1.04	0.65	0.47	0.36	0.30	0.26
0.6	32.73	7.36	2.98	1.56	0.96	0.65	0.49	0.39	0.33
0.7	45.26	10.32	4.21	2.21	1.34	0.90	0.65	0.51	0.42
0.8	59.82	13.78	5.67	2.98	1.80	1.20	0.86	0.65	0.52
0.9	76.41	17.75	7.36	3.88	2.35	1.56	1.11	0.83	0.65

	C_s Values								
	Q_s/Q_c								
A_s/A_c	0.1	0.2	0.3	0.4	0.5	0.6	0.7	0.8	0.9
0.1	0.13	0.16							
0.2	0.20	0.13	0.15	0.16	0.28				
0.3	0.90	0.13	0.13	0.14	0.15	0.16	0.20		
0.4	2.88	0.20	0.14	0.13	0.14	0.15	0.15	0.16	0.34
0.5	6.25	0.37	0.17	0.14	0.13	0.14	0.14	0.15	0.15
0.6	11.88	0.90	0.20	0.13	0.14	0.13	0.14	0.14	0.15
0.7	18.62	1.71	0.33	0.18	0.16	0.14	0.13	0.15	0.14
0.8	26.88	2.88	0.50	0.20	0.15	0.14	0.13	0.13	0.14
0.9	36.45	4.46	0.90	0.30	0.19	0.16	0.15	0.14	0.13

SD5-24 Cross, Diverging

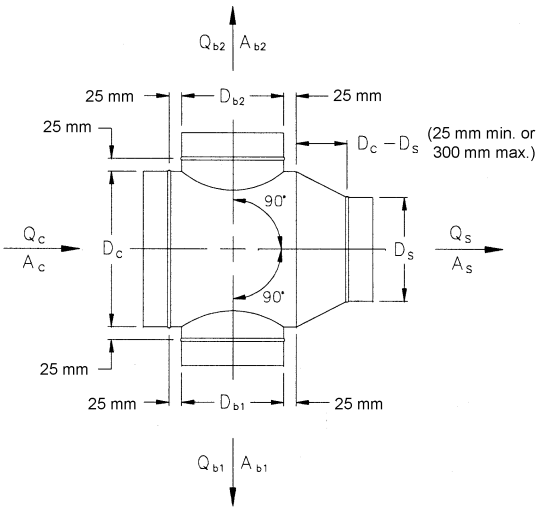

		C_{b1} Values								
		Q_{b1}/Q_c								
A_s/A_c	A_{b1}/A_c	0.1	0.2	0.3	0.4	0.5	0.6	0.7	0.8	0.9
0.20	0.1	2.07	2.08	1.62	1.30	1.08	0.93	0.81	0.72	0.64
	0.2		2.07	2.31	2.08	1.83	1.62	1.44	1.30	1.18
	0.3			2.07	2.34	2.24	2.08	1.91	1.76	1.62
	0.4			0.90	2.07	2.32	2.31	2.21	2.08	1.95
	0.5				1.28	2.07	2.30	2.33	2.27	2.18
	0.6					1.48	2.07	2.29	2.34	2.31
	0.7					0.55	1.60	2.07	2.27	2.33
	0.8						0.90	1.68	2.07	2.25
	0.9							1.12	1.74	2.07
0.35	0.1		3.25	3.11	2.69	2.32	2.03	1.80	1.61	1.46
	0.2			2.44	3.25	3.28	3.11	2.90	2.69	2.49
	0.3				1.69	2.88	3.25	3.31	3.23	3.11
	0.4					1.12	2.44	3.02	3.25	3.31
	0.5						0.69	2.04	2.73	3.09
	0.6							0.37	1.69	2.44
	0.7								0.11	1.38
	0.8									
	0.9									
0.55	0.1		1.50	1.56	1.38	1.20	1.06	0.94	0.84	0.77
	0.2			0.89	1.50	1.60	1.56	1.47	1.38	1.28
	0.3				0.38	1.20	1.50	1.59	1.59	1.56
	0.4					0.00	0.89	1.31	1.50	1.58
	0.5							0.61	1.09	1.36
	0.6								0.38	0.89
	0.7									0.17
	0.8									
	0.9									
0.80	0.1	1.20	0.62	0.80	1.28	1.99	2.92	4.07	5.44	7.02
	0.2	4.10	1.20	0.72	0.62	0.66	0.80	1.01	1.28	1.60
	0.3	8.99	2.40	1.20	0.81	0.66	0.62	0.64	0.70	0.80
	0.4	15.89	4.10	1.94	1.20	0.88	0.72	0.64	0.62	0.63
	0.5	24.80	6.29	2.91	1.74	1.20	0.92	0.77	0.68	0.63
	0.6	35.73	8.99	4.10	2.40	1.62	1.20	0.96	0.81	0.72
	0.7	48.67	12.19	5.51	3.19	2.12	1.55	1.20	0.99	0.85
	0.8	63.63	15.89	7.14	4.10	2.70	1.94	1.49	1.20	1.01
	0.9	80.60	20.10	8.99	5.13	3.36	2.40	1.83	1.46	1.20
1.00	0.1	1.20	0.62	0.80	1.28	1.99	2.92	4.07	5.44	7.02
	0.2	4.10	1.20	0.72	0.62	0.66	0.80	1.01	1.28	1.60
	0.3	8.99	2.40	1.20	0.81	0.66	0.62	0.64	0.70	0.80
	0.4	15.89	4.10	1.94	1.20	0.88	0.72	0.64	0.62	0.63
	0.5	24.80	6.29	2.91	1.74	1.20	0.92	0.77	0.68	0.63
	0.6	35.73	8.99	4.10	2.40	1.62	1.20	0.96	0.81	0.72
	0.7	48.67	12.19	5.51	3.19	2.12	1.55	1.20	0.99	0.85
	0.8	63.63	15.89	7.14	4.10	2.70	1.94	1.49	1.20	1.01
	0.9	80.60	20.10	8.99	5.13	3.36	2.40	1.83	1.46	1.20

	C_s Values								
	Q_s/Q_c								
A_s/A_c	0.1	0.2	0.3	0.4	0.5	0.6	0.7	0.8	0.9
0.1	0.13	0.16							
0.2	0.20	0.13	0.15	0.16	0.28				
0.3	0.90	0.13	0.13	0.14	0.15	0.16	0.20		
0.4	2.88	0.20	0.14	0.13	0.14	0.15	0.15	0.16	0.34
0.5	6.25	0.37	0.17	0.14	0.13	0.14	0.14	0.15	0.15
0.6	11.88	0.90	0.20	0.13	0.14	0.13	0.14	0.14	0.15
0.7	18.62	1.71	0.33	0.18	0.16	0.14	0.13	0.15	0.14
0.8	26.88	2.88	0.50	0.20	0.15	0.14	0.13	0.13	0.14
0.9	36.45	4.46	0.90	0.30	0.19	0.16	0.15	0.14	0.13

For the other branch, subscripts 1 and 2 change places.

SD5-25 Cross, Conical Branches Tapered into Body, Diverging

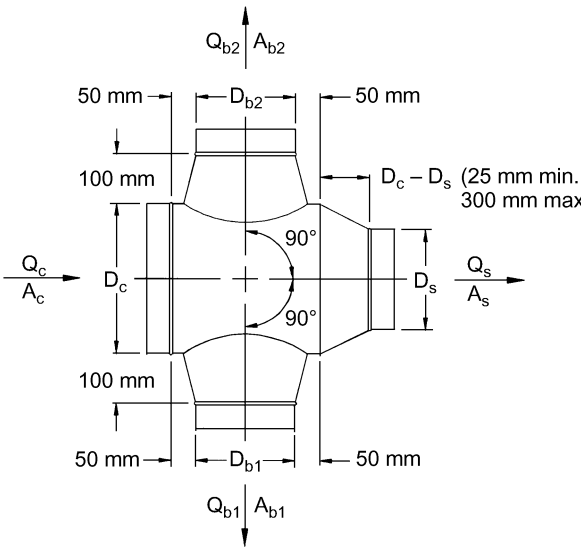

		C_{b1} Values								
		Q_{b1}/Q_c								
A_s/A_c	A_{b1}/A_c	**0.1**	**0.2**	**0.3**	**0.4**	**0.5**	**0.6**	**0.7**	**0.8**	**0.9**
0.20	0.1	2.07	2.08	1.62	1.30	1.08	0.93	0.81	0.72	0.64
	0.2		2.07	2.31	2.08	1.83	1.62	1.44	1.30	1.18
	0.3			2.07	2.34	2.24	2.08	1.91	1.76	1.62
	0.4			0.90	2.07	2.32	2.31	2.21	2.08	1.95
	0.5				1.28	2.07	2.30	2.33	2.27	2.18
	0.6					1.48	2.07	2.29	2.34	2.31
	0.7					0.55	1.60	2.07	2.27	2.33
	0.8						0.90	1.68	2.07	2.25
	0.9							1.12	1.74	2.07
0.35	0.1		3.25	3.11	2.69	2.32	2.03	1.80	1.61	1.46
	0.2			2.44	3.25	3.28	3.11	2.90	2.69	2.49
	0.3				1.69	2.88	3.25	3.31	3.23	3.11
	0.4					1.12	2.44	3.02	3.25	3.31
	0.5						0.69	2.04	2.73	3.09
	0.6							0.37	1.69	2.44
	0.7								0.11	1.38
	0.8									
	0.9									
0.55	0.1		1.50	1.56	1.38	1.20	1.06	0.94	0.84	0.77
	0.2			0.89	1.50	1.60	1.56	1.47	1.38	1.28
	0.3				0.38	1.20	1.50	1.59	1.59	1.56
	0.4					0.00	0.89	1.31	1.50	1.58
	0.5							0.61	1.09	1.36
	0.6								0.38	0.89
	0.7									0.17
	0.8									
	0.9									
0.80	0.1	0.65	0.24							
	0.2	2.98	0.65	0.33	0.24	0.18				
	0.3	7.36	1.56	0.65	0.39	0.29	0.24	0.20		
	0.4	13.78	2.98	1.20	0.65	0.43	0.33	0.27	0.24	0.21
	0.5	22.24	4.92	1.98	1.04	0.65	0.47	0.36	0.30	0.26
	0.6	32.73	7.36	2.98	1.56	0.96	0.65	0.49	0.39	0.33
	0.7	45.26	10.32	4.21	2.21	1.34	0.90	0.65	0.51	0.42
	0.8	59.82	13.78	5.67	2.98	1.80	1.20	0.86	0.65	0.52
	0.9	76.41	17.75	7.36	3.88	2.35	1.56	1.11	0.83	0.65
1.00	0.1	0.65	0.24							
	0.2	2.98	0.65	0.33	0.24	0.18				
	0.3	7.36	1.56	0.65	0.39	0.29	0.24	0.20		
	0.4	13.78	2.98	1.20	0.65	0.43	0.33	0.27	0.24	0.21
	0.5	22.24	4.92	1.98	1.04	0.65	0.47	0.36	0.30	0.26
	0.6	32.73	7.36	2.98	1.56	0.96	0.65	0.49	0.39	0.33
	0.7	45.26	10.32	4.21	2.21	1.34	0.90	0.65	0.51	0.42
	0.8	59.82	13.78	5.67	2.98	1.80	1.20	0.86	0.65	0.52
	0.9	76.41	17.75	7.36	3.88	2.35	1.56	1.11	0.83	0.65

	C_s Values								
	Q_s/Q_c								
A_s/A_c	**0.1**	**0.2**	**0.3**	**0.4**	**0.5**	**0.6**	**0.7**	**0.8**	**0.9**
0.1	0.13	0.16							
0.2	0.20	0.13	0.15	0.16	0.28				
0.3	0.90	0.13	0.13	0.14	0.15	0.16	0.20		
0.4	2.88	0.20	0.14	0.13	0.14	0.15	0.15	0.16	0.34
0.5	6.25	0.37	0.17	0.14	0.13	0.14	0.14	0.15	0.15
0.6	11.88	0.90	0.20	0.13	0.14	0.13	0.14	0.14	0.15
0.7	18.62	1.71	0.33	0.18	0.16	0.14	0.13	0.15	0.14
0.8	26.88	2.88	0.50	0.20	0.15	0.14	0.13	0.13	0.14
0.9	36.45	4.46	0.90	0.30	0.19	0.16	0.15	0.14	0.13

For the other branch, subscripts 1 and 2 change places

RECTANGULAR FITTINGS

CR3-1 Elbow, Smooth Radius, Without Vanes

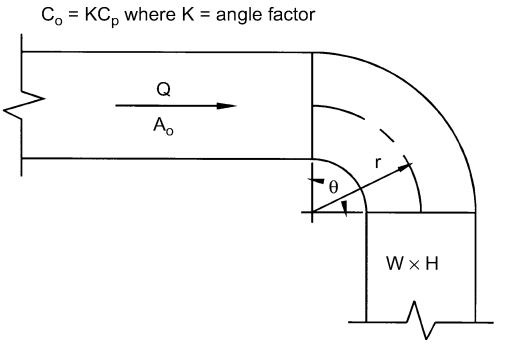

C_p Values											
	H/W										
r/W	0.25	0.50	0.75	1.00	1.50	2.00	3.00	4.00	5.00	6.00	8.00
0.50	1.53	1.38	1.29	1.18	1.06	1.00	1.00	1.06	1.12	1.16	1.18
0.75	0.57	0.52	0.48	0.44	0.40	0.39	0.39	0.40	0.42	0.43	0.44
1.00	0.27	0.25	0.23	0.21	0.19	0.18	0.18	0.19	0.20	0.21	0.21
1.50	0.22	0.20	0.19	0.17	0.15	0.14	0.14	0.15	0.16	0.17	0.17
2.00	0.20	0.18	0.16	0.15	0.14	0.13	0.13	0.14	0.14	0.15	0.15

Angle Factor *K*											
θ	0	20	30	45	60	75	90	110	130	150	180
K	0.00	0.31	0.45	0.60	0.78	0.90	1.00	1.13	1.20	1.28	1.40

CR3-3 Elbow, Smooth Radius, One Splitter Vane

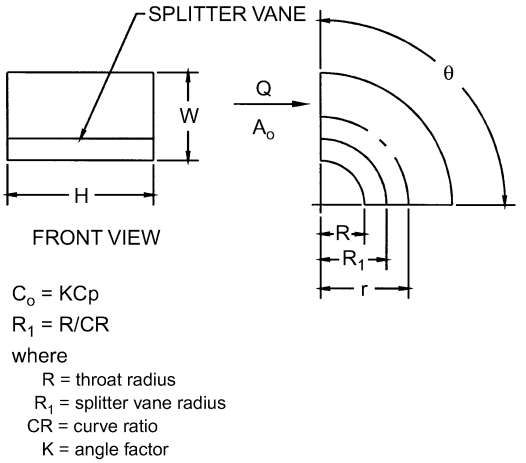

$C_o = KCp$
$R_1 = R/CR$
where
R = throat radius
R_1 = splitter vane radius
CR = curve ratio
K = angle factor

C_p Values											
	H/W										
r/W	0.25	0.50	1.00	1.50	2.00	3.00	4.00	5.00	6.00	7.00	8.00
0.55	0.52	0.40	0.43	0.49	0.55	0.66	0.75	0.84	0.93	1.01	1.09
0.60	0.36	0.27	0.25	0.28	0.30	0.35	0.39	0.42	0.46	0.49	0.52
0.65	0.28	0.21	0.18	0.19	0.20	0.22	0.25	0.26	0.28	0.30	0.32
0.70	0.22	0.16	0.14	0.14	0.15	0.16	0.17	0.18	0.19	0.20	0.21
0.75	0.18	0.13	0.11	0.11	0.11	0.12	0.13	0.14	0.14	0.15	0.15
0.80	0.15	0.11	0.09	0.09	0.09	0.09	0.10	0.10	0.11	0.11	0.12
0.85	0.13	0.09	0.08	0.07	0.07	0.08	0.08	0.08	0.08	0.09	0.09
0.90	0.11	0.08	0.07	0.06	0.06	0.06	0.06	0.07	0.07	0.07	0.07
0.95	0.10	0.07	0.06	0.05	0.05	0.05	0.05	0.05	0.06	0.06	0.06
1.00	0.09	0.06	0.05	0.05	0.04	0.04	0.04	0.05	0.05	0.05	0.05

Angle Factor *K*					
θ	0	30	45	60	90
K	0.00	0.45	0.60	0.78	1.00

Curve Ratio CR										
r/W	0.55	0.60	0.65	0.70	0.75	0.80	0.85	0.90	0.95	1.00
CR	0.218	0.302	0.361	0.408	0.447	0.480	0.509	0.535	0.557	0.577

Throat Radius/Width Ratio (*R*/*W*)										
r/W	0.55	0.60	0.65	0.70	0.75	0.80	0.85	0.90	0.95	1.00
R/W	0.05	0.10	0.15	0.20	0.25	0.30	0.35	0.40	0.45	0.50

CR3-6 Elbow, Mitered

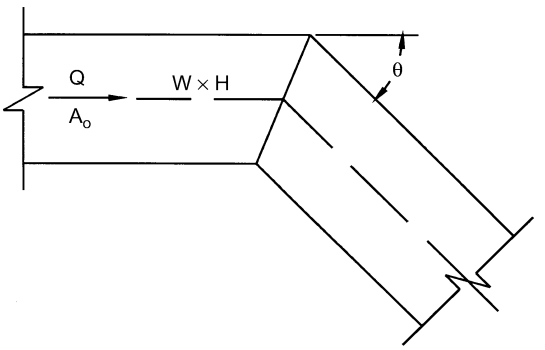

C_o Values											
	H/W										
θ	0.25	0.50	0.75	1.00	1.50	2.00	3.00	4.00	5.00	6.00	8.00
20	0.08	0.08	0.08	0.07	0.07	0.07	0.06	0.06	0.05	0.05	0.05
30	0.18	0.17	0.17	0.16	0.15	0.15	0.13	0.13	0.12	0.12	0.11
45	0.38	0.37	0.36	0.34	0.33	0.31	0.28	0.27	0.26	0.25	0.24
60	0.60	0.59	0.57	0.55	0.52	0.49	0.46	0.43	0.41	0.39	0.38
75	0.89	0.87	0.84	0.81	0.77	0.73	0.67	0.63	0.61	0.58	0.57
90	1.30	1.27	1.23	1.18	1.13	1.07	0.98	0.92	0.89	0.85	0.83

CR3-9 Elbow, Mitered, 90 Degree, Single-Thickness Vanes (Design 1)

$C_o = 0.11$

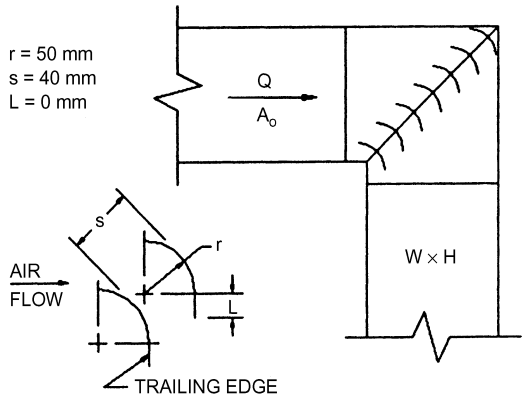

CR3-10 Elbow, Mitered, 90 Degree, Single-Thickness Vanes (Design 2)

$C_o = 0.12$

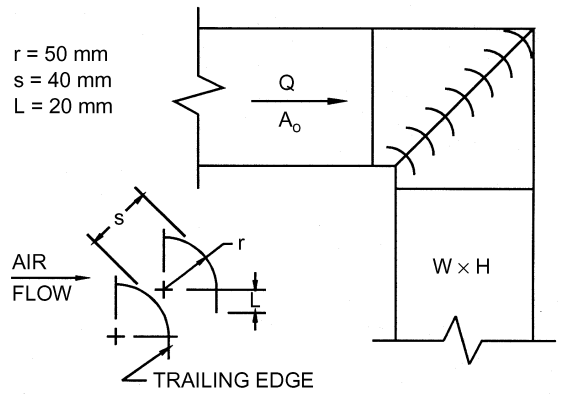

CR3-12 Elbow, Mitered, 90 Degree, Single-Thickness Vanes (Design 4)

$C_o = 0.33$

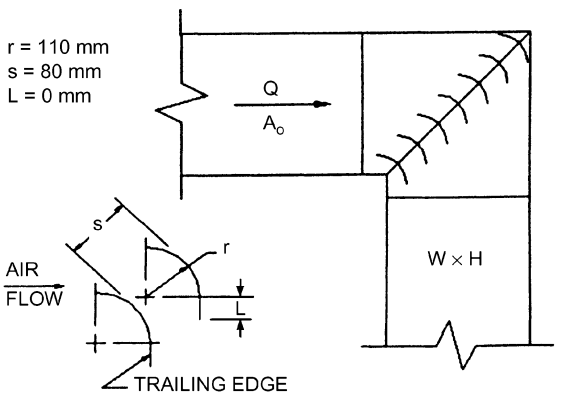

CR3-14 Elbow, Mitered, 90 Degree, Double-Thickness Vanes (Design 1)

$C_o = 0.38$

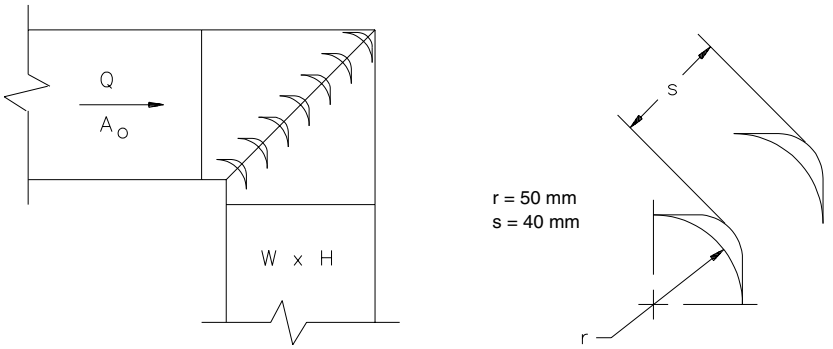

CR3-15 Elbow, Mitered, 90 Degree, Double-Thickness Vanes (Design 2)

$C_o = 0.25$

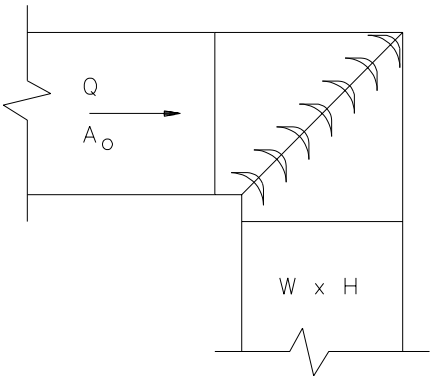

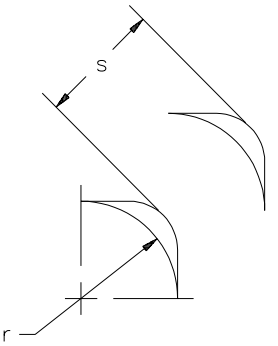

r = 50 mm
s = 60 mm

CR3-16 Elbow, Mitered, 90 Degree, Double-Thickness Vanes (Design 3)

$C_o = 0.41$

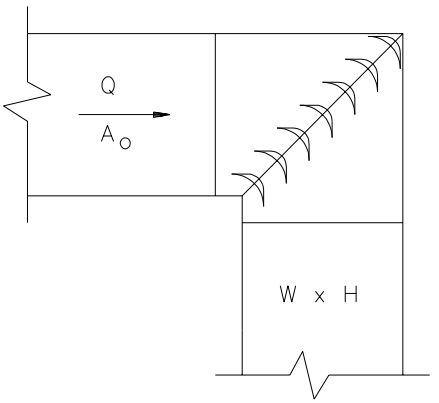

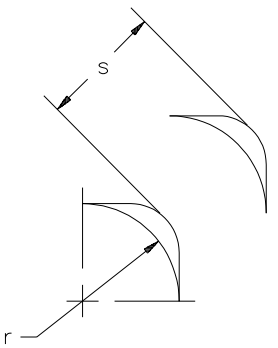

r = 110 mm
s = 80 mm

CR3-17 Elbow, Z-Shaped

	C_p Values													
	L/W													
H/W	**0.0**	**0.4**	**0.6**	**0.8**	**1.0**	**1.2**	**1.4**	**1.6**	**1.8**	**2.0**	**4.0**	**8.0**	**10.0**	**100.0**
0.25	0.00	0.68	0.99	1.77	2.89	3.97	4.41	4.60	4.64	4.60	3.39	3.03	2.70	2.53
0.50	0.00	0.66	0.96	1.72	2.81	3.86	4.29	4.47	4.52	4.47	3.30	2.94	2.62	2.46
0.75	0.00	0.64	0.94	1.67	2.74	3.75	4.17	4.35	4.39	4.35	3.20	2.86	2.55	2.39
1.00	0.00	0.62	0.90	1.61	2.63	3.61	4.01	4.18	4.22	4.18	3.08	2.75	2.45	2.30
1.50	0.00	0.59	0.86	1.53	2.50	3.43	3.81	3.97	4.01	3.97	2.93	2.61	2.33	2.19
2.00	0.00	0.56	0.81	1.45	2.37	3.25	3.61	3.76	3.80	3.76	2.77	2.48	2.21	2.07
3.00	0.00	0.51	0.75	1.34	2.18	3.00	3.33	3.47	3.50	3.47	2.56	2.28	2.03	1.91
4.00	0.00	0.48	0.70	1.26	2.05	2.82	3.13	3.26	3.29	3.26	2.40	2.15	1.91	1.79
6.00	0.00	0.45	0.65	1.16	1.89	2.60	2.89	3.01	3.04	3.01	2.22	1.98	1.76	1.66
8.00	0.00	0.43	0.63	1.13	1.84	2.53	2.81	2.93	2.95	2.93	2.16	1.93	1.72	1.61

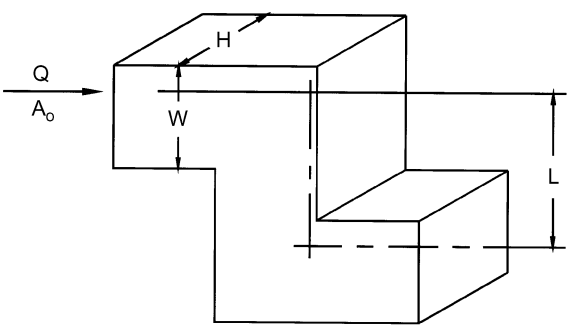

$C_o = K_r C_p$
where K_r = Reynolds number correction factor

Reynolds Number Correction Factor K_r									
Re/1000	**10**	**20**	**30**	**40**	**60**	**80**	**100**	**140**	**500**
K_r	1.40	1.26	1.19	1.14	1.09	1.06	1.04	1.00	1.00

CR6-1 Screen (Only)

	C_o Values												
	n												
A_1/A_o	0.30	0.35	0.40	0.45	0.50	0.55	0.60	0.65	0.70	0.75	0.80	0.90	1.00
0.2	155.00	102.50	75.00	55.00	41.25	31.50	24.25	18.75	14.50	11.00	8.00	3.50	0.00
0.3	68.89	45.56	33.33	24.44	18.33	14.00	10.78	8.33	6.44	4.89	3.56	1.56	0.00
0.4	38.75	25.63	18.75	13.75	10.31	7.88	6.06	4.69	3.63	2.75	2.00	0.88	0.00
0.5	24.80	16.40	12.00	8.80	6.60	5.04	3.88	3.00	2.32	1.76	1.28	0.56	0.00
0.6	17.22	11.39	8.33	6.11	4.58	3.50	2.69	2.08	1.61	1.22	0.89	0.39	0.00
0.7	12.65	8.37	6.12	4.49	3.37	2.57	1.98	1.53	1.18	0.90	0.65	0.29	0.00
0.8	9.69	6.40	4.69	3.44	2.58	1.97	1.52	1.17	0.91	0.69	0.50	0.22	0.00
0.9	7.65	5.06	3.70	2.72	2.04	1.56	1.20	0.93	0.72	0.54	0.40	0.17	0.00
1.0	6.20	4.10	3.00	2.20	1.65	1.26	0.97	0.75	0.58	0.44	0.32	0.14	0.00
1.2	4.31	2.85	2.08	1.53	1.15	0.88	0.67	0.36	0.40	0.31	0.22	0.10	0.00
1.4	3.16	2.09	1.53	1.12	0.84	0.64	0.49	0.38	0.30	0.22	0.16	0.07	0.00
1.6	2.42	1.60	1.17	0.86	0.64	0.49	0.38	0.29	0.23	0.17	0.13	0.05	0.00
1.8	1.91	1.27	0.93	0.68	0.51	0.39	0.30	0.23	0.18	0.14	0.10	0.04	0.00
2.0	1.55	1.03	0.75	0.55	0.41	0.32	0.24	0.19	0.15	0.11	0.08	0.04	0.00
2.5	0.99	0.66	0.48	0.35	0.26	0.20	0.16	0.12	0.09	0.07	0.05	0.02	0.00
3.0	0.69	0.46	0.33	0.24	0.18	0.14	0.11	0.08	0.06	0.05	0.04	0.02	0.00
4.0	0.39	0.26	0.19	0.14	0.10	0.08	0.06	0.05	0.04	0.03	0.02	0.01	0.00
6.0	0.17	0.11	0.08	0.06	0.05	0.04	0.03	0.02	0.02	0.01	0.01	0.00	0.00

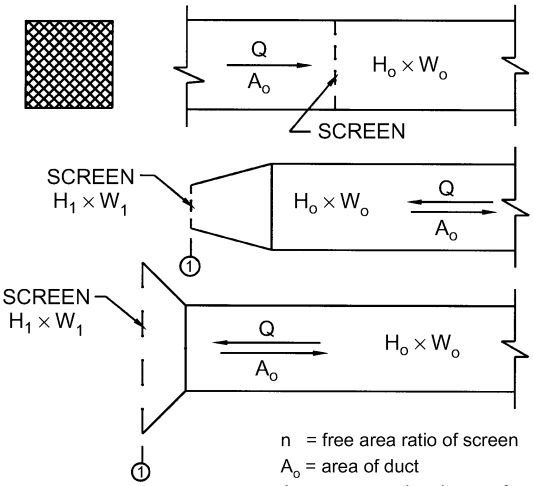

CR6-4 Obstruction, Smooth Cylinder in Rectangular Duct

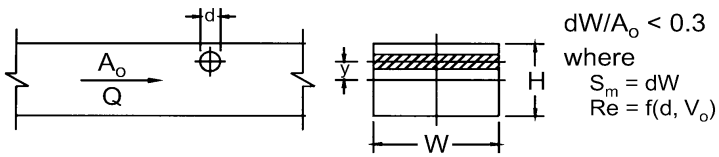

		C_o Values				
		S_m/A_o				
y/H	Re/1000	0.00	0.05	0.10	0.15	0.20
0.00	0.1	0.00	0.10	0.21	0.35	0.47
	0.5	0.00	0.08	0.17	0.28	0.38
	200	0.00	0.08	0.17	0.28	0.38
	300	0.00	0.07	0.16	0.26	0.35
	400	0.00	0.05	0.11	0.19	0.25
	500	0.00	0.04	0.09	0.14	0.19
	600	0.00	0.02	0.05	0.07	0.10
	1000	0.00	0.02	0.05	0.08	0.11
0.05	0.1	0.00	0.10	0.21	0.34	0.46
	0.5	0.00	0.08	0.17	0.27	0.37
	200	0.00	0.08	0.17	0.27	0.37
	300	0.00	0.07	0.15	0.25	0.34
	400	0.00	0.05	0.11	0.18	0.24
	500	0.00	0.04	0.08	0.13	0.18
	600	0.00	0.02	0.04	0.07	0.10
	1000	0.00	0.02	0.05	0.08	0.11
0.10	0.1	0.00	0.09	0.20	0.32	0.44
	0.5	0.00	0.07	0.16	0.26	0.35
	200	0.00	0.07	0.16	0.26	0.35
	300	0.00	0.07	0.15	0.24	0.32
	400	0.00	0.05	0.11	0.17	0.23
	500	0.00	0.04	0.08	0.13	0.18
	600	0.00	0.02	0.04	0.07	0.09
	1000	0.00	0.02	0.05	0.08	0.10
0.15	0.1	0.00	0.09	0.19	0.31	0.42
	0.5	0.00	0.07	0.15	0.25	0.34
	200	0.00	0.07	0.15	0.25	0.34
	300	0.00	0.06	0.14	0.23	0.31
	400	0.00	0.05	0.10	0.17	0.22
	500	0.00	0.04	0.08	0.12	0.17
	600	0.00	0.02	0.04	0.07	0.09
	1000	0.00	0.02	0.04	0.07	0.10
0.20	0.1	0.00	0.08	0.18	0.29	0.40
	0.5	0.00	0.07	0.14	0.24	0.32
	200	0.00	0.07	0.14	0.24	0.32
	300	0.00	0.06	0.13	0.22	0.29
	400	0.00	0.04	0.10	0.16	0.21
	500	0.00	0.03	0.07	0.12	0.16
	600	0.00	0.02	0.04	0.06	0.09
	1000	0.00	0.02	0.04	0.07	0.09
0.25	0.1	0.00	0.08	0.17	0.28	0.38
	0.5	0.00	0.06	0.14	0.22	0.30
	200	0.00	0.06	0.14	0.22	0.30
	300	0.00	0.06	0.12	0.20	0.28
	400	0.00	0.04	0.09	0.15	0.20
	500	0.00	0.03	0.07	0.11	0.15
	600	0.00	0.02	0.04	0.06	0.08
	1000	0.00	0.02	0.04	0.06	0.09
0.30	0.1	0.00	0.07	0.16	0.26	0.35
	0.5	0.00	0.06	0.13	0.21	0.28
	200	0.00	0.06	0.13	0.21	0.28
	300	0.00	0.05	0.12	0.19	0.26
	400	0.00	0.04	0.08	0.14	0.19
	500	0.00	0.03	0.06	0.10	0.14
	600	0.00	0.02	0.03	0.05	0.07
	1000	0.00	0.02	0.04	0.06	0.08
0.35	0.1	0.00	0.07	0.14	0.23	0.32
	0.5	0.00	0.05	0.11	0.19	0.25
	200	0.00	0.05	0.11	0.19	0.25
	300	0.00	0.05	0.11	0.17	0.23
	400	0.00	0.04	0.08	0.12	0.17
	500	0.00	0.03	0.06	0.09	0.13
	600	0.00	0.01	0.03	0.05	0.07
	1000	0.00	0.02	0.03	0.05	0.07
0.40	0.1	0.00	0.06	0.13	0.20	0.28
	0.5	0.00	0.05	0.10	0.16	0.22
	200	0.00	0.05	0.10	0.16	0.22
	300	0.00	0.04	0.09	0.15	0.20
	400	0.00	0.03	0.07	0.11	0.15
	500	0.00	0.02	0.05	0.08	0.11
	600	0.00	0.01	0.03	0.04	0.06
	1000	0.00	0.01	0.03	0.05	0.06

CR9-1 Damper, Butterfly

	C_o Values									
	θ									
H/W	0	10	20	30	40	50	60	65	70	90
0.12	0.04	0.30	1.10	3.00	8.00	23.00	60.00	100.00	190.00	99999
0.25	0.08	0.33	1.18	3.30	9.00	26.00	70.00	128.00	210.00	99999
1.00	0.08	0.33	1.18	3.30	9.00	26.00	70.00	128.00	210.00	99999
2.00	0.13	0.35	1.25	3.60	10.00	29.00	80.00	155.00	230.00	99999

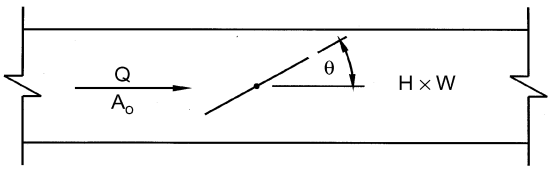

CR9-3 Damper, Parallel Blades

	C_o Values								
	θ								
L/R	0	10	20	30	40	50	60	70	80
0.3	0.52	0.79	1.49	2.20	4.95	8.73	14.15	32.11	122.06
0.4	0.52	0.84	1.56	2.25	5.03	9.00	16.00	37.73	156.58
0.5	0.52	0.88	1.62	2.35	5.11	9.52	18.88	44.79	187.85
0.6	0.52	0.92	1.66	2.45	5.20	9.77	21.75	53.78	288.89
0.8	0.52	0.96	1.69	2.55	5.30	10.03	22.80	65.46	295.22
1.0	0.52	1.00	1.76	2.66	5.40	10.53	23.84	73.23	361.00
1.5	0.52	1.08	1.83	2.78	5.44	11.21	27.56	97.41	495.31

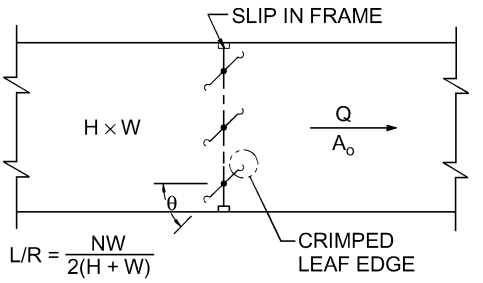

where
N = number of damper blades
W = duct dimension parallel to blade axis, mm
H = duct height, mm
L = sum of damper blade lengths, mm
R = perimeter of duct, mm

CR9-4 Damper, Opposed Blades

	C_o Values								
	θ								
L/R	0	10	20	30	40	50	60	70	80
0.3	0.52	0.79	1.91	3.77	8.55	19.46	70.12	295.21	807.23
0.4	0.52	0.85	2.07	4.61	10.42	26.73	92.90	346.25	926.34
0.5	0.52	0.93	2.25	5.44	12.29	33.99	118.91	393.36	1045.44
0.6	0.52	1.00	2.46	5.99	14.15	41.26	143.69	440.25	1163.09
0.8	0.52	1.08	2.66	6.96	18.18	56.47	193.92	520.27	1324.85
1.0	0.52	1.17	2.91	7.31	20.25	71.68	245.45	576.00	1521.00
1.5	0.52	1.38	3.16	9.51	27.56	107.41	361.00	717.05	1804.40

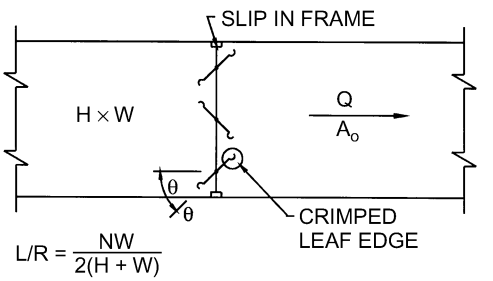

where
N = number of damper blades
W = duct dimension parallel to blade axis, mm
H = duct height, mm
L = sum of damper blade lengths, mm
R = perimeter of duct, mm

CR9-6 Fire Damper, Curtain Type, Type B

$C_o = 0.19$

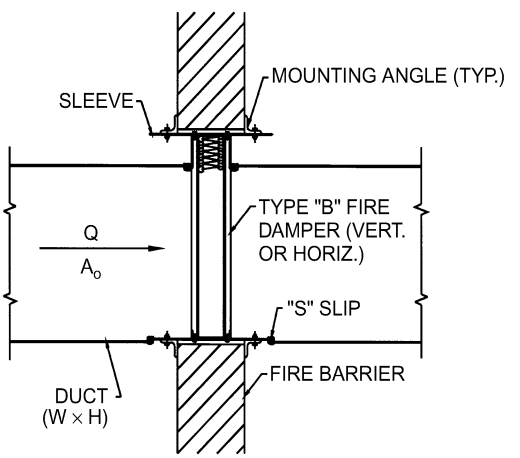

ER2-1 Bellmouth, Plenum to Round, Exhaust/Return Systems

	C_o Values												
	r/D_1												
A_o/A_1	0.00	0.01	0.02	0.03	0.04	0.05	0.06	0.08	0.10	0.12	0.16	0.20	10.00
1.5	0.22	0.20	0.15	0.14	0.12	0.10	0.09	0.07	0.05	0.04	0.03	0.01	0.01
2.0	0.13	0.11	0.08	0.08	0.07	0.06	0.05	0.04	0.03	0.02	0.02	0.01	0.01
2.5	0.08	0.07	0.05	0.05	0.04	0.04	0.03	0.02	0.02	0.01	0.01	0.00	0.00
3.0	0.06	0.05	0.04	0.03	0.03	0.02	0.02	0.02	0.01	0.01	0.01	0.00	0.00
4.0	0.03	0.03	0.02	0.02	0.02	0.01	0.01	0.01	0.01	0.01	0.00	0.00	0.00
8.0	0.01	0.01	0.01	0.00	0.00	0.00	0.00	0.00	0.00	0.00	0.00	0.00	0.00

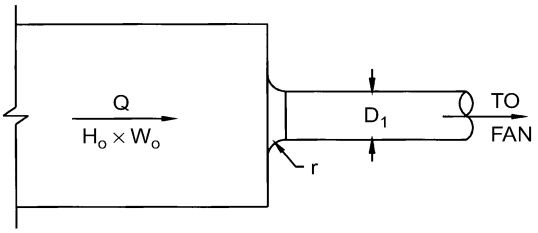

ER3-1 Elbow, 90 Degree, Variable Inlet/Outlet Areas, Exhaust/Return Systems

	C_o Values						
	W_1/W_o						
H/W_o	0.6	0.8	1.0	1.2	1.4	1.6	2.0
0.25	1.76	1.43	1.24	1.14	1.09	1.06	1.06
1.00	1.70	1.36	1.15	1.02	0.95	0.90	0.84
4.00	1.46	1.10	0.90	0.81	0.76	0.72	0.66
100.00	1.50	1.04	0.79	0.69	0.63	0.60	0.55

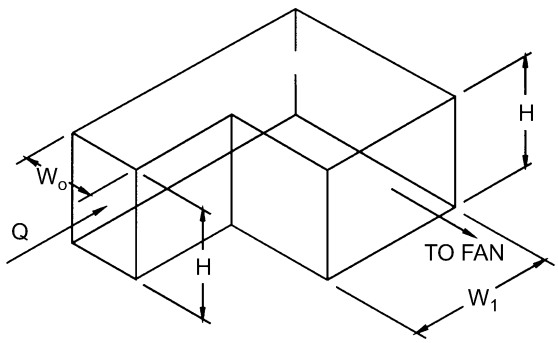

ER4-1 Transition, Rectangular, Two Sides Parallel, Symmetrical, Exhaust/Return Systems

	C_o Values									
	θ									
A_o/A_1	10	15	20	30	45	60	90	120	150	180
0.06	0.26	0.27	0.40	0.56	0.71	0.86	1.00	0.99	0.98	0.98
0.10	0.24	0.26	0.36	0.53	0.69	0.82	0.93	0.93	0.92	0.91
0.25	0.17	0.19	0.22	0.42	0.60	0.68	0.70	0.69	0.67	0.66
0.50	0.14	0.13	0.15	0.24	0.35	0.37	0.38	0.37	0.36	0.35
1.00	0.00	0.00	0.00	0.00	0.00	0.00	0.00	0.00	0.00	0.00
2.00	0.23	0.20	0.20	0.20	0.24	0.28	0.54	0.78	1.02	1.09
4.00	0.81	0.64	0.64	0.64	0.88	1.12	2.78	4.38	5.65	6.60
6.00	1.82	1.44	1.44	1.44	1.98	2.53	6.56	10.20	13.00	15.20
10.00	5.03	5.00	5.00	5.00	6.50	8.02	19.10	29.10	37.10	43.10

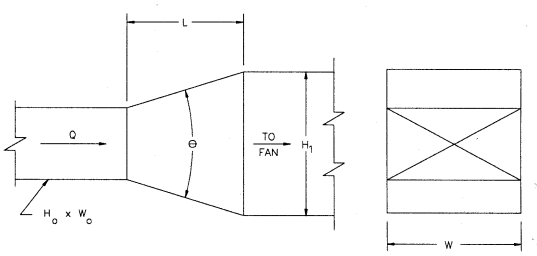

A_0/A_1 < or > 1

ER4-3 Transition, Rectangular to Round, Exhaust/Return Systems

	C_o Values									
	θ									
A_o/A_1	10	15	20	30	45	60	90	120	150	180
0.06	0.30	0.54	0.53	0.65	0.77	0.88	0.95	0.98	0.98	0.93
0.10	0.30	0.50	0.53	0.64	0.75	0.84	0.89	0.91	0.91	0.88
0.25	0.25	0.36	0.45	0.52	0.58	0.62	0.64	0.64	0.64	0.64
0.50	0.15	0.21	0.25	0.30	0.33	0.33	0.33	0.32	0.31	0.30
1.00	0.00	0.00	0.00	0.00	0.00	0.00	0.00	0.00	0.00	0.00
2.00	0.24	0.28	0.26	0.20	0.22	0.24	0.49	0.73	0.97	1.04
4.00	0.89	0.78	0.79	0.70	0.88	1.12	2.72	4.33	5.62	6.58
6.00	1.89	1.67	1.59	1.49	1.98	2.52	6.51	10.14	13.05	15.14
10.00	5.09	5.32	5.15	5.05	6.50	8.05	19.06	29.07	37.08	43.05

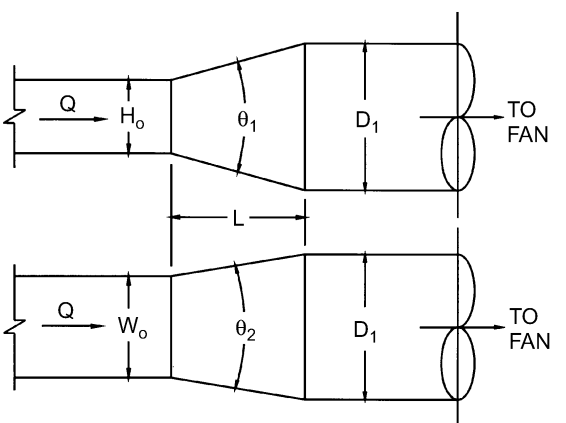

A_o/A_1 < or > 1
θ is larger of θ_1 and θ_2

ER5-2 Tee, Round Tap to Rectangular Main, Converging

Q_b/Q_c	0.1	0.2	0.3	0.4	0.5	0.6	0.7	0.8	0.9	1.0
C_b	−12.25	−1.31	0.64	0.94	1.27	1.43	1.40	1.45	1.52	1.49

Q_s/Q_c	0.1	0.2	0.3	0.4	0.5	0.6	0.7	0.8	0.9
C_s	2.15	11.91	6.54	3.74	2.23	1.33	0.76	0.38	0.10

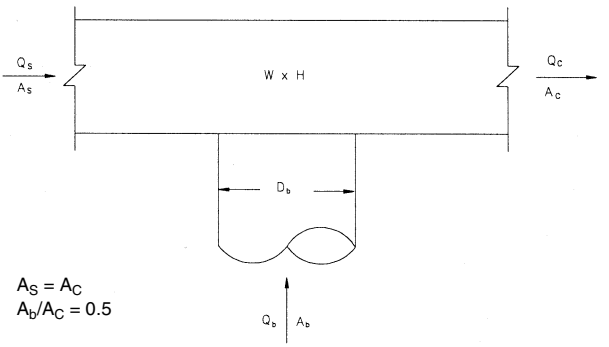

$A_S = A_C$
$A_b/A_C = 0.5$

ER5-3 Tee, 45 Degree Entry Branch, Converging

Q_b/Q_c	0.1	0.2	0.3	0.4	0.5	0.6	0.7	0.8	0.9	1.0
C_b	-18.00	-3.25	-0.64	0.53	0.76	0.79	0.93	0.79	0.90	0.91

Q_s/Q_c	0.1	0.2	0.3	0.4	0.5	0.6	0.7	0.8	0.9
C_s	2.15	11.91	6.54	3.74	2.23	1.33	0.76	0.38	0.10

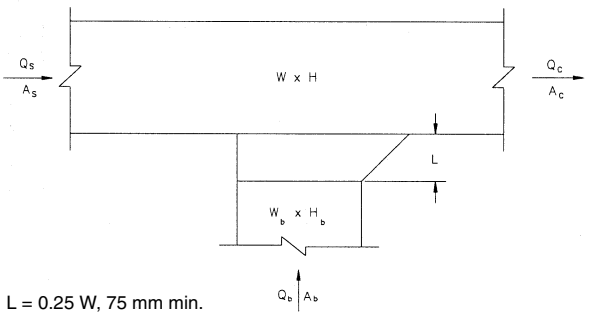

L = 0.25 W, 75 mm min.
$A_S = A_C$
$A_b/A_C = 0.5$

ER5-4 Wye, Symmetrical, Dovetail, Q_b/Q_c = 0.5, Converging

A_b/A_c	0.5	1.0
C_b	0.23	0.28

Branches are identical, $Q_{b1} = Q_{b2} = Q_b$, and $C_{b1} = C_{b2} = C_b$

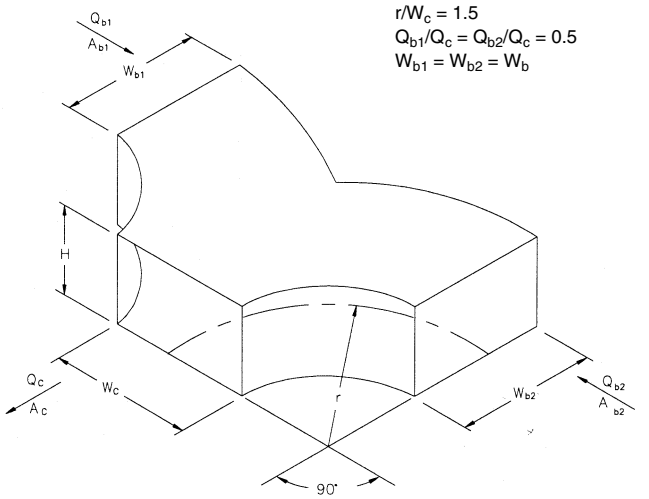

$r/W_c = 1.5$
$Q_{b1}/Q_c = Q_{b2}/Q_c = 0.5$
$W_{b1} = W_{b2} = W_b$

ER7-1 Fan Inlet, Centrifugal, SWSI, 90 Degree Smooth Radius Elbow (Square)

	C_o Values			
	L/H			
r/H	0.0	2.0	5.0	10.0
0.50	2.50	1.60	0.80	0.80
0.75	2.00	1.20	0.67	0.67
1.00	1.20	0.67	0.33	0.33
1.50	1.00	0.57	0.30	0.30
2.00	0.80	0.47	0.26	0.26

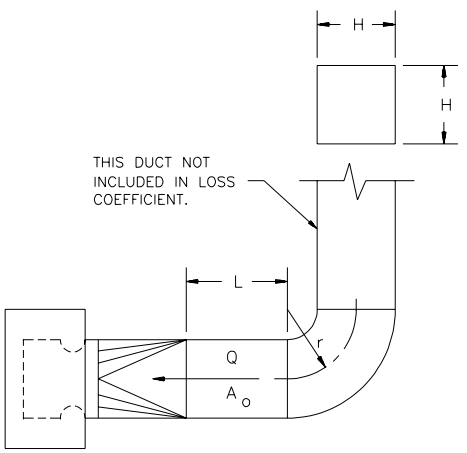

SR1-1 Conical Bellmouth/Sudden Contraction, Plenum to Rectangular, Supply Air Systems

		C_o Values									
		θ									
A_o/A_1	L/D_h	0	10	20	30	45	60	90	120	150	180
0.10	0.025	0.46	0.43	0.42	0.40	0.38	0.37	0.38	0.40	0.43	0.46
	0.050	0.46	0.42	0.38	0.33	0.30	0.28	0.31	0.36	0.41	0.46
	0.075	0.46	0.39	0.32	0.28	0.23	0.21	0.26	0.32	0.39	0.46
	0.100	0.46	0.36	0.30	0.23	0.19	0.17	0.23	0.30	0.38	0.46
	0.150	0.46	0.34	0.25	0.18	0.15	0.14	0.21	0.29	0.37	0.46
	0.300	0.46	0.31	0.22	0.16	0.13	0.13	0.20	0.28	0.37	0.46
	0.600	0.46	0.25	0.17	0.12	0.10	0.11	0.19	0.27	0.36	0.46
0.20	0.025	0.42	0.40	0.38	0.36	0.34	0.34	0.35	0.37	0.39	0.42
	0.050	0.42	0.38	0.35	0.30	0.27	0.25	0.29	0.33	0.37	0.42
	0.075	0.42	0.36	0.30	0.25	0.21	0.19	0.24	0.30	0.36	0.42
	0.100	0.42	0.33	0.27	0.21	0.18	0.15	0.21	0.27	0.35	0.42
	0.150	0.42	0.31	0.23	0.17	0.13	0.13	0.19	0.26	0.34	0.42
	0.300	0.42	0.28	0.20	0.15	0.12	0.12	0.18	0.26	0.34	0.42
	0.600	0.42	0.23	0.15	0.11	0.10	0.10	0.17	0.25	0.33	0.42
0.40	0.025	0.34	0.32	0.31	0.29	0.28	0.27	0.28	0.30	0.32	0.34
	0.050	0.34	0.31	0.28	0.25	0.22	0.20	0.23	0.26	0.30	0.34
	0.075	0.34	0.29	0.24	0.20	0.17	0.16	0.19	0.24	0.29	0.34
	0.100	0.34	0.27	0.22	0.17	0.14	0.12	0.17	0.22	0.28	0.34
	0.150	0.34	0.25	0.18	0.14	0.11	0.10	0.15	0.21	0.27	0.34
	0.300	0.34	0.23	0.16	0.12	0.10	0.10	0.15	0.21	0.27	0.34
	0.600	0.34	0.18	0.12	0.09	0.08	0.08	0.14	0.20	0.27	0.34
0.60	0.025	0.25	0.24	0.23	0.22	0.20	0.20	0.21	0.22	0.23	0.25
	0.050	0.25	0.23	0.21	0.18	0.16	0.15	0.17	0.19	0.22	0.25
	0.075	0.25	0.21	0.18	0.15	0.13	0.12	0.14	0.18	0.21	0.25
	0.100	0.25	0.20	0.16	0.13	0.11	0.09	0.12	0.16	0.21	0.25
	0.150	0.25	0.19	0.14	0.10	0.08	0.08	0.11	0.16	0.20	0.25
	0.300	0.25	0.17	0.12	0.09	0.07	0.07	0.11	0.15	0.20	0.25
	0.600	0.25	0.14	0.09	0.07	0.06	0.06	0.10	0.15	0.20	0.25
0.80	0.025	0.15	0.14	0.13	0.13	0.12	0.12	0.12	0.13	0.14	0.15
	0.050	0.15	0.13	0.12	0.11	0.10	0.09	0.10	0.12	0.13	0.15
	0.075	0.15	0.13	0.10	0.09	0.08	0.07	0.08	0.10	0.13	0.15
	0.100	0.15	0.12	0.10	0.07	0.06	0.05	0.07	0.10	0.12	0.15
	0.150	0.15	0.11	0.08	0.06	0.05	0.04	0.07	0.09	0.12	0.15
	0.300	0.15	0.10	0.07	0.05	0.04	0.04	0.07	0.09	0.12	0.15
	0.600	0.15	0.08	0.05	0.04	0.03	0.04	0.06	0.09	0.12	0.15
0.90	0.025	0.09	0.08	0.08	0.08	0.07	0.07	0.07	0.08	0.08	0.09
	0.050	0.09	0.08	0.07	0.06	0.06	0.05	0.06	0.07	0.08	0.09
	0.075	0.09	0.07	0.06	0.05	0.04	0.04	0.05	0.06	0.08	0.09
	0.100	0.09	0.07	0.06	0.04	0.04	0.03	0.04	0.06	0.07	0.09
	0.150	0.09	0.07	0.05	0.04	0.03	0.03	0.04	0.06	0.07	0.09
	0.300	0.09	0.06	0.04	0.03	0.03	0.02	0.04	0.05	0.07	0.09
	0.600	0.09	0.05	0.03	0.02	0.02	0.02	0.04	0.05	0.07	0.09

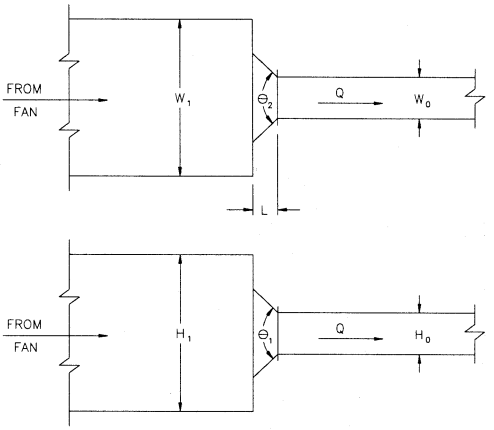

$$Dh = \frac{2\,H_0 W_0}{(H_0 + W_0)}$$

θ is larger of θ_1 and θ_2

SR2-1 Abrupt Exit

H/W	0.1	0.2	0.9	1.0	1.1	4.0	5.0	10.0
C_o	1.55	1.55	1.55	2.00	1.55	1.55	1.55	1.55

$C_o = 1.0$

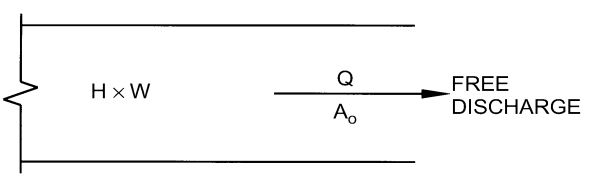

Note: Table is LAMINAR flow; $C_o = 1.0$ is TURBULENT flow.

SR2-3 Plain Diffuser (Two Sides Parallel), Free Discharge

		C_o Values								
		θ								
A_1/A_o	Re/1000	8	10	14	20	30	45	60	90	120
1	50	0.00	0.00	0.00	0.00	0.00	0.00	0.00	0.00	0.00
	100	0.00	0.00	0.00	0.00	0.00	0.00	0.00	0.00	0.00
	200	0.00	0.00	0.00	0.00	0.00	0.00	0.00	0.00	0.00
	400	0.00	0.00	0.00	0.00	0.00	0.00	0.00	0.00	0.00
	2000	0.00	0.00	0.00	0.00	0.00	0.00	0.00	0.00	0.00
2	50	0.50	0.51	0.56	0.63	0.80	0.96	1.04	1.09	1.09
	100	0.48	0.50	0.56	0.63	0.80	0.96	1.04	1.09	1.09
	200	0.44	0.47	0.53	0.63	0.74	0.93	1.02	1.08	1.08
	400	0.40	0.42	0.50	0.62	0.74	0.93	1.02	1.08	1.08
	2000	0.40	0.42	0.50	0.62	0.74	0.93	1.02	1.08	1.08
4	50	0.34	0.38	0.48	0.63	0.76	0.91	1.03	1.07	1.07
	100	0.31	0.36	0.45	0.59	0.72	0.88	1.02	1.07	1.07
	200	0.26	0.31	0.41	0.53	0.67	0.83	0.96	1.06	1.06
	400	0.22	0.27	0.39	0.53	0.67	0.83	0.96	1.06	1.06
	2000	0.22	0.27	0.39	0.53	0.67	0.83	0.96	1.06	1.06
6	50	0.32	0.34	0.41	0.56	0.70	0.84	0.96	1.08	1.08
	100	0.27	0.30	0.41	0.56	0.70	0.84	0.96	1.08	1.08
	200	0.24	0.27	0.36	0.52	0.67	0.81	0.94	1.06	1.06
	400	0.20	0.24	0.36	0.52	0.67	0.81	0.94	1.06	1.06
	2000	0.18	0.24	0.34	0.50	0.67	0.81	0.94	1.05	1.05

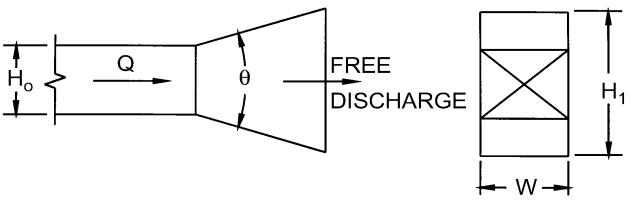

SR2-5 Pyramidal Diffuser, Free Discharge

		C_o Values								
		θ								
A_1/A_o	Re/1000	8	10	14	20	30	45	60	90	120
1	50	0.00	0.00	0.00	0.00	0.00	0.00	0.00	0.00	0.00
	100	0.00	0.00	0.00	0.00	0.00	0.00	0.00	0.00	0.00
	200	0.00	0.00	0.00	0.00	0.00	0.00	0.00	0.00	0.00
	400	0.00	0.00	0.00	0.00	0.00	0.00	0.00	0.00	0.00
	2000	0.00	0.00	0.00	0.00	0.00	0.00	0.00	0.00	0.00
2	50	0.65	0.68	0.74	0.82	0.92	1.05	1.10	1.08	1.08
	100	0.61	0.66	0.73	0.81	0.90	1.04	1.09	1.08	1.08
	200	0.57	0.61	0.70	0.79	0.89	1.04	1.09	1.08	1.08
	400	0.50	0.56	0.64	0.76	0.88	1.02	1.07	1.08	1.08
	2000	0.50	0.56	0.64	0.76	0.88	1.02	1.07	1.08	1.08
4	50	0.53	0.60	0.69	0.78	0.90	1.02	1.07	1.09	1.09
	100	0.49	0.55	0.66	0.78	0.90	1.02	1.07	1.09	1.09
	200	0.42	0.50	0.62	0.74	0.87	1.00	1.06	1.08	1.08
	400	0.36	0.44	0.56	0.70	0.84	0.99	1.06	1.08	1.08
	2000	0.36	0.44	0.56	0.70	0.84	0.99	1.06	1.08	1.08
6	50	0.50	0.57	0.66	0.77	0.91	1.02	1.07	1.08	1.08
	100	0.47	0.54	0.63	0.76	0.98	1.02	1.07	1.08	1.08
	200	0.42	0.48	0.60	0.73	0.88	1.00	1.06	1.08	1.08
	400	0.34	0.44	0.56	0.73	0.86	0.98	1.06	1.08	1.08
	2000	0.34	0.44	0.56	0.73	0.86	0.98	1.06	1.08	1.08
10	50	0.45	0.53	0.64	0.74	0.85	0.97	1.10	1.12	1.12
	100	0.40	0.48	0.62	0.73	0.85	0.97	1.10	1.12	1.12
	200	0.34	0.44	0.56	0.69	0.82	0.95	1.10	1.11	1.11
	400	0.28	0.40	0.55	0.67	0.80	0.93	1.09	1.11	1.11
	2000	0.28	0.40	0.55	0.67	0.80	0.93	1.09	1.11	1.11

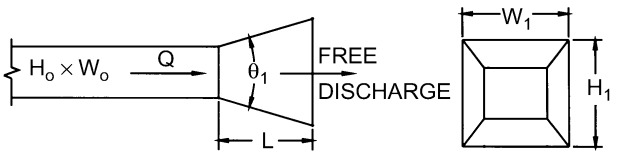

θ is larger of θ_1 and θ_2

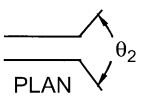

SR2-6 Pyramidal Diffuser, with Wall

L/D_h	0.5	1.0	2.0	3.0	4.0	5.0	6.0	8.0	10.0	12.0	14.0
C_o	0.49	0.40	0.30	0.26	0.23	0.21	0.19	0.17	0.16	0.15	0.14
θ	26	19	13	11	9	8	7	6	6	5	5

θ is the optimum angle.

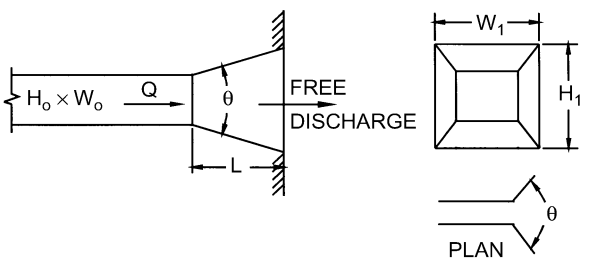

SR3-1 Elbow, 90 Degree, Variable Inlet/Outlet Areas, Supply Air Systems

	C_o Values						
	W_o/W_1						
H/W_1	0.6	0.8	1.0	1.2	1.4	1.6	2.0
0.25	0.63	0.92	1.24	1.64	2.14	2.71	4.24
1.00	0.61	0.87	1.15	1.47	1.86	2.30	3.36
4.00	0.53	0.70	0.90	1.17	1.49	1.84	2.64
100.00	0.54	0.67	0.79	0.99	1.23	1.54	2.20

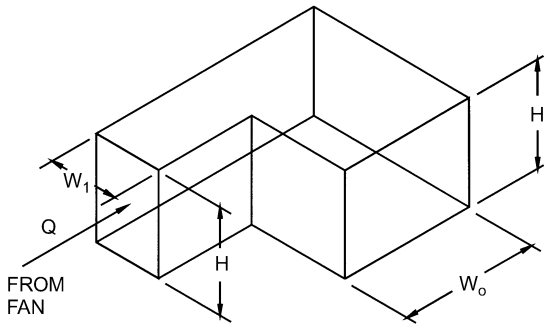

SR4-1 Transition, Rectangular, Two Sides Parallel, Symmetrical, Supply Air Systems

	C_o Values									
	θ									
A_o/A_1	10	15	20	30	45	60	90	120	150	180
0.10	0.05	0.05	0.05	0.05	0.07	0.08	0.19	0.29	0.37	0.43
0.17	0.05	0.04	0.04	0.04	0.05	0.07	0.18	0.28	0.36	0.42
0.25	0.05	0.04	0.04	0.04	0.06	0.07	0.17	0.27	0.35	0.41
0.50	0.06	0.05	0.05	0.05	0.06	0.07	0.14	0.20	0.26	0.27
1.00	0.00	0.00	0.00	0.00	0.00	0.00	0.00	0.00	0.00	1.00
2.00	0.56	0.52	0.60	0.96	1.40	1.48	1.52	1.48	1.44	1.40
4.00	2.72	3.04	3.52	6.72	9.60	10.88	11.20	11.04	10.72	10.56
10.00	24.00	26.00	36.00	53.00	69.00	82.00	93.00	93.00	92.00	91.00
16.00	66.56	69.12	102.40	143.36	181.76	220.16	256.00	253.44	250.88	250.88

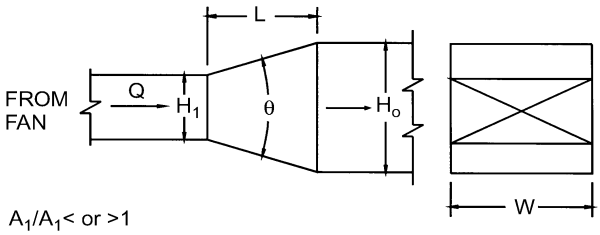

SR4-3 Transition, Round to Rectangular, Supply Air Systems

	C_o Values									
	θ									
A_o/A_1	10	15	20	30	45	60	90	120	150	180
0.10	0.05	0.05	0.05	0.05	0.07	0.08	0.19	0.29	0.37	0.43
0.17	0.05	0.05	0.05	0.04	0.06	0.07	0.18	0.28	0.36	0.42
0.25	0.06	0.05	0.05	0.04	0.06	0.07	0.17	0.27	0.35	0.41
0.50	0.06	0.07	0.07	0.05	0.06	0.06	0.12	0.18	0.24	0.26
1.00	0.00	0.00	0.00	0.00	0.00	0.00	0.00	0.00	0.00	0.00
2.00	0.60	0.84	1.00	1.20	1.32	1.32	1.32	1.28	1.24	1.20
4.00	4.00	5.76	7.20	8.32	9.28	9.92	10.24	10.24	10.24	10.24
10.00	30.00	50.00	53.00	64.00	75.00	84.00	89.00	91.00	91.00	88.00
16.00	76.80	138.24	135.68	166.40	197.12	225.28	243.20	250.88	250.88	238.08

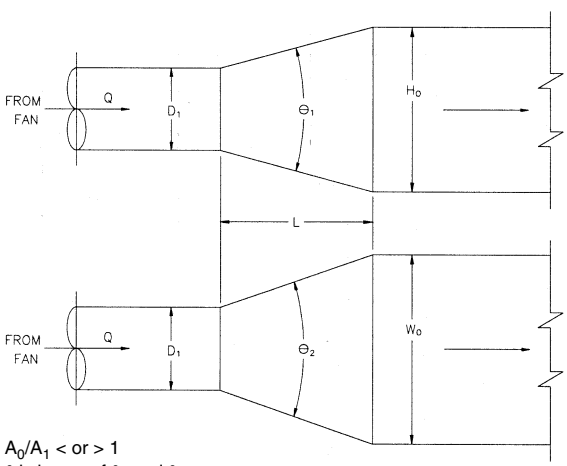

SR5-1 Smooth Wye of Type $A_s + A_b \geq A_c$, Branch 90° to Main, Diverging

		C_b Values								
		Q_b/Q_c								
A_s/A_c	A_b/A_c	0.1	0.2	0.3	0.4	0.5	0.6	0.7	0.8	0.9
0.50	0.25	3.44	0.70	0.30	0.20	0.17	0.16	0.16	0.17	0.18
	0.50	11.00	2.37	1.06	0.64	0.52	0.47	0.47	0.47	0.48
	1.00	60.00	13.00	4.78	2.06	0.96	0.47	0.31	0.27	0.26
0.75	0.25	2.19	0.55	0.35	0.31	0.33	0.35	0.36	0.37	0.39
	0.50	13.00	2.50	0.89	0.47	0.34	0.31	0.32	0.36	0.43
	1.00	70.00	15.00	5.67	2.62	1.36	0.78	0.53	0.41	0.36
1.00	0.25	3.44	0.78	0.42	0.33	0.30	0.31	0.40	0.42	0.46
	0.50	15.50	3.00	1.11	0.62	0.48	0.42	0.40	0.42	0.46
	1.00	67.00	13.75	5.11	2.31	1.28	0.81	0.59	0.47	0.46

		C_s Values								
		Q_s/Q_c								
A_s/A_c	A_b/A_c	0.1	0.2	0.3	0.4	0.5	0.6	0.7	0.8	0.9
0.50	0.25	8.75	1.62	0.50	0.17	0.05	0.00	–0.02	–0.02	0.00
	0.50	7.50	1.12	0.25	0.06	0.05	0.09	0.14	0.19	0.22
	1.00	5.00	0.62	0.17	0.08	0.08	0.09	0.12	0.15	0.19
0.75	0.25	19.13	3.38	1.00	0.28	0.05	–0.02	–0.02	0.00	0.06
	0.50	20.81	3.23	0.75	0.14	–0.02	–0.05	–0.05	–0.02	0.03
	1.00	16.88	2.81	0.63	0.11	–0.02	–0.05	0.01	0.00	0.07
1.00	0.25	46.00	9.50	3.22	1.31	0.52	0.14	–0.02	–0.05	–0.01
	0.50	35.00	6.75	2.11	0.75	0.24	0.00	–0.10	–0.09	–0.04
	1.00	38.00	7.50	2.44	0.81	0.24	–0.03	–0.08	–0.06	–0.02

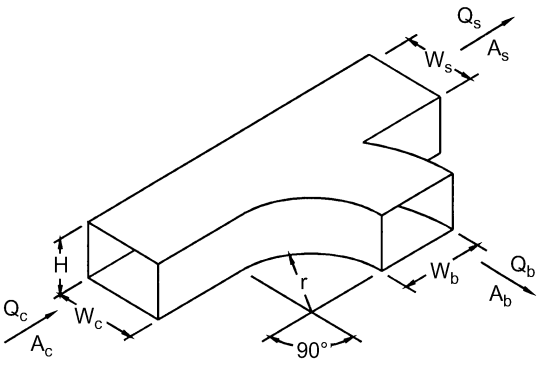

SR5-3 Wye of the Type $A_s + A_b > A_c$, $A_s = A_c$, 45 Degree, Diverging

	C_b Values								
	Q_b/Q_c								
A_b/A_c	0.1	0.2	0.3	0.4	0.5	0.6	0.7	0.8	0.9
0.1	0.60	0.52	0.57	0.58	0.64	0.67	0.70	0.71	0.73
0.2	2.24	0.56	0.44	0.45	0.51	0.54	0.58	0.60	0.62
0.3	5.94	1.08	0.52	0.41	0.44	0.46	0.49	0.52	0.54
0.4	10.56	1.88	0.71	0.43	0.35	0.31	0.31	0.32	0.34
0.5	17.75	3.25	1.14	0.59	0.40	0.31	0.30	0.30	0.31
0.6	26.64	5.04	1.76	0.83	0.50	0.36	0.32	0.30	0.30
0.7	37.73	7.23	2.56	1.16	0.67	0.44	0.35	0.31	0.30
0.8	49.92	9.92	3.48	1.60	0.87	0.55	0.42	0.35	0.32

Q_s/Q_c	0.1	0.2	0.3	0.4	0.5	0.6	0.8	1.0
C_s	32.00	6.50	2.22	0.87	0.40	0.17	0.03	0.00

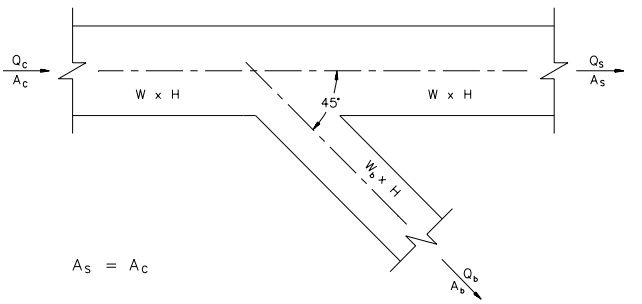

SR5-5 Tee of the Type $A_s + A_b > A_c$, $A_s = A_c$ Diverging

	C_b Values								
	Q_b/Q_c								
A_b/A_c	0.1	0.2	0.3	0.4	0.5	0.6	0.7	0.8	0.9
0.1	2.06	1.20	0.99	0.87	0.88	0.87	0.87	0.86	0.86
0.2	5.16	1.92	1.28	1.03	0.99	0.94	0.92	0.90	0.89
0.3	10.26	3.13	1.78	1.28	1.16	1.06	1.01	0.97	0.94
0.4	15.84	4.36	2.24	1.48	1.11	0.88	0.80	0.75	0.72
0.5	24.25	6.31	3.03	1.89	1.35	1.03	0.91	0.84	0.78
0.6	34.56	8.73	4.04	2.41	1.64	1.22	1.04	0.94	0.87
0.7	46.55	11.51	5.17	3.00	2.00	1.44	1.20	1.06	0.96
0.8	60.80	14.72	6.54	3.72	2.41	1.69	1.38	1.20	1.07

Q_s/Q_c	0.1	0.2	0.3	0.4	0.5	0.6	0.8	1.0
C_s	32.00	6.50	2.22	0.87	0.40	0.17	0.03	0.00

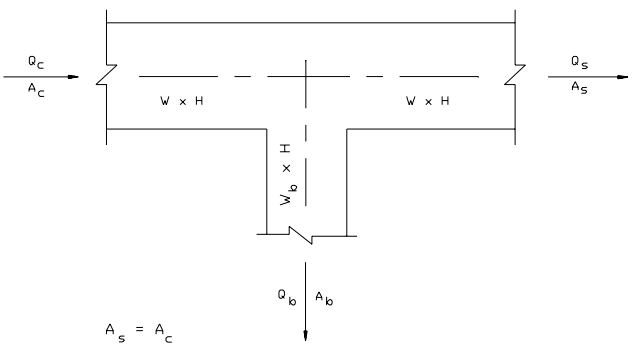

SR5-11 Tee, Rectangular Main to Round Tap, Diverging

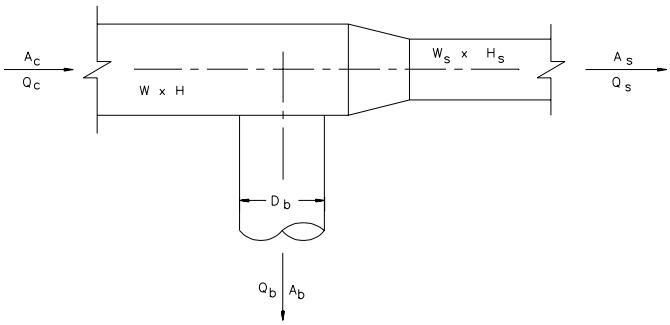

	C_b Values								
	Q_b/Q_c								
A_b/A_c	0.1	0.2	0.3	0.4	0.5	0.6	0.7	0.8	0.9
0.1	1.58	0.94	0.83	0.79	0.77	0.76	0.76	0.76	0.75
0.2	4.20	1.58	1.10	0.94	0.87	0.83	0.80	0.79	0.78
0.3	8.63	2.67	1.58	1.20	1.03	0.94	0.88	0.85	0.83
0.4	14.85	4.20	2.25	1.58	1.27	1.10	1.00	0.94	0.90
0.5	22.87	6.19	3.13	2.07	1.58	1.32	1.16	1.06	0.99
0.6	32.68	8.63	4.20	2.67	1.96	1.58	1.35	1.20	1.10
0.7	44.30	11.51	5.48	3.38	2.41	1.89	1.58	1.38	1.24
0.8	57.71	14.85	6.95	4.20	2.94	2.25	1.84	1.58	1.40
0.9	72.92	18.63	8.63	5.14	3.53	2.67	2.14	1.81	1.58

	C_s Values								
	Q_s/Q_c								
A_s/A_c	0.1	0.2	0.3	0.4	0.5	0.6	0.7	0.8	0.9
0.1	0.04								
0.2	0.98	0.04							
0.3	3.48	0.31	0.04						
0.4	7.55	0.98	0.18	0.04					
0.5	13.18	2.03	0.49	0.13	0.04				
0.6	20.38	3.48	0.98	0.31	0.10	0.04			
0.7	29.15	5.32	1.64	0.60	0.23	0.09	0.04		
0.8	39.48	7.55	2.47	0.98	0.42	0.18	0.08	0.04	
0.9	51.37	10.17	3.48	1.46	0.67	0.31	0.15	0.07	0.04

SR5-13 Tee, 45 Degree Entry Branch, Diverging

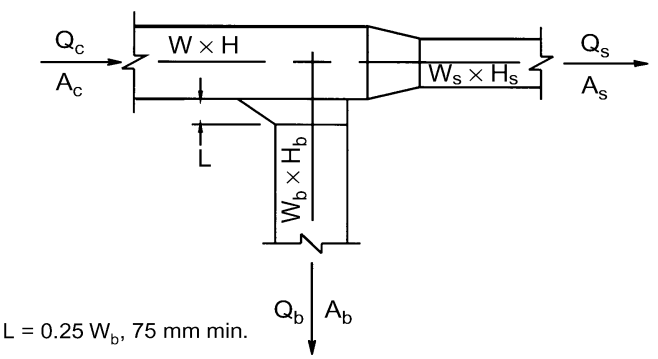

	C_b Values								
	Q_b/Q_c								
A_b/A_c	0.1	0.2	0.3	0.4	0.5	0.6	0.7	0.8	0.9
0.1	0.73	0.34	0.32	0.34	0.35	0.37	0.38	0.39	0.40
0.2	3.10	0.73	0.41	0.34	0.32	0.32	0.33	0.34	0.35
0.3	7.59	1.65	0.73	0.47	0.37	0.34	0.32	0.32	0.32
0.4	14.20	3.10	1.28	0.73	0.51	0.41	0.36	0.34	0.32
0.5	22.92	5.08	2.07	1.12	0.73	0.54	0.44	0.38	0.35
0.6	33.76	7.59	3.10	1.65	1.03	0.73	0.56	0.47	0.41
0.7	46.71	10.63	4.36	2.31	1.42	0.98	0.73	0.58	0.49
0.8	61.79	14.20	5.86	3.10	1.90	1.28	0.94	0.73	0.60
0.9	78.98	18.29	7.59	4.02	2.46	1.65	1.19	0.91	0.73

	C_s Values								
	Q_s/Q_c								
A_s/A_c	0.1	0.2	0.3	0.4	0.5	0.6	0.7	0.8	0.9
0.1	0.04								
0.2	0.98	0.04							
0.3	3.48	0.31	0.04						
0.4	7.55	0.98	0.18	0.04					
0.5	13.18	2.03	0.49	0.13	0.04				
0.6	20.38	3.48	0.98	0.31	0.10	0.04			
0.7	29.15	5.32	1.64	0.60	0.23	0.09	0.04		
0.8	39.48	7.55	2.47	0.98	0.42	0.18	0.08	0.04	
0.9	51.37	10.17	3.48	1.46	0.67	0.31	0.15	0.07	0.04

SR5-14 Wye, Symmetrical, Dovetail, Q_b/Q_c = 0.5, Diverging

A_b/A_c	0.5	1.0
C_b	0.30	1.00

Branches are identical: $Q_{b1} = Q_{b2} = Q_b$, and $C_{b1} = C_{b2} = C_b$

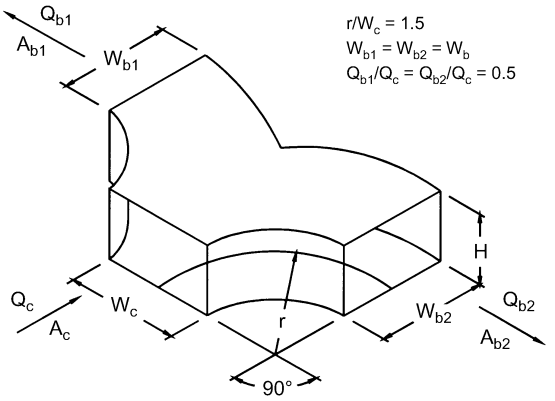

SR7-1 Fan, Centrifugal, Without Outlet Diffuser, Free Discharge

A_b/A_o	0.4	0.5	0.6	0.7	0.8	0.9	1.0
C_o	2.00	2.00	1.00	0.80	0.47	0.22	0.00

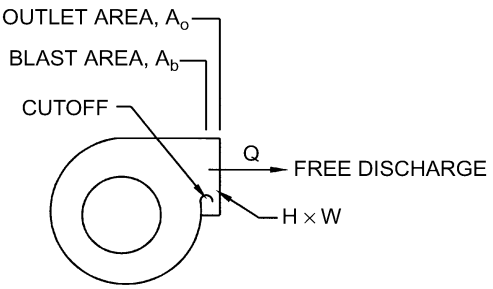

SR7-2 Plane Asymmetric Diffuser at Centrifugal Fan Outlet, Free Discharge

	C_o Values					
	A_1/A_o					
θ	1.5	2.0	2.5	3.0	3.5	4.0
10	0.51	0.34	0.25	0.21	0.18	0.17
15	0.54	0.36	0.27	0.24	0.22	0.20
20	0.55	0.38	0.31	0.27	0.25	0.24
25	0.59	0.43	0.37	0.35	0.33	0.33
30	0.63	0.50	0.46	0.44	0.43	0.42
35	0.65	0.56	0.53	0.52	0.51	0.50

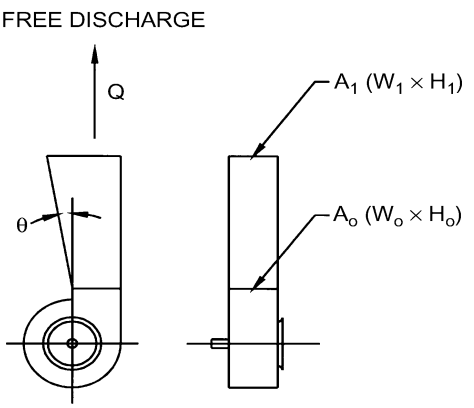

SR7-5 Fan Outlet, Centrifugal, SWSI, with Elbow (Position A)

	C_o Values					
	L/L_e					
A_b/A_o	0.00	0.12	0.25	0.50	1.00	10.00
0.4	3.20	2.50	1.80	0.80	0.00	0.00
0.5	2.20	1.80	1.20	0.53	0.00	0.00
0.6	1.60	1.40	0.80	0.40	0.00	0.00
0.7	1.00	0.80	0.53	0.26	0.00	0.00
0.8	0.80	0.67	0.47	0.18	0.00	0.00
0.9	0.53	0.47	0.33	0.18	0.00	0.00
1.0	0.53	0.47	0.33	0.18	0.00	0.00

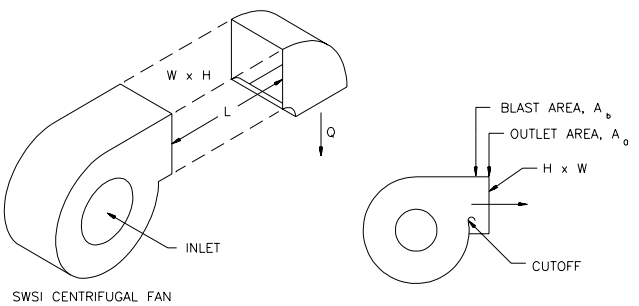

SR7-6 Fan Outlet, Centrifugal, SWSI, with Elbow (Position B)

	C_o Values					
	L/L_e					
A_b/A_o	0.00	0.12	0.25	0.50	1.00	10.00
0.4	3.80	3.20	2.20	1.00	0.00	0.00
0.5	2.90	2.20	1.60	0.67	0.00	0.00
0.6	2.00	1.60	1.20	0.53	0.00	0.00
0.7	1.40	1.00	0.67	0.33	0.00	0.00
0.8	1.00	0.80	0.53	0.26	0.00	0.00
0.9	0.80	0.67	0.47	0.18	0.00	0.00
1.0	0.67	0.53	0.40	0.18	0.00	0.00

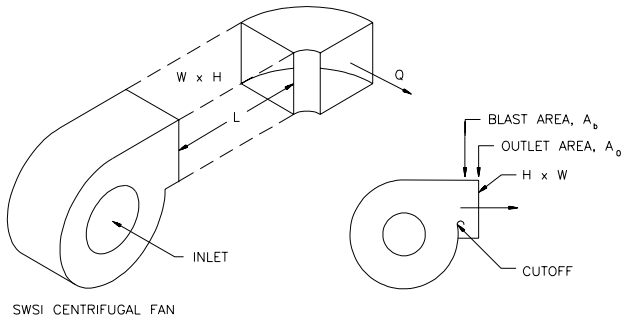

SR7-7 Fan Outlet, Centrifugal, SWSI, with Elbow (Position C)

	C_o Values					
	L/L_e					
A_b/A_o	0.00	0.12	0.25	0.50	1.00	10.00
0.4	5.50	4.50	3.20	1.60	0.00	0.00
0.5	3.80	3.20	2.20	1.00	0.00	0.00
0.6	2.90	2.50	1.60	0.80	0.00	0.00
0.7	2.00	1.60	1.00	0.53	0.00	0.00
0.8	1.40	1.20	0.80	0.33	0.00	0.00
0.9	1.20	0.80	0.67	0.26	0.00	0.00
1.0	1.00	0.80	0.53	0.26	0.00	0.00

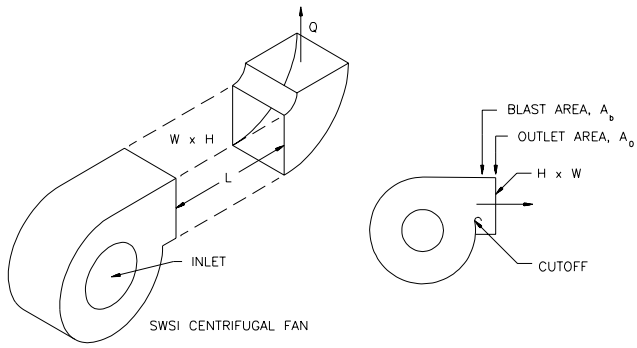

SR7-8 Fan Outlet, Centrifugal, SWSI, with Elbow (Position D)

	C_o Values					
	L/L_e					
A_b/A_o	0.00	0.12	0.25	0.50	1.00	10.00
0.4	5.50	4.50	3.20	1.60	0.00	0.00
0.5	3.80	3.20	2.20	1.00	0.00	0.00
0.6	2.90	2.50	1.60	0.80	0.00	0.00
0.7	2.00	1.60	1.00	0.53	0.00	0.00
0.8	1.40	1.20	0.80	0.33	0.00	0.00
0.9	1.20	0.80	0.67	0.26	0.00	0.00
1.0	1.00	0.80	0.53	0.26	0.00	0.00

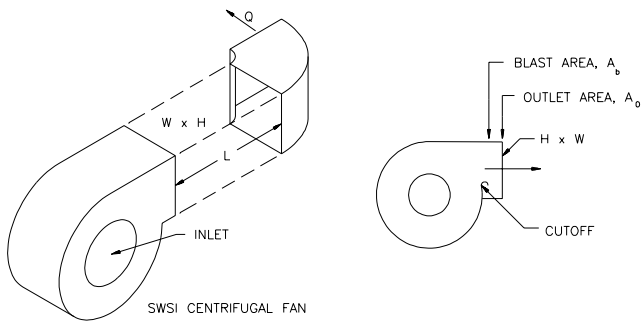

SR7-9 Fan Outlet, Centrifugal, DWDI, with Elbow (Position A)

	C_o					
	L/L_e					
A_b/A_o	0.00	0.12	0.25	0.50	1.00	10.00
0.4	3.20	2.50	1.80	0.80	0.00	0.00
0.5	2.20	1.80	1.20	0.53	0.00	0.00
0.6	1.60	1.40	0.80	0.40	0.00	0.00
0.7	1.00	0.80	0.53	0.26	0.00	0.00
0.8	0.80	0.67	0.47	0.18	0.00	0.00
0.9	0.53	0.47	0.33	0.18	0.00	0.00
1.0	0.53	0.47	0.33	0.18	0.00	0.00

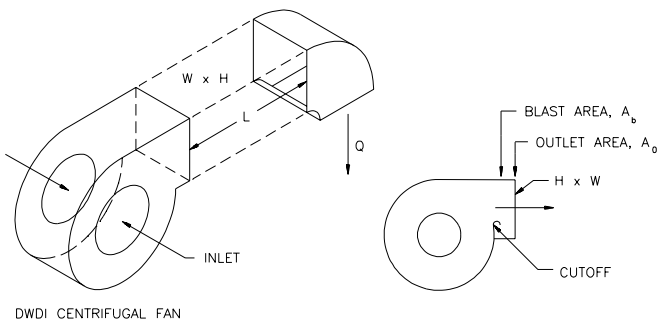

SR7-10 Fan Outlet, Centrifugal, DWDI, with Elbow (Position B)

	C_o					
	L/L_e					
A_b/A_o	0.00	0.12	0.25	0.50	1.00	10.00
0.4	4.80	4.00	2.90	1.30	0.00	0.00
0.5	3.60	2.90	2.00	0.84	0.00	0.00
0.6	2.50	2.00	1.50	0.66	0.00	0.00
0.7	1.80	1.30	0.84	0.41	0.00	0.00
0.8	1.25	1.00	0.66	0.33	0.00	0.00
0.9	1.00	0.84	0.59	0.23	0.00	0.00
1.0	0.84	0.66	0.50	0.23	0.00	0.00

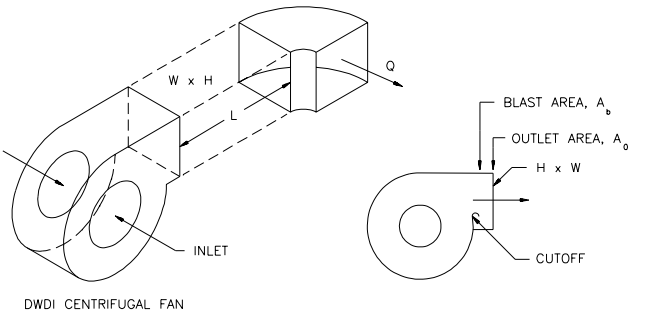

SR7-11 Fan Outlet, Centrifugal, DWDI, with Elbow (Position C)

	C_o					
	L/L_e					
A_b/A_o	0.00	0.12	0.25	0.50	1.00	10.00
0.4	5.50	4.50	3.20	1.60	0.00	0.00
0.5	3.80	3.20	2.20	1.00	0.00	0.00
0.6	2.90	2.50	1.60	0.80	0.00	0.00
0.7	2.00	1.60	1.00	0.53	0.00	0.00
0.8	1.40	1.20	0.80	0.33	0.00	0.00
0.9	1.20	0.80	0.67	0.26	0.00	0.00
1.0	1.00	0.80	0.53	0.26	0.00	0.00

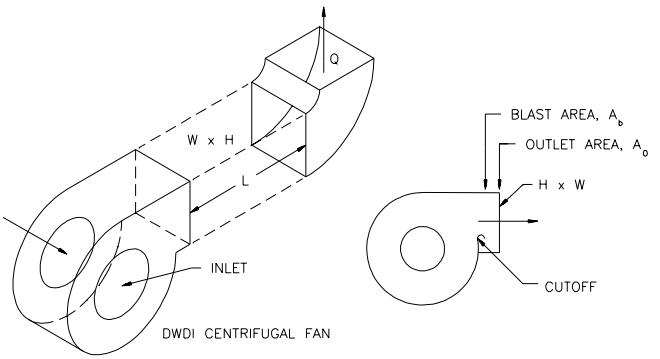

SR7-12 Fan Outlet, Centrifugal, DWDI, with Elbow (Position D)

	C_o					
	L/L_e					
A_b/A_o	0.00	0.12	0.25	0.50	1.00	10.00
0.4	4.70	3.80	2.70	1.40	0.00	0.00
0.5	3.20	2.70	1.90	0.85	0.00	0.00
0.6	2.50	2.10	1.40	0.68	0.00	0.00
0.7	1.70	1.40	0.85	0.45	0.00	0.00
0.8	1.20	1.00	0.68	0.26	0.00	0.00
0.9	1.00	0.68	0.57	0.22	0.00	0.00
1.0	0.85	0.68	0.45	0.22	0.00	0.00

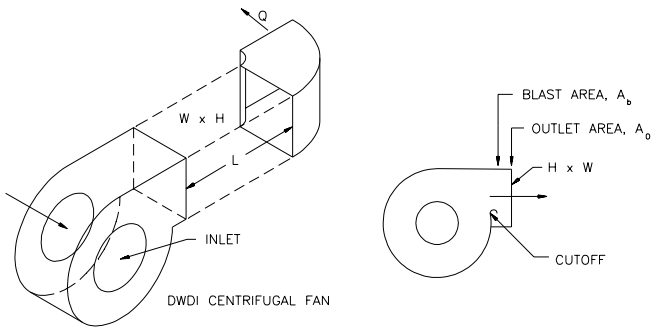

SR7-17 Pyramidal Diffuser at Centrifugal Fan Outlet with Ductwork

	C_1 Values					
	A_o/A_1					
θ	1.5	2.0	2.5	3.0	3.5	4.0
10	0.10	0.18	0.21	0.23	0.24	0.25
15	0.23	0.33	0.38	0.40	0.42	0.44
20	0.31	0.43	0.48	0.53	0.56	0.58
25	0.36	0.49	0.55	0.58	0.62	0.64
30	0.42	0.53	0.59	0.64	0.67	0.69

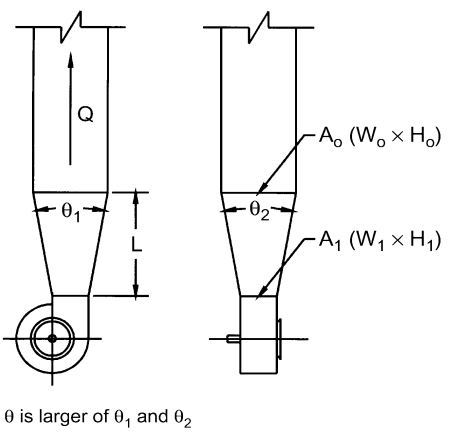

θ is larger of θ_1 and θ_2